UNIVERSITY OF CALIFORNIA, SAN DIEGO

Insights into the regulation of NF-kappaB and mediation of the cellular stress response by NF-kappaB

A Dissertation submitted in partial satisfaction of the requirements for the degree Doctor of Philosophy

in

Chemistry

by

Jessica Ho

Committee in Charge:

Professor Gourisankar Ghosh, Chair
Professor Timothy Baker
Professor Randy Hampton
Professor David Hendrickson
Professor Jack Johnson

2010

..

The Dissertation of Jessica Ho is approved, and it is acceptable in quality and form for publication on microfilm and electronically:

_____

_____

_____

_____

_____

Chair

UNIVERSITY OF CALIFORNIA, SAN DIEGO

2010

Dedication

This thesis is dedicated to my parents, Jonathan, James, and Anthony because they always believed in me, and were unquestionalbly patient and encouraging when things got really hard.

Table of Contents

List of Abbreviations

ARD	ankyrin repeat domain
Bcl-2	B cell lymphoma 2
cDNA	coding DNA
DTT	dithiothreitol
FasL	Fas Ligand
FLAG	peptide with sequence Asp-Tyr-Lys-Asp-Asp-Asp-Asp-Lys
GO	glucose oxidase
GRR	glycine rich region
H_2O_2	hydrogen peroxide
HEPES	(4-(2-hydroxyethyl)-1-piperazineethanesulfonic acid)
IAP	inhibitor of apoptosis
IκB	inhibitor of NF-κB
IKK	IκB kinase complex
IP	immunoprecipitation
IPTG	isopropyl β-D-1-thiogalactopyranoside
J	Joules
kDa	kilodalton
MEF	mouse embryonic fibroblast cells
mU	milli unit of activity

MW	molecular weight
NF-κB	nuclear factor-κB
NLS	nuclear localization signal
PAGE	polyacrylamide gel electrophoresis
PAR	poly(ADP-ribose)
PARP	poly(ADP) ribose polymerase
PCR	polymerase chain reaction
PMSF	phenylmethanesulfonylfluoride
qPCR	real time quantitative PCR
ROS	reactive oxygen species
RHR	rel homology region
RP	regulatory particle
SDS	sodium dodecyl sulfate
TAD	transcription activation domain
TCEP	tris(2-carboxyethyl)phosphine
TNFα	tumor necrosis factor alpha
TRIS	tris(hydroxymethyl)aminomethane
Ub	ubiquitin
UV	ultraviolet light
XIAP	X-linked Inhibitor of Apoptosis Protein

List of Figures

List of Tables

Acknowledgements

I would like to thank my advisor, Gouri Ghosh, for seeing potential in me and giving me a chance to conduct research in his laboratory, when no one else would. All of our discussions and scientific challenges during these last 6 years has made me a better scientist. I would also like to thank Alexander Hoffmann for being so kind as to allow me to attend his lab's sub-group meetings and for always being generous with his scientific input and equipment. I would also like to thank Dan Donoghue for accepting me as a trainee on the Growth Regulation and Oncogenesis Training Grant. By attending the monthly meetings, I was introduced to a plethora of other scientists, who, with his encouragement, I would approach for their scientific expertise when my project veered from traditional aspects in our lab.

I have also been blessed to do research surrounded by a great group of people from the Gouri Ghosh, Partho Ghosh, and Alex Hoffmann laboratories. In particular, I would like to thank Jacky Ngo for being a great source of support, for always taking time and being patient teaching me the basics in protein biochemistry, and for

introducing me to terrific restaurants and being a great dinner buddy. I would like to thank Don Vu for his constant support and listening ear, I will always remember how he saved me from staying overnight in the lab during my 1st proteasome prep by showing me all these nifty lab tricks. I would also like to thank Anu Moorthy, Erika Mathes, Amanda Fusco, Smarajit Polley, Zhihua Tao, and Zhong for their scientific input and support. I would also like to thank Brent Hamaoka, Johanne Le Coq, Jyothi Kumaran, and Byron Hetrick for always taking time out of their busy schedules to listen to my practice talks. I would like to thank Shannon Werner, Ellen O'Dea, Vincent Shih, Jon Almaden, Soumen Basak, Kim Ngo, and Masa Asagiri for their scientific input and technical support. I would also like to thank Olga Savinova and Sulakshana Mukherjee for being great role models for women in science. I will always remember and have been inspired by their wealth of knowledge, inquisitive nature, strength, and perseverance; I have learned so much from working with them. I would like to thank Anthony Farina for his unending support and patience. I will never forget how he always took what he learned and taught me, encouraged me to talk to other scientists, always tried to find someone he knew to help me whenever I was stuck, and believed in me. I would not have been able to complete my studies without his help. Finally, I would like to thank my

dad, mom, my brothers, Jon and James for being pillars of strength and support, which unquestionalbly helped me get through my PhD. Every time I got too caught up with work, they were always there to remind me that there was a world outside of science, that they did not care if my protein was active or not, and that they would always love me, regardless of the outcome. I would like to thank my dad and mom for their unwavering belief in me, Jon for always making me laugh with youtube videos so that I could see the lighter side of things, and James for flying to San Diego to bring me food, buying me two laptops just because, and for finding the best free online versions of Microsoft Office, Adobe Illustrator, and Endnote for me.

Parts of the research described in my dissertation is in the process of being published or in preparation for submission and my collaborators are cited both in the text and acknowledgements of each chapter. Permission has been extended to include this material. Chapter 2, has been submitted for publication as it may appear in PLoS One, 2010. Ho, Jessica Q.; Asagiri, Masataka; Hoffmann, Alexander; Ghosh, Gourisankar. "NF-κB potentiates caspase independent hydrogen peroxide induced cell death". The dissertation author was the primary author of this paper. Parts of Chapter 3 and Chapter 4 are

adapted from a manuscript in preparation, 2010. Ho, Jessica Q.; Hyunh, Kim; Mathes, Erika; Ghosh, Gourisankar. "PA28αβ bound 20S proteasome is responsible for the degradation of free IκBα". The dissertation author the primary author. Kim Hyunh and Erika Mathes performed some of the experiments and are co-authors.

Vita

2004	B.S, University California, San Diego
2007	M.S, University of California, San Diego
2010	Ph.D, University of California, San Diego

Publications

Ho. J.Q., Asagiri, M., Hoffmann, A., Ghosh, G. NF-κB potentiates hydrogen peroxide induced cell death. *PloS One (submitted)*

Ho, J.Q., Hyunh, K, Mathes, E. Ghosh, G. Regαβ bound 20S proteasome is responsible for free IκBα turnover. (In preparation)

Moorthy, A., Savinova, O., **Ho, J.Q.**, Wang, V., Vu, D., Ghosh, G. The 20S proteasome processes NF-κB1 p105 into p50 in a translation-independent manner. The EMBO Journal (2006) 25, 1945–1956.

Abstract of the Dissertation

Insights into the regulation of NF-kappaB and mediation of the cellular stress response by NF-kappaB

by

Jessica Ho

Doctor of Philosophy in Chemistry

University of California, San Diego, 2010

Professor Gourisankar Ghosh, Chair

NF-κB is a pleiotropic transcription factor, which is instrumental in regulating diverse cellular processes such as inflammation and cell survival. Enhanced NF-κB activity, due either to prolonged NF-κB activation upon exposure to cellular stress or misregulation of NF-κB, can lead to many neurodegenerative diseases as well as cancer. Thus, in this study, biological and biochemical approaches were used to

characterize how NF-κB regulates the cellular stress response and how NF-κB activity itself is regulated. Chapter 1 introduces oxidative stress, which is the specific cellular stress used in this study, and reviews how oxidative stress affects all cellular components, including the proteasome and NF-κB. Chapter 2 characterizes the mechanism of NF-κB's cell death promoting function in response to oxidative stress and shows that NF-κB signaling actually promotes cell death. Furthermore, we suggest that NF-κB promotes cell death through the repression of pro-survival genes and induction of pro-death genes. Chapter 3 focuses on whether oxidized 20S proteasome enhances the ubiquitin independent degradation of NF-κB inhibitor molecule IκBγ. We clearly show that the 20S proteasome is able to degrade IκBγ in an ubiquitin independent manner. Preliminary LC-MS/MS data suggests that the 20S proteasome, which displays enhanced activity towards IκBγ, can undergo cysteic acid modification. We suggest that mild oxidative stress can enhance proteasome activity, while severe oxidative stress impairs proteasomal activity. Chapter 4 provides strong evidence suggesting that PA28αβ bound 20S proteasome is responsible for the ubiquitin independent degradation of another NF-κB inhibitor molecule, free IκBα. All together, this work delineates how NF-κB signaling can mediate cell death in response to oxidative stress, how oxidative stress

can potentially increase the ubiquitin independent degradation of IκBγ by enhancing the proteolytic activity of the 20S proteasome, and how PA28αβ bound 20S proteasome is responsible for the ubiquitin independent degradation of free IκBα.

Chapter 1: Introduction

1.1 Reactive oxygen species and reactive nitrogen species

Reactive oxygen species (ROS) and reactive nitrogen species (RNS) have been implicated in the pathogenesis of age related diseases, such as cancer, arteriosclerosis, and degenerative disorders. ROS include free radical species, superoxide anion ($O_2^{\bullet -}$) and hydroxyl radical ($\bullet OH$), and non- radical species, hydrogen peroxide (H_2O_2). RNS include nitric oxide ($NO\bullet$) and peroxynitrite ($ONOO^-$)(Trachootham et al., 2008). Intracellular ROS and RNS both arise from exogenous and endogenous sources (Fig 1.1). Exogenous sources arise from UV, X-ray, or gamma ray irradiation, and also atmospheric pollutants and chemicals (Valko et al., 2006). Endogenous sources arise mainly from the mitochondria, where, during aerobic respiration, a single electron is added onto molecular oxygen by cytochrome c oxidase to produce the superoxide anion. The addition of an electron to oxygen is due to electron leakage from complex I and III of the electron transport chain (Cadenas, 1989). The superoxide anion can then be converted to H_2O_2 and O_2 by mitochondrial superoxide dismutases (SOD) (Engelhardt, 1999). Since H_2O_2 is a non-polar molecule, it can diffuse into other cellular compartments (Veal et al., 2007). In the presence of reduced transition metals, such as Fe(II) and sometimes copper, H_2O_2 can be

further converted to •OH, through the Fenton/Harber-Weiss reaction (Valko et al., 2006; Wardman and Candeias, 1996). Additionally, ROS are produced by membrane bound NADPH oxidase, present on both phagocytic immune cells and non-immune cells. Phagocytic cells, such as neutrophils, use NADPH oxidase to generate H_2O_2 as a cytotoxic agent to kill invading microbes. In non-immune cells, binding of various growth factors and cytokines bind to their corresponding membrane bound receptors, which activates NADPH oxidase. Once activated, NADPH oxidase produces the superoxide anion, which is then converted to H_2O_2 by cytoplasmic SODs. (Geiszt and Leto, 2004; Veal et al., 2007). In addition, both microsomes and peroxisomes produce H_2O_2, where microsomes produce up to 80% of the H_2O_2 concentration under hypoxia conditions and peroxisomes produce H_2O_2 under physiological conditions. RNS, NO•, is generated through the following nitric oxide synthase isozymes: mitochondrial nitric oxide synthase (mtNOS), neuronal NOS (nNOS), endothelial NOS (eNOS), and inducible NOS (iNOS) (Ghafourifar and Cadenas, 2005; Trachootham et al., 2008).

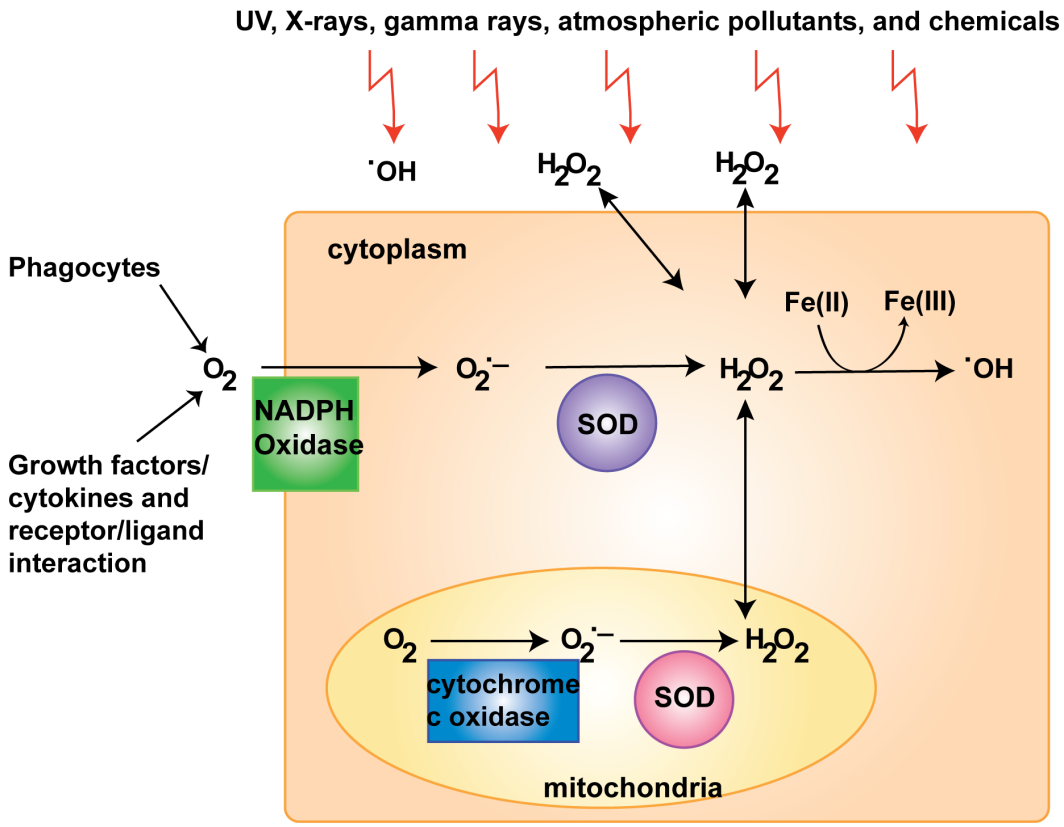

Figure 1.1: Sources of exogenous and endogenous of ROS

Exogenous ROS, such as hydrogen peroxide (H_2O_2) and the hydroxyl radical (•OH), can be produced by UV, X-ray, or gamma ray irradiation, and also atmospheric pollutants and chemicals. Endogenous ROS arise in the following manner. Superoxide anion ($O_2^{\bullet -}$) is formed by cytochrome c oxidase in the mitochondria during aerobic respiration, and by membrane bound NADPH oxidase which are activated by phagocytes and by the binding of growth factors and cytokines to their cognate receptors. The superoxide anion is then further converted to H_2O_2 through mitochondria or cytoplasmic superoxide dismutases (SOD), respectively. In the presence of iron, Fe(II), H_2O_2 is converted to •OH through the Fenton reaction. H_2O_2 is able to diffuse through membranes, as shown by the double- sided arrow, since H_2O_2 is a non-polar molecule. This figure is adapted from (Veal et al., 2007).

1.2 Oxidative stress and its consequences

Different levels of ROS can induce different biological outputs (Fig 1.2). For example, transient and low levels of ROS elicit an anti-oxidant response, where expression of antioxidant transcription Nrf-2 is up-regulated. However, when ROS/RNS overwhelm the anti-oxidant capabilities of the cell, a state of oxidative stress can ensue. Increased levels of oxidative stress can either promote cell proliferation and cell survival or promote cell death (Gloire et al., 2006b). In general, ROS at moderate/ intermediate levels promote inflammation, cell proliferation and cell survival, which eventually can lead to aberrant cell survival and growth, resulting in cancer. This is because ROS act as secondary messengers in many signal transduction pathways, involving NF-κB, AP-1, and HIF, that promote these particular cellular responses. In contrast, severe increases in ROS induce excessive cell death, which eventually can lead to the gradual decline of tissue function, followed by aging and degenerative disorders (Hensley et al., 2000; Lander, 1997; Trachootham et al., 2008). Thus, ROS are known to have a "two-faced" character, in that ROS can initiate and promote carcinogenesis, yet also act as an anti- tumourigenic species by inducing cellular senescence and cell death (Valko et al., 2006).

The actual concentration of ROS required to induce either cell survival or cell death is highly cell type dependent. For example, the concentration of H_2O_2 required to induce apoptotic cell death in mammalian cells actually varies 20 fold among different cell types (Veal et al., 2007). While it has been estimated that the basal level of H_2O_2 is in the nM range (Chance et al., 1979) and that an intermediate level of oxidative stress is in the 10-100μM range (Gloire et al., 2006b; Lander, 1997), these values can still vary depending on the cell type. Generally, it is thought that genetically unstable cells, which already contain both ROS induced DNA mutations and loss of tumor suppressor gene p53, are able to adapt to survive, evade cell death, and proliferate in response to moderate increases in cellular levels of ROS. However, exposure of normal or aging cells to high levels of ROS, results in the accumulation of irreversible damage to DNA, lipids, and protein. Thus, these cells, as opposed to the genetically unstable cells, are more prone to oxidative stress induced cell death (Trachootham et al., 2008).

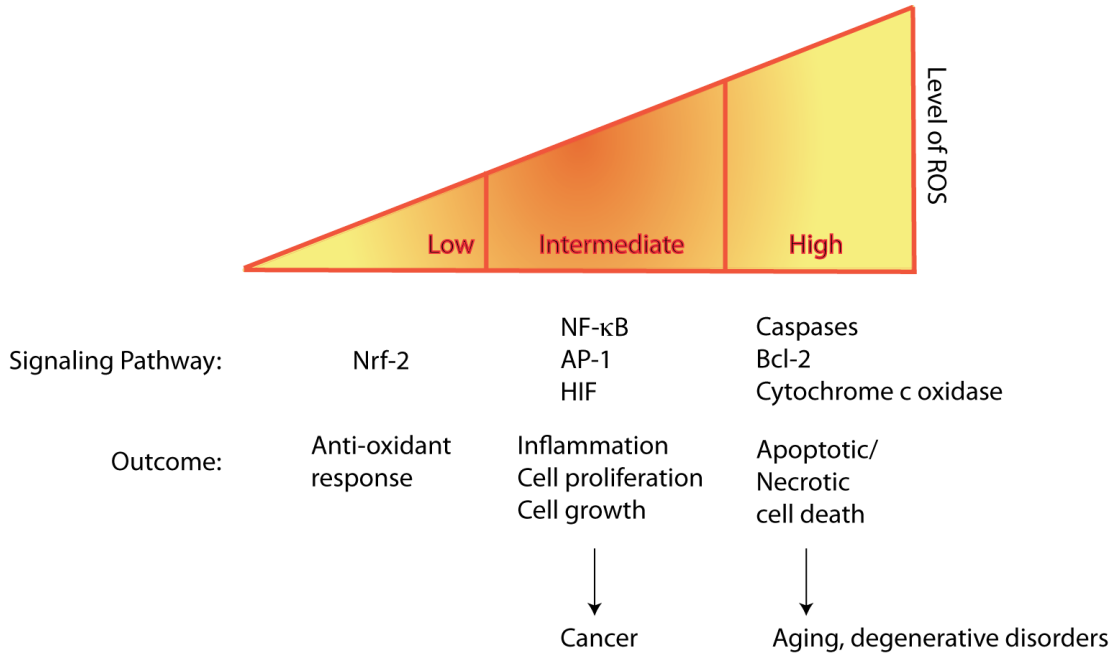

Figure 1.2: Biological outputs of different levels of ROS

Different levels of ROS result in different biological outputs. Low levels of ROS result in an anti-oxidant response, where anti-oxidant transcription factors such as Nrf-2 are up-regulated. Both intermediate and high levels of ROS, which overwhelm the cells anti-oxidant system, produce a state of oxidative stress. While intermediate levels of ROS triggers an inflammatory response as well as cell growth and proliferation, which can eventually lead to cancer, a high level of ROS can trigger either apoptotic or necrotic cell death, which can eventually lead to aging and degenerative disorders. This figure is adapted from (Gloire et al., 2006b).

1.3 Antioxidant Defenses

Since ROS are both potent regulators of eukaryotic signal transduction and also cytotoxic agents, the level of intracellular ROS is tighly regulated, by both non-enzymatic and enzymatic anti-oxidants. Non- enzymatic antioxidants include Vitamin C, Vitamin E, carotenoids, thiol oxidants (glutathione, thioredoxin, and lipoic acid), flavonoids, and selenium. Enzymatic anti-oxidants include superoxide dismutases (SOD), catalases, glutathione peroxidases, and thioredoxin peroxidases (peroxiredoxin) (Veal et al., 2007). As previously stated, SOD catalyze the conversion of the superoxide anion to H_2O_2. However, SODs often work in conjunction with both catalses and glutathione peroxidases to remove intracellular H_2O_2. Distinct isoforms of SODs exist in different cellular compartments, in that SOD1 (CuZnSOD) is found in the cytoplasm, nucleus, and lysosomes, while SOD2 (MnSOD) and SOD3 are found in the mitochondria and extracellular matrix, respectively (Bafana et al., 2010). H_2O_2 produced by SOD can then be further converted to H_2O and oxygen through the activity of catalases. Catalases are highly efficent enzymes, most commonly found in peroxisomes, which contain high levels of H_2O_2, yet catalases can also be found in the cytosol or mitochondria of regular cells (Valko et al.,

2006). They utilize their heme prosthetic group to eliminate H_2O_2, where it has been estimated that it can scavenge ~6 million molecules of H_2O_2/ min (Trachootham et al., 2008).

Anti-oxidant molecule, glutathione peroxidase (GPX) also catalyzes the reduction of H_2O_2 to H_2O, which requires the cyclic oxidation/ reduction of the catalytic cysteine(SH) or selenocysteine(SeH) of GPX (Fig1.3) (Valko et al., 2007). GPX-SeH is oxidized to GPX-SeOH upon the reduction of H_2O_2, and only returns to its reduced state upon its reaction with two glutathione (GSH) molecules. The first reaction with GSH converts it to GPX-SeSG, and the second reaction with GSH converts it to its original reduced state (GPX-SeH), releasing GS-SG as the by product (Veal et al., 2007). Since the recycling of GPX-SeOH involves the oxidation of reduced glutathione (GSH), GPX catalyses the following reaction:

$$2GSH + H_2O_2 \rightarrow GS\text{-}SG + 2H_2O$$

where GSH is the reduced monomeric form of glutathione and GS-SG is the oxidized and dimeric form of glutathione connected by a disulfide bond (Valko et al., 2006). In order to complete the cycle, the oxidized glutathione (GS-SG) is reduced by glutathione reductase, which

requires NADPH provided by the pentose phosphate pathway. Glutathione reductase catalyzes the following reaction:

GS-SG + NADPH + H^+ 2GSH + $NADP^+$

(Casagrande et al., 2002; Valko et al., 2006). The complete cycle is shown in (Fig 1.3).

Thioredoxin peroxidase or peroxiredoxins (Prx) operate similarly to GPXs, in that the conversion of H_2O_2 to H_2O utilizes the cyclic oxidation/ reduction of its catalytic cysteine (SH), which is coupled to the consumption of NADPH provided again by the pentose phosphate pathway (Fig.1.3) (Veal et al., 2007). The typical 2-cysteine peroxiredoxin (2-Cys Prx) is a homodimeric species, where each monomer contains two active site cysteine residues (SH) (Wood et al., 2003). Upon reduction of H_2O_2, one of the Prx-SH active site residues becomes oxidized to Prx-SOH. This SOH group then reacts with the SH group from the other monomer to form a disulfide bond, which prevents further oxidation of the species. This covalently attached dimeric species undergoes reduction back to the original sulfhydryl form by the oxidation of thioredoxin (Trx) catalyzed by thioredoxin reductase. Trx is then reduced due to the consumption of NADPH (Chevallet et al., 2003; Veal et al., 2007; Veal et al., 2004). The complete

cycle is shown in (Fig 1.3).

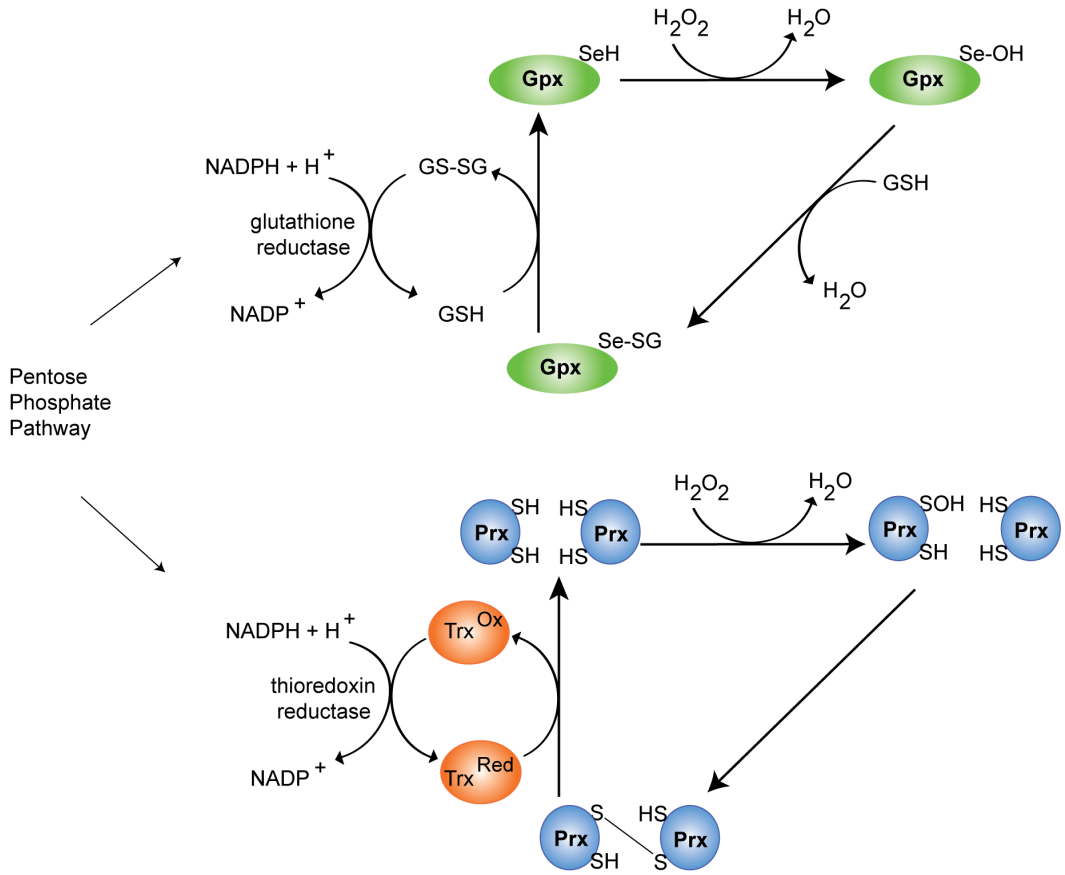

Figure 1.3: Glutathione Peroxidase (Gpx) and Peroxireductase (Prx) Systems

Gpx and Prx reduce hydrogen peroxide to water through the redox cycling of their catalytic seloncysteine (SeH) or cysteine (SH) residues, respectively. Upon reduction of H_2O_2, the active sites of Gpx and Prx are oxidized to Se-OH and S-OH. Subsequently, Gpx-SeOH reacts first with glutathione (GSH) to form Gpx-SeSG, and then another GSH molecule to revert to its original reduced form (Gpx-SeH), releasing GS-SG, two GSH molecules connected by a disulfide bond, in the process. In the case of Prx, Prx-SOH forms a disulfide bond with the active site SH residue of the other subunit of the Prx homodimer, which in turn is reduced by the subsequent oxidation of thioredoxin (Trx^{Ox}). Both GS-SG and Trx^{Ox} are reduced by glutathione reductase and thioredoxin reductase, respectively. This reaction is coupled to the NADPH oxidation, which is provided by the pentose phosphate pathway. This figure is adapted from (Veal et al., 2007).

1.4 Oxidative damage to DNA, Lipids, and Proteins

In the cases where the anti-oxidant systems are overwhelmed by severe levels of ROS, DNA, lipids and proteins undergo oxidative damage (Trachootham et al., 2008). The hydroxyl radical interacts with all components of DNA, the purine and pyrimidine bases as well as the deoxyribose backbone. In general, ROS causes single/double stranded DNA breaks, modifications of purine, pyrimidine, or deoxyribose units, and DNA cross-linking (Valko et al., 2007). Moderate levels of DNA damage trigger cell cycle arrest and initiate DNA repair processes to ensure DNA integrity. However, excessive DNA damage and failure in DNA repair processes induces apoptosis and can also lead to genomic instability and eventually cancer (Marnett, 2000; Valko et al., 2006). A common and easily formed, oxidized DNA product is 8-hydroxyguanine (8-OH-G), which is formed by reaction of a hydroxyl radical with guanine. 8-OH-G is used as a biomarker for oxidative DNA damage in an organism and can be used as potential marker for carcinogenesis (Cooke et al., 2003).

Lipids are also susceptible to oxidative modification and damage. The hydroxyl radical can attack the polyunsaturated fatty

acid residues of phospholipids, which results in lipid peroxidation (Marnett, 1999). Lipid peroxidation generates lipid radicals, which can attack subsequent lipid molecules, resulting in a chain reaction. Lipid peroxidation generated by products, malondialdehyde (MDA) and 4-hydroxy-2nonenal (HNE), can functionally alter both DNA bases and proteins, which results in genetic mutations and altered signal transduction pathways, respectively (Trachootham et al., 2008).

Proteins also undergo oxidative modification, which can be either reversible or irreversible, depending on the extent of oxidative damage (Valko et al., 2007). Residues such as lysine, arginine, histidine, proline, and threonine are particularly susceptible to metal catalyzed oxidation, which produces protein carbonyl derivatives that are commonly used as a quantitative marker of protein oxidation (Trachootham et al., 2008). Cysteine and methionine residues are both susceptible to reversible/irreversible oxidation by disulfide bond mediated cross- linking, hyperoxidation (Woo et al., 2003b), and adduct formation between proteins and lipid peroxides, which produces large protein aggregates that are unable to be degraded by the proteasomal degradation system (Trachootham et al., 2008; Valko et al., 2006).

1.5 Modulation of protein activity by hyperoxidation of cysteine residues

Hyperoxidation of cysteine residues is known to modulate the activities of many proteins, such as Peroxiredoxins (Prxs), MMP-7 (matrix metallo-proteinase-7), glyceraldehyde-3-phosphate dehydrogenase, carbonic anhydrase III, mitogen-activated protein kinase phosphatase-3 (MKP3), and protein tyrosine phosphatase-1B (Lim et al., 2008). The hyperoxidation of cysteine residues is determined by the pKa of the cysteine thiloate anion, which is conferred by the protein's local environment. For example, a typical Prx molecule exists as an obligate homodimer, where each monomer subunit contains two conserved active site thiol groups (Cys-SH), located at the N and C terminus (Wood et al., 2003). Under both normal and oxidative stress conditions, the N terminal Cys-SH can be selectively oxidized by H_2O_2 to Cys-SOH (the sulfenic acid) and either react with another active site's C terminal Cys-SH to form a disulfide bond or become further oxidized to Cys-SO_2H (the sulfinic acid), which results in the inactivation of the enzyme (Fig 1.4) (Bozonet et al., 2005; Chevallet et al., 2003). The increased susceptibility of sulfenic acid to be converted to sulfinic acid is related to the fact that disulfide bond formation in Prx is a relatively slow

process (Veal et al., 2007). Thus, this hyperoxidation event can occur in the presence of low H_2O_2 concentrations and is thought to act as a molecular switch, in which inactivation of Prx by hyperoxidation allows for the occurrence signal transduction responses, which involve redox activated transcription factors. Interestingly, in PrxI, the Cys-SO_2H can be reversed back to the catalytically active Cys-SH form through the activity of sulfiredoxin proteins. This demonstrates that cysteine sulfinylation is a precisely regulated cellular mechanism (Chang et al., 2004; Woo et al., 2003a; Woo et al., 2005; Woo et al., 2003b; Wood et al., 2003; Yang et al., 2002).

Irreversible modification, cysteic acid (Cys-SO_3H) formation, has also been reported for human PrxI, as well as its yeast homologue, Tsa1p. In the case of Tsa1p, Cys-SO_3H modification actually switches Tsa1p's activity from a peroxidase to an effective molecular chaperone (Chevallet et al., 2003; Lim et al., 2008; Rabilloud et al., 2002; Wagner et al., 2002). While hyperoxidation of PrxI's catalytic cysteine results in the inactivation of Prx, oxidation of cysteine residues can also lead to activation of enzymes, such as in the case of MMP-7. MMP-7, which mediates plaque rupture in atherosclerosis, is secreted as an inactive pro-protein, where its cysteine switch domain protects the latent form

of the enzyme from cleavage. However, it becomes active upon sulfinic acid formation of the cysteine present in the cysteine switch by hypochlorous acid (Fu et al., 2001b). Thus, cysteine oxidation plays an important role in modulating protein activity in a variety of cellular processes.

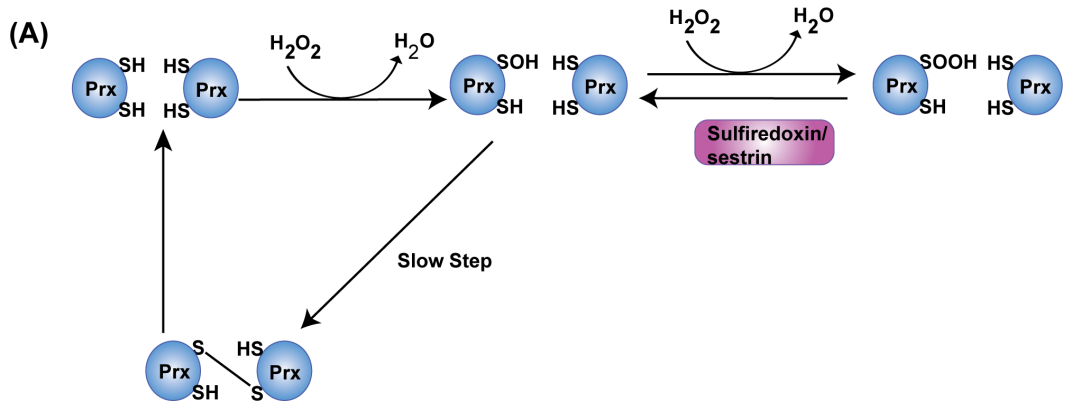

(B) thiol (-SH)
sulfenic acid (Cys-SOH)
sulfinic acid (Cys-SO_2H)
sulfonic acid/cysteic acid (Cys-SO_3H)

Figure 1.4: Hyperoxidation of peroxiredoxin (Prx)

(A) Prx reduces hydrogen peroxide (H_2O_2) to water through the redox cycling of their catalytic cysteine (Cys-SH) residues. Upon reduction of H_2O_2, the active site Cys-SH is oxidized to Cys-SOH. Subsequently, the Cys-SOH can either form a disulfide bond with the active site of another Cys-SH residue present on the other subunit of the Prx homodimer, or undergo to Cys-SO_2H. This hyperoxidation event further inactivates the enzyme, and can be reversed by the actions of sulfiredoxins or sestrins. **(B)** The nomenclature is given for all of the states of cysteine oxidation.

1.6 The proteasomal degradation system and oxidative stress

The 26S proteasome, which consists of the 20S catalytic core and two 19S regulatory particles, is the major cellular component that carries out protein degradation. Under oxidative stress, the 26S proteasome has been shown to be extremely susceptible to oxidative damage, which results in a decrease in its ability to degrade substrates in an ubiquitin dependent manner (Davies, 2001; Reinheckel et al., 1998). Ubiquitin- activating enzymes (E1) also become oxidatively damaged and rendered inactive under this condition (Shringarpure et al., 2003; Trachootham et al., 2008), further illustrating that the ubiquitin dependent degradation pathway is impaired under oxidative stress. However, the 20S proteasome remains more resistant to oxidative damage than the 26S proteasome, such that the 20S proteasome retains its ability to degrade proteins (Reinheckel et al., 1998). Due to its lack of a ubiquitin recognition motif, which is present in the 19S regulatory particle, the 20S proteasome degrades proteins in a ubiquitin independent manner (Bader et al., 2007). Degradation of proteins in a ubiquitin independent manner is facilitated by the fact that, under oxidative stress, many proteins become partially unfolded, which also results in the exposure of their hydrophobic residues (Bader and Grune,

2006; Voss and Grune, 2007). In the cases of histones (1, 2A, 2B, 3, 4), hemoglobin, α-Casein, and ferritin, hydrophobic residues act as a degradation signal for the 20S proteasome (Grune et al., 2003). Thus, the 20S proteasome is thought to be an active participant of the anti-oxidant response, since it removes oxidatively damaged proteins. However, severely oxidatively damaged proteins, which are cross-linked to each other and form higher order oligomers, are resistant to proteasomal degradation (Bader et al., 2007; Grune et al., 2003; Grune et al., 1995; Voss and Grune, 2007).

1.7 NF-κB and oxidative stress

1.7.1 NF-κB

Nuclear factor- κB, is a ubiquitously expressed transcription factor that is critically involved in the regulation of a variety of cellular processes, such as the innate and adaptive immune response, inflammation, cellular survival, proliferation, differentiation, cell adhesion, and the cellular stress response (Gilmore, 2006). It was first identified as a protein that binds to a specific DNA sequence within the intronic enhancer of the immunoglobulin- κ light chain in mature B and plasma cells (Sen and Baltimore, 1986; Singh et al., 1986). However, it is now known to mediate the afore- mentioned processes by transcriptional regulation of NF-κB target genes, which include cytokines, chemokines, adhesion molecules, and cell survival/death promoting factors (Mankan et al., 2009). Since NF-κB is integral to a variety of cell processes, NF-κB signaling is evolutionary conserved and thus, NF- κB proteins are found in a multitude of species, ranging from *Drosophilia* to humans, but not in yeast and *C. elegans* (Ghosh et al., 1998; Sullivan et al., 2007).

In mammals, NF-κB is actually a family of proteins that are

comprised of homo- and heterodimers of five proteins: RelA (p65), RelB, c- Rel, p50, and p52, which are encoded by the genes *rela*, *relb*, *crel*, *nfkb1*, and *nfkb2*, respectively. Both p50 and p52 are smaller processed proteins from larger precursor molecules, p105 and p100, respectively. All five NF-κB proteins can form homo- and hetero- dimers in a combinatorial manner, which allows for regulation of distinct sets of genes.

All of these proteins share a highly conserved Rel Homology Region (RHR), which is comprised of an amino terminal domain (NTD), responsible for DNA recognition, and a dimerization domain (DimD), responsible for dimerization, and a nuclear localization signal (NLS)(Bakkar and Guttridge, 2010; Gilmore, 2006; O'Dea and Hoffmann, 2009). However, the C- terminal ends of the NF-κB proteins differ and can be grouped into two classes. Class I consists of p105 and p100 whose C- terminal regions contain multiple copies of ankyrin repeats, which act as inhibitors of NF-κB (see 1.7.2 for more detail). Class II consists of RelA, RelB, and c-Rel, because they all contain C- terminal transactivating domains (TADs), which are thought to assist in gene activation (Huxford et al., 1999). RelB differs from the other NF-κB family members in that it contains an N-terminal leucine zipper (LZ) domain,

which is required for full RelB dependent transcription activation (Dobrzanski et al., 1993). Class I molecules are generally not transcriptionally active, but only become active upon dimerization with Class II molecules. This is because both p50 and p52 lack TAD domains, unlike p65, c-Rel, and RelB. Thus, p50 and p52 homodimers are both repressors of transcription (Franzoso et al., 1992; Huxford et al., 1999). The domain organization of all NF-κB family members is shown in (Fig 1.5).

Upon translocation to the nucleus, NF-κB dimers bind to 9-10 base pair DNA sites, called κB sites, with the consensus sequence, 5'-GGGRNWYYCC-3', where R is a purine base, N is any nucleotide, W is A or T, and Y is a pyrimidine base (Gilmore, 2006; Hoffmann et al., 2006).

As previously stated, NF-κB is integral to a variety of cellular processes. Table 1.1 provides the defects and phenotypes corresponding to knock out of NF-κB proteins. While *nfkb1*$^{-/-}$ mice remain viable, which is surprising given p105/p50's ubiquitous presence, *nfkb1*$^{-/-}$ mice are defective in stress response and have impaired innate and adaptive immune functions. *nfkb2*$^{-/-}$ mice also have impaired immune responses, in that they display impaired B- lymphocyte

maturation and abnormal T-cell function (Gerondakis et al., 2006). *rela*$^{-/-}$ mice are embryonically lethal and are also sensitive to TNFα induced cell death, strongly illustrating RelA's survival function (Beg and Baltimore, 1996; Beg et al., 1995). *relb*$^{-/-}$ mice develop hematopoietic abnormalities given that RelB is highly expressed in the thymus and lymph nodes. The impairment in B-cell survival and proliferation is the primary defect in *crel*$^{-/-}$ mice, which is indicative of c-rel's importance in immune function (Gerondakis et al., 2006). Since c-rel is predominately expressed in hematopoietic cells, such as lymphocytes, c-rel is essential for the normal function of proper functioning of B- and T- cells, macrophages, and dendritic cells (Courtois and Gilmore, 2006).

Since NF-κB is vital for a variety of cellular processes, its mis-regulation can lead to a host of diseases. Table 1.2 provides a list of mutations in NF-κB proteins, which have been shown to play a central role in many diseases. Mutation in the promoter regions of *nfkb1* can result in ulcerative colitis and oral carcinoma. The human *crel* gene is the most common target for somatic cell genetic ablation among all NF-κB family members and NF-κB signaling components (Courtois and Gilmore, 2006). The *crel* gene is typically amplified in many types of B cell lymphoma (Gilmore et al., 2004). It is thought that increased gene

copy number of *crel* leads to over-expression of the c-rel protein, which then overwhelms the IκB inhibitory system. This results in the chronic and oncogenic activation of c-rel target genes (Gilmore et al., 2001).

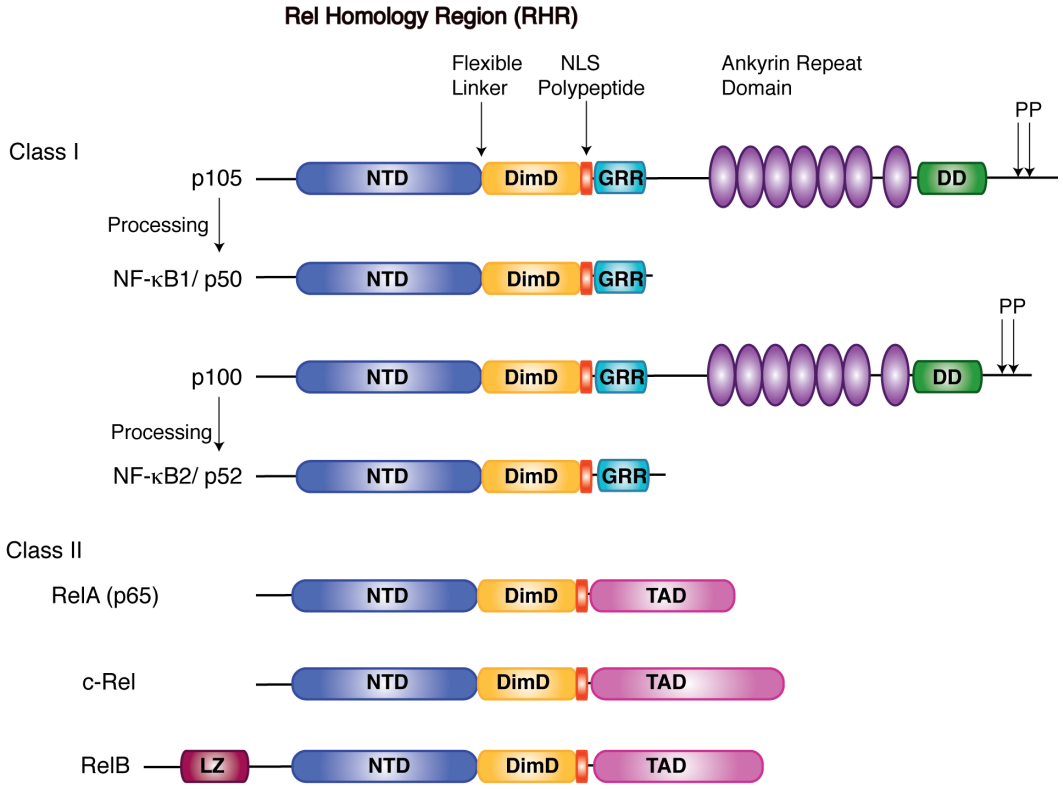

Figure 1.5: Domain organization of NF-κB Class I and II molecules

NF-κB proteins are grouped into either Class I or II depending on the absence or presence of the transactivation domain (TAD), respectively. The Rel homology domain (RHD) consists of the N- terminal domain (NTD), the Dimerization domain (DimD), and the nuclear localization signal (NLS). For p105 and p100, a glycine rich region (GRR) immediately follows the end of the RHR, and the site of processing is thought to occur shortly after the end of the GRR. P donates phosphorylation sites, and LZ denotes leucine zipper domain. This figure was adapted from (Huxford et al., 1999).

Table 1.1: Knockout Phenotypes for NF-κB Transcription Factors

Genotype	Lethality	Defect/ Phenotype
nfkb1$^{-/-}$	No	B cells: marginal zone and CD5+ peritoneal B cells reduced, response to LPS diminished, impaired humoral immune response NK cells: enhanced proliferation and increased IFNγ production Macrophages: impaired ERK mitogen-activated protein kinase signaling in response to TLR signals
nfkb2$^{-/-}$	No	B cells: impaired development Dendritic cells: enhanced function Defective secondary lymphoid development
rela$^{-/-}$	Yes	Defective in leukocyte recruitment and T-cell dependent responses Impaired secondary lymphoid organ development TNFα induced cell death in hepatocytes, macrophages, and fibroblasts
relb$^{-/-}$	No	T cells: reduced proliferation and survival of CD4+ or CD8+, impaired Th1 differentiation Dendritic cells: lack of certain populations and functional defects Defects in secondary lymphoid organ structure and germinal center formation
crel$^{-/-}$	No	B cells: cell-cycle and survival defects T cells: defects in CD4 and CD8 T- cell responses Neuronal survival defects

Adapted from (Gerondakis et al., 2006)

Table 1.2: NF-κB mutations and human diseases

Gene	Type of mutation	Disease
nfkb1	Mutation in promoter	Ulcerative colitis and Oral carcinoma
crel	Gene amplification	Hodgkin's Lymphoma, Diffuse large B-cell lymphoma, Follicular lymphoma

Adapted from (Courtois and Gilmore, 2006)

1.7.2 The IκB Family

NF-κB is regulated on many levels, from protein synthesis to post-translational modifications. However, its central regulators are the IκB family of proteins. Primarily cytoplasmic IκBs consist of IκBα, IκBβ, IκBε, also known as classical IκBs, and p105 and p100, also known as non-classical IκBs (Fig 1.6). Both of these groups of proteins inhibit NF-κB activity (Huxford et al., 1999; Savinova et al., 2009). Primarily nuclear IκBs consist of Bcl-3, IκBζ, and IκB-NS (Fig 1.6), where they act as co-activators of p50 and p52 containing dimers, or, as in the case of Bcl-3, act as de-repressors of transcription, in which Bcl-3 removes transcriptionally repressive p50 homodimers from DNA (Mankan et al., 2009; Michel et al., 2001). Each IκB is known to have different affinities for different NF-κB dimers. For example, both IκBα and IκBβ predominately associate with RelA/p50 and p50/c-Rel heterodimers (Mankan et al., 2009), while Bcl-3 is known to associate with p50 and p52 homodimers (Franzoso et al., 1992). p105 and p100 inhibitory complexes can bind to and accommodate all NF-κB proteins (p50, RelA, RelB, c-Rel, p52), and thus form large oligomeric complexes (~600kDa), while classical IκBs are smaller and contain stochiometric ratios between NF-κB and IκBs (Savinova et al., 2009). Structural studies

of classical IκBα or IκBβ with RelA: p50 heterodimer or RelA:RelA homodimer, respectively, reveals that IκB makes multiple contacts with the NF-κB dimers, and masks NF-κB's NLS as well as interferes with NF-κB's DNA binding region (Huxford et al., 1998; Jacobs and Harrison, 1998; Malek et al., 2003).

All IκB's share a common domain, called the Ankyrin Repeat Domain (ARD), which contains 6 to 7 ankyrin repeats, each of which are 30 aa long (Fig 1.6). The ARD makes extensive contacts with NF-κB bound dimers, demonstrating that the ARD is an essential component of the IκB molecule. IκBα and IκBβ are the only IκBs to contain a C-terminal PEST domain (Huxford et al., 1999; Michel et al., 2001). PEST domains are defined as polypeptide regions enriched in proline (P), glutamic acid (E), serine (S), and threonine (T), and are flanked by positively charged residues, which are disallowed within the PEST sequence (Rechsteiner and Rogers, 1996). Generally, the PEST domain serves as a proteolytic signal (Rogers et al., 1986), although not entirely in the case of IκBα (Mathes et al., 2008). Bcl-3 contains another ankyin repeat in place of the PEST domain (Michel et al., 2001). Most IκBs also contain a signal responsive element (SRD), which contains both phosphorylation and ubiquitination sites for signal responsive

degradation. Post-translational modification of this region frees NF-κB to bind to DNA. The actual sites for IKK phosphorylation and ubiquitination are conserved in all 3 classical IκB's (O'Dea and Hoffmann, 2009).

The C terminal portions of p105 and p100 are called IκBγ and IκBδ, respectively. The site of processing in p105 and p100 to produce p50 and p52, respectively, occurs some residues following the GRR (Bakkar and Guttridge, 2010; Moorthy et al., 2006). p105 and p100 also contain an additional domain called the death domain, which is generally thought to facilitate interactions with death inducing proteins. The DD of p100 has been thought to interact with other death receptor molecules, such as FasL and TNF Receptor, to induce cell death (Hacker and Karin, 2002; Wang et al., 2002). Interestingly, the DD of p105 has been reported to have an additional role, in which it acts as a docking site for the IκB kinase, IKK. This interaction is required for the signal induced IKK dependent phosphorylation of p105 on its SRE, which results then in the degradation of p105 (Beinke et al., 2002).

Table 1.3 summarizes common defects and phenotypes associated with knock- out of classical IκB molecules. For example, *ikba*$^{-/-}$ mice die within 7-10 days after birth due to severe wide spread

inflammatory dermatitis and an amplified granulocytic compartment. Unlike the *ikba*$^{-/-}$ mice, *ikbe*$^{-/-}$ mice remain viable and display only subtle immune system defects. This suggests that aside from IκBα, all other IκBs are functionally redundant in lymphoid cells (Gerondakis et al., 2006). Additionally, knock out of IκBε results in the up-regulation of both IκBα and IκBβ further implying that IκB's functionally compensate for each other (Mankan et al., 2009).

Table 1.4 summarizes disease mutations associated with NF-κB signaling. In humans, patients with EDA-ID (Anhidrotic ectodermal dysplasia with immunodeficiency) and impaired T cell proliferation have an inherited heterozygous missense mutation in *ikba*, in which phosphorylation on Ser 32 by IKK is abolished. HL cells, which are cells from a common B-cell lymphoma, are known to contain several types of mutations in *ikba*, all of which induce a loss of function in IκBα (Courtois and Gilmore, 2006). This results in the constitutive activation of NF-κB and up-regulation of NF-κB pro-survival and growth promoting genes (Hinz et al., 2001). Gene rearrangements can lead to the over-expression of NF-κB co-activator, Bcl-3, which contributes to human B-cell malignancies (Courtois and Gilmore, 2006).

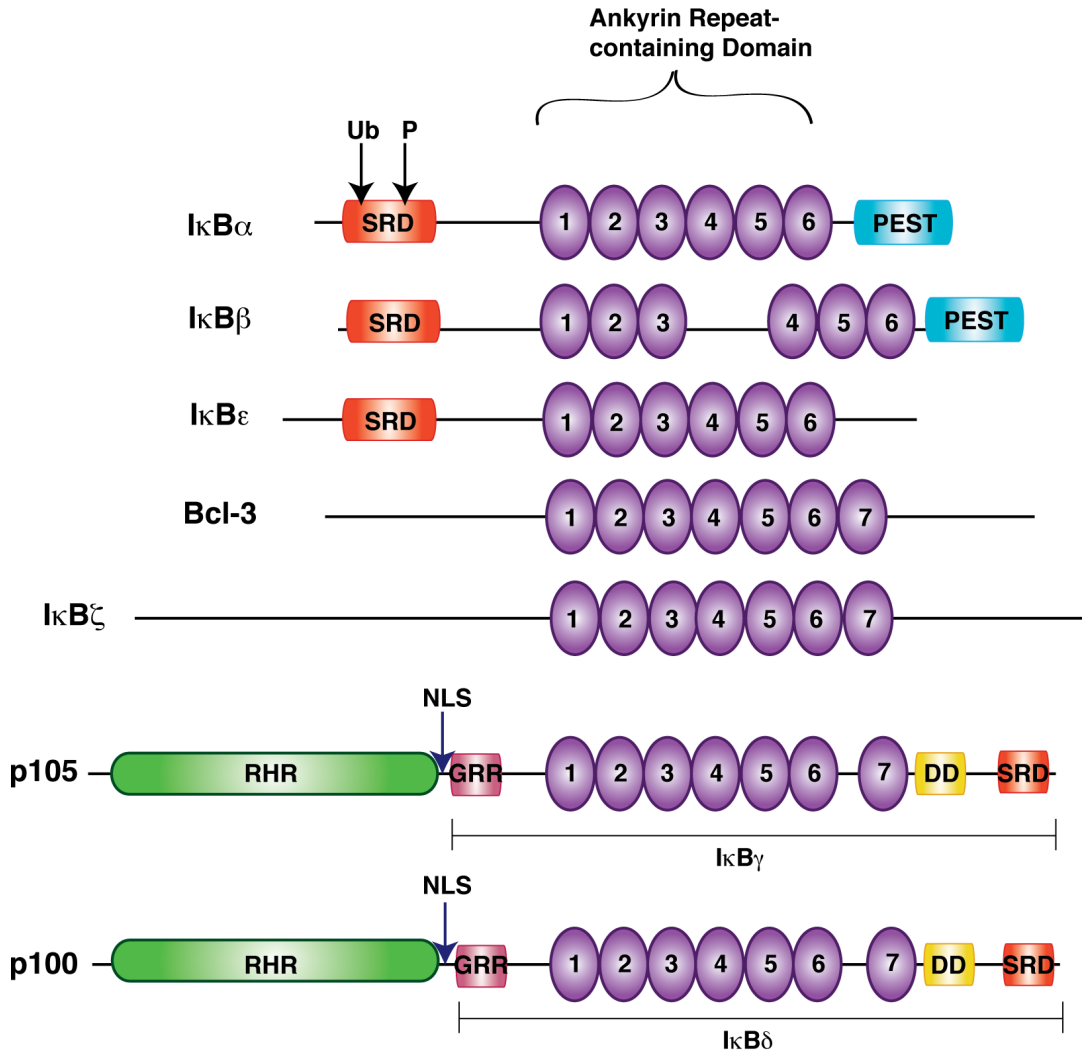

Figure 1.6: Domain organization of IκBs

All IκB's contain an Ankyrin Repeat Domain (ARD). Both classical IκBs (IκBα, IκBβ, IκBε) and non-classical IκBs (p105, p100) contain a Signal Response Domain (SRD). IκBα and IκBβ also contain a Pro, Glu, Ser, Thr rich region called the PEST domain. p105 and p100 can be processed into p50 and p52, respectively, and the C-terminal portions are called IκBγ and IκBδ, respectively. In addition to the SRD and ARD, these C-terminal portions also include the glycine rich region (GRR) and Death Domain (DD). Nuclear IκBs include Bcl-3 and IκBζ. This figure is adapted from (Bakkar and Guttridge, 2010).

Table 1.3: Knockout Phenotypes for IκB molecules

Genotype	Lethality	Defect/ Phenotype
ikba$^{-/-}$	Yes, 7-10 days after birth	B cells: enhanced proliferation T cells: reduced proliferation Severe inflammatory dermatitis
ikbe$^{-/-}$	No	Increased expression of certain Ig isotypes and cytokines
bcl3$^{-/-}$	No	T cells: defective Th1 and Th2 differentiation Disrupted splenic architecture

Adapted from (Gerondakis et al., 2006)

Table 1.4: IκB mutations and human disease

Gene	Type of mutation	Disease
ikba	Susceptibility to polymorphisms	Multiple myeloma
ikba	Inherited gene mutation	Anhidrotic ectodermal dysplasia with immunodeficiency, plus impaired T-cell proliferation
bcl3	Inherited gene mutation	Nonsyndromic cleft lip

Adapted from (Courtois and Gilmore, 2006)

1.7.3 NF-κB Activation Pathways

In unstimulated cells, NF-κB dimers generally exists in a latent form, due to their interaction with IκBs, which prevents nuclear localization and DNA binding (Baeuerle and Baltimore, 1988; Baldwin, 1996; Karin and Ben-Neriah, 2000; Sen and Baltimore, 1986). NF-κB can be activated through several different pathways (Fig 1.7). NF- κB can be activated via the "classical" or "canonical" activation pathway upon binding of inflammatory cytokines (TNFα, IL-1β) or pathogen derived substrates (lipopolysacccharide (LPS)) to their cognate receptors (Mankan et al., 2009). This results in the activation of the IκB kinase complex, IKK, which consists of 2 catalytic subunits, IKKα and IKKβ, and the scaffolding protein, NEMO (NF-κB essential modifier or IKKγ). Once activated, IKKβ phosphorylates the IκB bound NF-κB (Karin and Ben-Neriah, 2000; Sen and Baltimore, 1986). In general, the canonical pathway involves the classical IκBs, most commonly IκBα. IκBα is phosphorylated on Ser32 and Ser36, which then results in its K48-linked ubiquitination on Lys21 and 22 by the E3 ubiquitin ligase, β-TrCp. This serves as a degradation signal for its degradation by the 26S proteasome, which then frees NF-κB, most commonly RelA:p50 heterodimer, to translocate to the nucleus and bind to DNA (Gilmore,

2006).

The "non-canonical" or "alternative" pathway involves the activation of p100/RelB complexes during B- and T-cell development. This pathway is only activated in the cases of stimulation with Lymphotoxin B (LTβ), CD40 Ligand (CD40L), and B-cell activating factor (BAFF), which then results in the activation of NF-κB inducing kinase, NIK. Activated NIK phosphorylates the IKK complex, which consists of only two IKKα molecules, on their activation loops. The activated IKK complex then phosphorylates p100 in its SRD, which signals for and causes the partial degradation of the C-terminal portion of p100, thus producing the processed product, p52, and liberation of the p52: RelB heterodimer (Hacker and Karin, 2002; Sun and Ley, 2008).

The processing of p105 to p50 is also another NF-κB activation pathway, and is different than p100 processing because it occurs in a constitutive manner (Beinke et al., 2002). The 20S proteasome is thought to be responsible for p105 processing, in that it endoproteolytically cleaves p105 and selectively degrades the C-terminus of p105 in a ubiquitin independent manner, thus producing p50. This processing event occurs only in fully synthesized p105 molecules and requires the

GRR domain of p105 (Moorthy et al., 2006). The production of a p50: p50 homodimer could serve to activate transcription upon binding of nuclear IκBs, Bcl-3 or IκBζ (Mankan et al., 2009; Michel et al., 2001). In response to certain stimuli (TNFα, LPS), phosphorylation by an IKK complex, containing IKKα, IKKβ, and NEMO, induces the complete degradation of p105, which could also release p50 associated with other Rel containing NF-κB molecules into the nucleus to activate transcription (Gilmore, 2006; Sun and Ley, 2008).

Classical IκBs (α/β/ε) and non-classical IκBs (p105 and p100) are all NF-κB target genes, which provides a negative feedback mechanism (Basak et al., 2007; Hoffmann et al., 2006; Kearns et al., 2006). For example, upon stimulation with TNFα, NF-κB is activated via the canonical activation pathway, which results in the degradation of IκBα bound NF-κB. Upon translocation to the nucleus, NF-κB induces the expression of many genes, including IκBα, which can then bind and inhibit NF-κB. This prevents aberrant NF-κB activity (Werner et al., 2005). Each IκB protein has different rates of degradation and re-synthesis in response to a stimulus, which is critical for the temporal responsiveness of NF-κB signaling (Hoffmann et al., 2006).

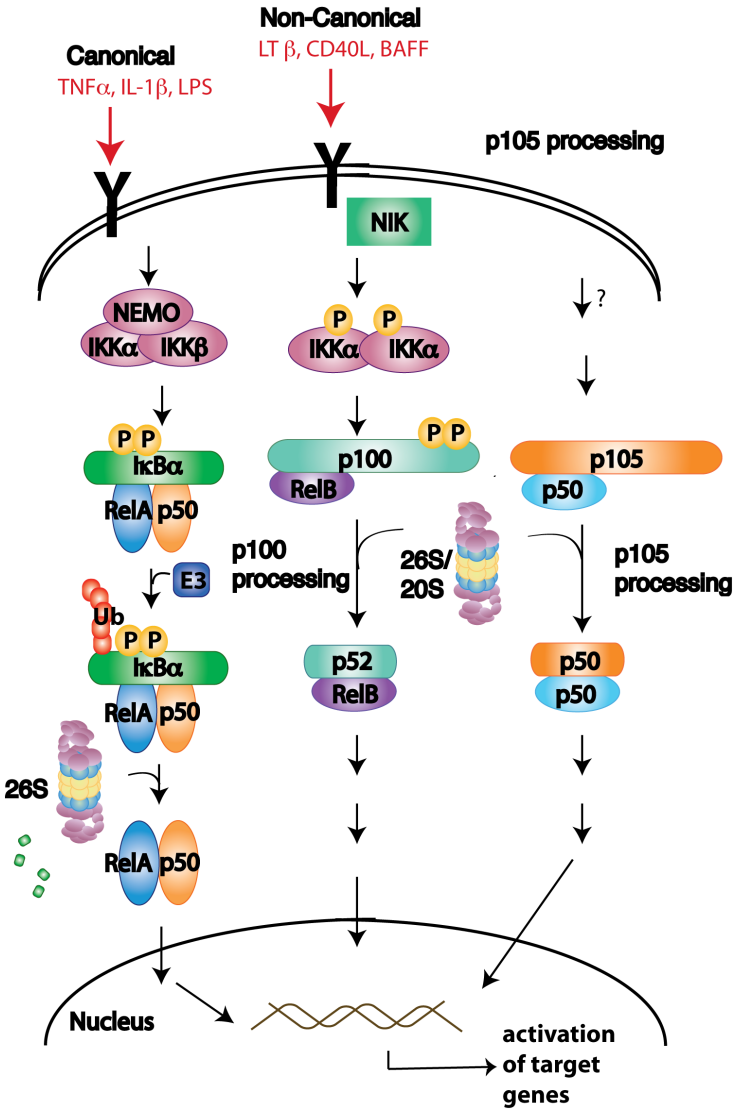

Figure 1.7: Different pathways of NF-κB activation

The canonical NF-κB activation pathway involves stimulation by TNFα, IL-1β, or LPS, which then activates an IKK complex composed of IKKα, IKKβ, and NEMO. This then results in the degradation of NF-κB bound IκB, which is most commonly IκBα. While the canonical pathway generally involves classical IκB molecules, the non-canonical pathway involves the processing of non-classical IκB molecule, p100. This pathway is activated by a different set of stimuli (LTβ, CD40L, BAFF), and involves an IKK complex composed of two IKKα molecules. p105 processing differs from p100 processing in that p105 processing occurs in a constitutive manner. The 20S proteasome carries out p105 processing. This figure is adapted from (Gilmore, 2006).

1.7.4 ROS and NF-κB

NF-κB was the first protein shown to be redox regulated, where direct addition of H_2O_2 was shown to activate NF-κB in Jurkat cells (Schreck et al., 1991). Later studies demonstrate that NF-κB activation in response to H_2O_2 is cell type dependent. Additionally, even in cases where NF-κB activation is seen, NF-κB can be activated via several different pathways, depending on the cell type (Oliveira-Marques et al., 2009). For example, in murine T lypmphocytes cells, NF-κB bound IκBα is phosphorylated on Tyr42, which results in the degradation of IκBα in a proteasome independent manner (Schoonbroodt et al., 2000). However, in HeLa cells, H_2O_2 activates Src, which then activates both Abl and PKCδ. Activated Abl and PKCδ phosphorylate and activate PKD. PKD then activates the IKK complex, which results in the canonical activation of NF-κB (Storz et al., 2004; Storz and Toker, 2003).

Perhaps the most well characterized role of ROS in NF-κB signaling is the role of ROS in mediating crosstalk between the NF-κB and JNK signal transduction pathways (Figure 1.8). Stimulation of cells with TNFα results in activation of the MAP Kinase signaling cascade and subsequent JNK activation (Gloire et al., 2006b). While JNK activation is

usually down-regulated by MKPs (MAP Kinase Phosphatases), the binding of TNFα to TNF Receptor also produces ROS, which inactivates the active site cysteine residue of MKPs. In cells lacking RelA, this then results in the prolonged activation of JNK, which induces cell death (Kamata et al., 2005). However, cell death is always averted in cells containing RelA, because RelA containing homo- or hetero-dimers are also activated upon stimulation with TNFα. NF-κB then up-regulates the production of pro-survival protein and anti-oxidant enzymes. The anti-oxidant enzymes, such as Mn-SOD, then decrease the intracellular amount of ROS, which results in the activation of MKPs, down-regulation of JNK signaling, and cell survival (Papa et al., 2006).

While ROS are known to induce the translocation of NF-κB to the nucleus, nuclear binding and gene expression also undergoes redox regulation (Gloire and Piette, 2009). For example, chromatin remodeling has been shown to be enhanced by ROS. ROS produced by cigarette smoke induced phosphorylation, nitration, and carbonylation on HDACs (Histone Deaceylase), which results in the ubiquitination and degradation of HDACs. Since HDAC activity results in DNA compaction and inhibition of transcription, degradation of HDACs leads to uncontrolled transcription of pro-inflammatory genes

(Rajendrasozhan et al., 2008). Additionally, transcription factors often contain critical cysteine residues on their DNA binding domains, such that the DNA binding of transcription factors is redox regulated. While oxidation of the cytoplasm enhances NF-κB translocation to the nucleus, NF-κB requires reducing conditions to bind to DNA (Gloire and Piette, 2009). For example, Cys62 of p50 is oxidized in the cytoplasm, but upon translocation to the nucleus, is rapidly reduced to allow for DNA binding (Nishi et al., 2002).

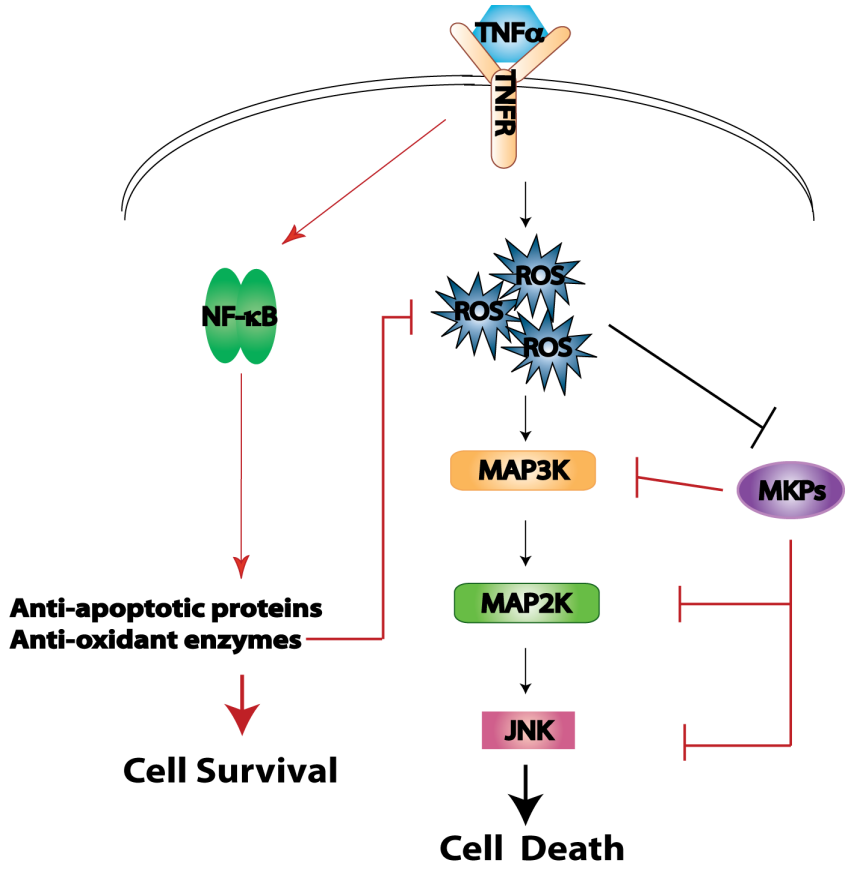

Figure 1.8: ROS mediates crosstalk between NF-κB and JNK signaling pathways

Binding of TNFα to its cognate receptor, TNFR, can induce ROS production. In the absence of NF-κB, this leads to the inactivation of MAP Kinase Phosphatases (MKPs) and thus sustained JNK activation and cell death (black arrows/ lines). However, when NF-κB is present, it is also activated in response to TNFα stimulation. This in turn induces expression of both anti-apoptotic proteins and anti-oxidant enzymes. The anti-oxidant enzymes decrease the level of intracellular ROS, which then results in the activation of MKPs and down-regulation of JNK signaling, and cell survival (red arrows/ lines).

1.8 Focus of Study

NF-κB is a pleiotropic transcription factor, which is present in almost all cell types, and is instrumental in regulating diverse processes such as inflammation, cell growth, and cell survival/death. To fully understand the functional aspects of NF-κB, it is essential to characterize both NF-κB signaling as well as the regulation of NF-κB. Therefore, my work is focused on characterizing the NF-κB signaling response to cellular stress and examining the proteasomal system in involved in regulating NF-κB activity. While NF-κB's pro-survival role has been extensively characterized, the precise mechanism of its pro-cell death role remains elusive. Thus, one area of this study is to characterize and determine the mechanism of NF-κB's response to hydrogen peroxide induced fibroblast cell death. The other area of study focuses on identifying and characterizing the degradation system, which carries out the ubiquitin- independent turn-over of NF-κB inhibitor molecules, IκBγ and IκBα.

Chapter 2: NF-κB Potentiates Caspase Independent Hydrogen Peroxide Induced Cell Death

2.1 Introduction

Mammalian cells are constantly exposed to reactive oxygen species (ROS), such as hydrogen peroxide (H_2O_2). Exogenous ROS arise from irradiation (UV, X-ray, γ-ray) and atmospheric pollutants, while endogenous ROS are mainly produced by the incomplete reduction of oxygen by cytochrome c during cellular respiration (Cadenas, 1989). However, when the antioxidant capabilities of the cell are overwhelmed by ROS, a state of oxidative stress ensues, which can result in damage to DNA, proteins, and lipids (Valko et al., 2006). Moreover, high and/or persistent levels of ROS result in aberrant cell death, which leads to aging and neurodegenerative disorders (Behl and Moosmann, 2002; Trachootham et al., 2008). In particular, ROS induced fibroblast cell death can cause chronic obstructive pulmonary disease (Carnevali et al., 2003; Nakamura et al., 1995) as well as inadequate wound healing following myocardial infarction/reperfusion (Takahashi et al., 2002; Xiao et al., 2010). ROS induces cell death by modulating cell signaling pathways. A prominent signaling pathway involved in mediating the cell survival/cell death fate is the nuclear factor-kB (NF-κB) pathway (Trachootham et al., 2008).

NF-κB is a family of transcription factors, which are comprised of five family members: RelA/ p65, RelB, c-rel, nfkb1/p50, and nfkb2/p52, that form homo- or hetero-dimers in a combinatorial manner. In resting cells, the NF-κB dimers are retained in the cytoplasm by forming stable complexes with NF-κB inhifbitor molecules, IκB (α/β/ε). In the canonical activation pathway, stimulation with an extracellular stimulus, such as tumor necrosis factor α (TNFα), a pro-inflammatory cytokine, leads to phosphorylation of IκBα on serines 32 and 36 by IKK, the IκB kinase. This results in the ubiquitination of IkBa, which signals for the degradation of IκBα by the 26S proteasome. The freed NF-κB dimers can then translocate to the nucleus and activate transcription of their target genes (Baldwin, 1996; Ghosh et al., 1998; Karin and Ben-Neriah, 2000).

Activation of NF-κB by exogenous H_2O_2 has been found to be highly cell- type dependent, in which NF-κB is activated in a variety of cell lines such as Jurkat T cells and HeLa cells (Schreck et al., 1991; Storz and Toker, 2003), whereas NF-κB activation is inhibited in other cell lines such as murine neutrophils (Zmijewski et al., 2007). In cases where activation of NF-κB occurs, several mechanisms of NF-κB activation have been reported. While canonical activation of NF-κB via IKK-dependent IkBa degradation has been reported, other reports focus on

an atypical mechanism of NF-κB activation in response to stimulation with H_2O_2 (Livolsi et al., 2001; Takada et al., 2003). This atypical mechanism involves an IKK independent mechanism and Tyr42 phosphorylation of IκBα, and only occurs in the absence of SHIP-1 (Gloire et al., 2006a; Gloire et al., 2006b). The pathway of NF-κB activation in other cell lines, such as in mouse embryonic fibroblasts (MEFs), has yet to be delineated.

The anti-cell death role of NF-κB has been extensively characterized. RelA deficient cultured cells undergo apoptotic cell death upon treatment with TNFα due to deficiencies in pro-survival and anti-oxidant gene transcription (Beg and Baltimore, 1996; Papa et al., 2006). RelA deficiency also leads to embryonic lethality accompanied by massive apoptosis in the embryonic liver (Beg et al., 1995). In response to a variety of other stimuli, such as ionizing radiation and chemotherapeutic drugs, RelA also appears to have an anti-apoptotic effect (Barkett and Gilmore, 1999). Finally, NF-κB suppression of apoptosis in cancer cells is a central event in cancer biology, as well as in chemoresistance of tumor cells (Kucharczak et al., 2003). However, there have also been a few scattered reports addressing the pro-cell death function of NF-κB in response to atypical NF-κB activators

(Campbell et al., 2004; Campbell et al., 2006; Ho et al., 2005; Lin et al., 1998; Liu et al., 2006b). Yet, the mechanism by which NF-κB mediates a pro-cell death response remains elusive.

In the present study, we sought to define NF-κB's role in immortalized MEF cell death induced by chronic insult with H_2O_2. Here we present evidence that unremitting exposure to H_2O_2 induces a caspase independent but PARP dependent cell death and that NF-κB potentiates cell death through the DNA binding activity of RelA, which is induced through the canonical activation pathway. Given that NF-κB dependent pro-survival genes, Bcl-2 and XIAP, were significantly repressed, while NF-κB dependent pro-death genes, TNFα and Fas Ligand, were induced in response to H_2O_2, we suggest that NF-κB mediates its pro- cell death function through the repression of pro-survival genes and induction of pro-death genes.

2.2 Materials and Methods

2.2.1 Cell culture, reagents, and antibodies

Immortalized MEF cells were cultured in humidified incubators at 37°C, 5% (v/v) $C0_2$ and were grown in Dulbecco's modified Eagle's medium (DMEM) supplemented with 10% bovine calf serum (BCS) (Invitrogen) and 100 U/ml penicillin–streptomycin–glutamine (1XPSG) (Invitrogen). 293T were grown in a similar manner, but with DMEM supplemented with 10% Fetal Calf Serum (Invitrogen). Cells were stimulated for various periods with TNFα (Roche Biochemicals), glucose oxidase (Sigma Aldrich), or H_2O_2 (Sigma). Cells were labeled with CFSE (5- (and 6-) carboxyfluorescein diacetate, N-succinimidyl ester) (Sigma Aldrich), H_2DCFDA (Invitrogen), or propidium iodide (Sigma). Cells were treated with z-VAD-fmk (caspase inhibitor VI) and DPQ (Parp Inhibitor III), which were both purchased from Calbiochem. Antibodies against IκBα (sc371), IKKα (sc7184), RelA (sc372), and αtubulin (sc5286) were purchased from Santa Cruz Biotechnology. Antibodies against IKKγ (#559675), pro-caspase 3 (#611048), active caspase 3 (#559565), PARP1 (#556362), and PAR (#551813) were purchased from BD

Pharmingen. [γ-32P] ATP (3000Ci/mmol) was purchased from MP Biomedicals.

2.2.2 Generation of oxidative stress

A concentrated stock of glucose oxidase (GO) solution (40 U/ml) dissolved in 50mM sodium acetate pH 5.1 was stored at -80°C. A fresh aliquot was used for every experiment. Cells were first grown to 95-98% confluency and the media was then removed. Glucose oxidase was diluted to 25 mU/ml with fresh media supplemented with 10% BCS and PSG. This mixture was then added to the cells, and incubated in the humidified incubators at 37°C, 5% (v/v) $C0_2$ for the indicated periods of time.

2.2.3 Measurement of ROS production

Measurement of intracellular ROS production was carried out as described in (Hayakawa et al., 2003). Briefly, after media was replaced with 1xDPBS, cells were incubated with 10uM DCFH-DA for 30 min. Cells were then extensively washed with 1xDPBS and incubated with 25 mU/ml GO for the indicated period. Cells were then washed again with 1xDPBS and incubated with fixing solution (20% ethanol 0.1% Tween-20)

for 15 min. Cell extract was then centrifuged and the resulting supernatants were collected and fluorescence emission scans were performed with a Fluoromax-P instrument (J. Y. Horiba, Inc.) using an excitation and emission bandpass of 5 nm and excitation of 492nm and emission of 526nm.

2.2.4 Cell Death Assay

MEF cell death was quantified by determining the normalized value of propidium iodide (PI) incorporation.

The normalized value of PI incorporation=$\left(\frac{(FI_{TreatedPI}/FI_{TreartedCFSE})}{(FI_{UntreatedPI}/FI_{UntreatedCFSE})}\right)$,

where FI= fluorescence intensity of PI reading or CFSE reading of either GO treated or untreated samples. In order to account for changes in cell number, cells were labeled with CFSE prior to treatment with GO, where a minimum of $2x10^6$ cells was re-suspended in 1xDPBS (Invitrogen) and labeled for 5min with 5 uM CFSE at room temperature. Following quenching of the reaction with two washes of media containing 10% BCS, the cells were plated such that forty-eight hours after labeling, the cells reached 90- 95% confluency. The cells were then treated with GO, UV, or left untreated) for various periods. After

treatment, each plate was then washed twice with 1XDPBS supplemented with 100mg/ml $CaCl_2$ and 100mg/ml Mg_2Cl_2, followed by the addition of freshly prepared 10 ug/ml of PI, dissolved in 1XDPBS containing $CaCl_2$ and $MgCl_2$. The PI solution was incubated with the plated cells in the dark for 15min at RT and then removed, followed by three washes with 1XPBS containing $CaCl_2$ and $MgCl_2$. To facilitate the removal of adherent cells, Puck's buffer (5.4 mM KCl, 0.14 M NaCl, 4.2 mM $NaHCO_3$, 5.6 mM D-glucose dextrose, 10 mM Hepes, 1 mM EDTA, pH 7.3- 7.4), was then added to the plate and allowed to incubate with the cells in the dark for 15min RT. For UV treated cells, cells floating the media were also collected, treated with PI, and combined with the adherent cells following removal of the adherent cells from the plate. Upon collection of the cells, the fluorescence intensity for PI and CFSE were then taken for each time point with a Fluoromax-P instrument (J. Y. Horiba, Inc.) using an excitation and emission bandpass of 5 nm. PI intensity was measured with an excitation of 535 nm and emission of 617 nm. CFSE intensity was measured with an excitation of 492 nm and emission of 517 nm.

2.2.5 Molecular Biology

IκBα constructs were cloned into the retrovirus vector pBabe-puro between the restriction sites *Eco*RI and *Sal*I. Mutagenesis reactions were performed with the Stratagene Quickchange Mutagenesis kit. The following primers were used to clone the RelA mutant R35AY36A: forward: 5'- CGGGGCATGCGATTCGCCGCAAAATGCGAGGGGCGC-3', reverse: 5'- GCGCCCCTCGCATTTTGCGGCGAATCGCATGCCCCG-3' .

2.2.6 Retroviral transgenic system

293T cells were transiently transfected using Lipofectamine 2000 (Invitrogen) containing 7 ug of the indicated retroviral vector and with 3 ug of pCl-Eco (Imgenex). Serum free DMEM containing the Lipofectamine and DNA mixture was removed 6 hours later and replaced with DMEM supplemented with 10% FBS and 1xPSG. Cells were allowed to grow for 38–42 hours post transfection. The media was then filtered with a 0.45 uM filter and placed onto the *nfkb*$^{-/-}$ cells along with 8 μg/ml polybrene (Sigma). These cells were then grown for another 48 hours before selection with 2.5 μg/ml puromycin (Calbiochem).

2.2.7 Preparation of cytoplasmic and nuclear extracts for electrophoretic mobility shift assays (EMSAs)

Following addition of GO, cells were washed twice with cold phosphate buffered saline (PBS) and then pelleted with PBS +1 mM EDTA. Collected cells were lysed with 100ul cytoplasmic lysis buffer (10 mM Hepes-KOH, pH 7.9, 60 mM KCl, 1 mM EDTA, 0.5% NP-40, 1 mM DTT and 1 mM PMSF) and, following a 2 minute incubation on ice, vortexed to induce complete lysis. The nuclei were then pelleted at 0.5 x g, re-suspended in 30 ul of nuclear extract buffer (250 mM Tris-HCl, pH 7.5, 60 mM KCl, 1 mM EDTA, 1 mM DTT and 1 mM PMSF), and lysed by 3 freeze–thaw cycles. Nuclear lysates were then cleared by 13 k rpm centrifugation for 10min at 4°C. Protein concentrations were normalized by Bradford assay.

2.2.8 Electrophoretic mobility shift assays (EMSAs)

EMSA experiments were carried out as described in (Mathes et al., 2008) using a ^{32}P- labeled oligonucleotide probe (5'-GCTACAA**GGGACTTTCC**GCTG**GGGACTTTCC**AGGGAGG -3'), which corresponds to the κB site of the HIV-1 LTR. This radio-labeled strand was

then bound to its complimentary strand, followed by incubatation with nuclear extract.

2.2.9 Western Blots

Cells were lysed using RIPA buffer (20 mM Tris pH7.5, 200 mM NaCl, 1% Triton-X 100, 2 mM DTT, 5 mM p- nitrophenyl phosphate, 2 mM sodium orthovanadate, 1X protease inhibitor cocktail (sigma)) and normalized by Bradford assay. Whole cell extracts were then resolved by SDS- PAGE gel, followed by semi-dry transfer onto a nitrocellulose membrane (Whatman). The membranes were then blocked with either 0.2% IBlock or 5% BSA, which was dissolved in TBS-Tween buffer (25mM Tris-HCl, pH7.5, 140mM NaCl, 0.1% Tween). Membranes were developed using ECL chemiluminescnece reagent (PerkinElmer) and visualized by film. Quantitation of western blots was performed with ImageQuant TL (Amersham Biosciences).

2.2.10 *In vitro* IKK kinase assay

Kinase assays were carried out as described in (Werner et al., 2005) with some modifications. Briefly, cells were stimulated with TNFα or GO and pelleted in an identical manner in the preparation of EMSA samples. Pelleted cells were then lysed with 100ul cytoplasmic lysis buffer (10 mM Hepes-KOH, pH 7.9, 250 mM NaCl, 1 mM EDTA, 0.5% NP-40, 0.2% Tween 20, 2 mM DTT, 1 mM PMSF, 20 mM β-glycerophosphate, 10 mM NaF and 0.1 mM Na_3VO_4) and normalized by Bradford assay. The cytoplasmic extracts were then incubated with 1ug of IKKγ monoclonal antibody for 2 hrs at 4°C, followed by addition of protein G agarose conjugated beads (Amersham) for one hour at 4°C. The beads were then washed twice with cytoplasmic lysis buffer and once with kinase wash buffer (20 mM Hepes pH 7.7, 100 mM NaCl, 10 mM MgCl2, 2 mM DTT, 1 mM PMSF, 20 mM β-glycerophosphate, 10 mM NaF and 0.1 mM Na_3VO_4). A reaction mixture of kinase buffer, 20 uM adenosine 5'-triphosphate (ATP), 10 mCi [^{32}P] ATP, and 2.0 mg of recombinant GST–IκBα(1–54) substrate was incubated with the beads at 30°C for 30 min. The reaction was quenched with SDS loading buffer and boiling for 5min at 95°C. The reaction was resolved by 10% SDS

PAGE and was visualized by PhosphorImager (Molecular Dynamics) and quantitated by ImageQuant TL.

2.2.11 Quantitative Reverse Transcription PCR (qPCR)

Cells were either untreated or treated with 25 mU/ml GO, where serum free media was used in both cases. Following 4 hours, cells were homogenized using the QIAshredder (QIAGEN). RNA was isolated using the RNeasy kit (QIAGEN) and further purified with DNase I digestion (QIAGEN). By following the manufacturer's directions, cDNA was synthesized from 1ug of RNA using the Superscript III First Strand synthesis kit (Invitrogen) with Oligo$(dT)_{20}$ as primers (Invitrogen). The cDNA was diluted 1:10 following its synthesis. Each qPCR reaction (total volume 10ul) contained the appropriate amount of primers, 2ul of cDNA (occasionally 4ul of cDNA for low expressing genes), and 2x SYBR green (Kapa Biosystems). Product accumulation was monitored by SYBR Green fluorescence with Eppendorf Mastercycler ep *realplex*. The internal control gene marker, GAPDH, was determined not to be affected by 25 mU/ml GO and the primers of genes of interest were verified to be equally efficient as GAPDH, following the directions specified in (Livak and Schmittgen, 2001; Schmittgen and Livak, 2008).

The relative gene expression levels were then determined using the 2^(-DDCT) method. The primers used for the qPCR reaction are presented in Table 2.1. The average, standard deviation, and p value (calculated using the Student's t test) were calculated and plotted using Microsoft Excel.

Table 2.1: Primers used for qPCR analysis

	Forward primer (5'-3')	Reverse primer (5'-3')	Citations
GAPDH	AATGTGTCCGTCGTGGATCT	CATCGAAGGTGGAAGAGTGG	Ghislettie et al, 2009
TNFα	CCAGACCCTCACACTCAGATC	CACTTGGTGGTTTGCTACGAC	Ghislettie et al, 2007
Fas Ligand	ACCCCCACTCAAGGTCCAT	CGAAGTACAACCCAGTTTCGT	PrimerBank ID: 6753818a2
Fas Receptor	AATCGCCTATGGTTGTTGACC	TTGGTATGGTTTCACGACTGG	PrimerBank ID: 6679751a3
Bax	TGAAGACAGGGGCCTTTTTG	AATTCGCCGGAGACACTCG	PrimerBank ID: 6680770a1
XIAP	GCAAGAGCTGGATTTTATGCTT	TGCCCCTTCTCATCCAATAG	Primer 3
Bcl-2	ATGCCTTTGTGGAACTATATGGC	GGTATGCACCCAGAGTGATGC	Wu et al, 2008
Bcl-xL	GACAAGGAGATGCAGGTATTGG	TCCCGTAGAGATCCACAAAAGT	PrimerBank ID: 31981887a1
cIAP-1	TCAGTGACCTCGTTATAGGCTT	TCACACACGTCAAATGTTGGAA	PrimerBank ID: 6680696a2
p53	GCGTAAACGCTTCGAGATGTT	TTTTTATGGCGGGAAGTAGACTG	PrimerBank ID: 6755881a1

The following primer sequences are provided (in 5' to 3' fashion) for the genes analyzed by qPCR. Primers obtained from the Primer Bank (Spandidos et al., 2008; Spandidos et al., 2010; Wang and Seed, 2003)are given with the PrimerBank ID. Primers obtained from various papers are also indicated in the citation field (Ghisletti et al., 2009; Ghisletti et al., 2007; Wu and Miyamoto, 2008). Primers designed using Primer3 software are denoted as Primer 3 in the citation field.

2.3 Results

2.3.1 H_2O_2 is being continuously produced via GO

In chronic obstructive pulmonary disease and inadequate wound healing following myocardial infarction/reperfusion, chronic insult of ROS to fibroblast cells can lead to aberrant cell death (Carnevali et al., 2003; Takahashi et al., 2002; Xiao et al., 2010). We attempted to simulate this condition by generating persistent oxidative stress in immortalized MEFs with glucose oxidase (GO). It has been shown that addition of GO to the media produces continuous levels of intracellular H_2O_2, as opposed a bolus addition of H_2O_2 (de Oliveira-Marques et al., 2007), which we were also able to verify (J.Ho, data not shown). Intracellular ROS generation was verified by staining with DCFH-DA, a commonly used membrane permeable dye that fluoresces upon its oxidation to DCF by intracellular ROS (Hayakawa et al., 2003). Accordingly, ROS was produced in MEFs throughout the duration of treatment with 25 mU/ml GO (Fig 2.1). To roughly estimate the amount of intracellular H_2O_2 that GO was producing, known concentrations of H_2O_2 were also added in a bolus fashion to the cells and the intensity of fluorescence monitored. Based on the H_2O_2 standard curve, we estimated that, within the first 3 hrs of treatment with 25 mU/ml GO, less

than 50 mM of H_2O_2 was being produced, and following 3 hrs, roughly 50-100 mM of H_2O_2 was produced (Fig 2.1).

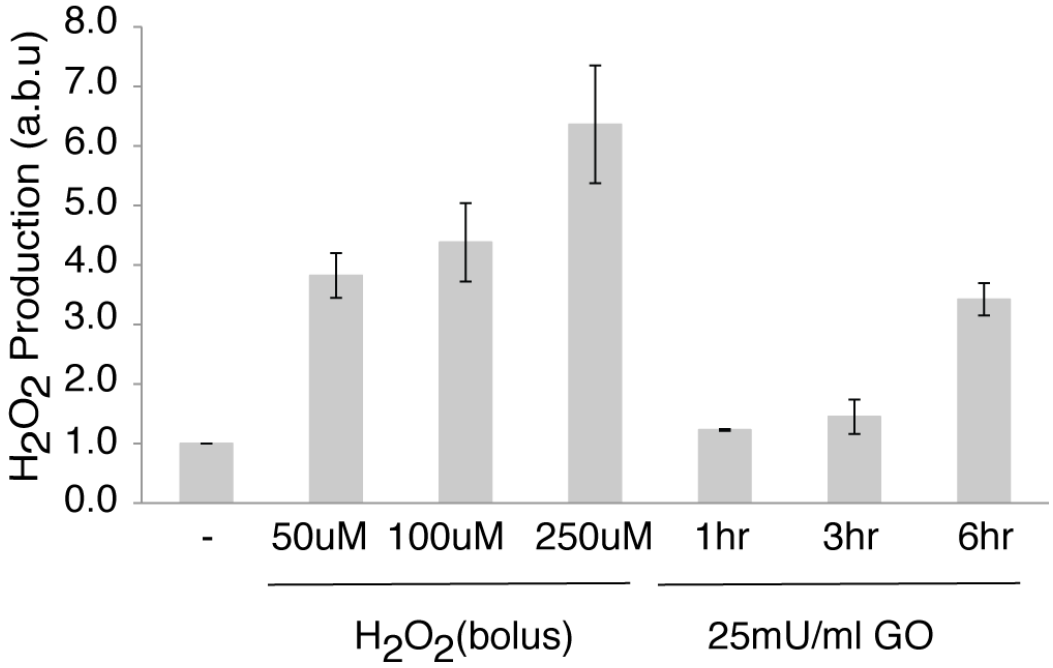

Figure 2.1: Intracellular H_2O_2 is continuously being produced in MEFs using gluocose oxidase (GO)

Wild type (wt) MEFs were either untreated (-) or treated with 25 mU/ml GO for the indicated periods of time. H_2O_2 readings for the H_2O_2 standard curve were taken 10 min after addition. All H_2O_2 levels are shown as normalized to untreated samples and are given in arbitrary units (a.b.u).

2.3.2 Chronic H_2O_2 insult induces a caspase independent but PARP dependent fibroblast cell death

We next determined the effect of prolonged H_2O_2 exposure (via 25 mU/ml GO) on MEFs. Significant cell death occurred within 5 hrs after GO treatment, as quantitated by the increase in propidium iodide (PI) incorporation, which correlates to a loss in membrane integrity. PI incorporation increased even further 6 hrs following treatment (Fig 2.2A). Since an increase in oxidative stress can switch the cell death mode from a caspase dependent to a caspase independent cell death mode (Gardner et al., 1997), we set out to determine whether GO generated H_2O_2 involved caspases. Treatment with irreversible general caspase inhibitor, z-VAD-fmk, was unable to prevent cell death. In agreement with these results, immunoblots against the cleaved form of caspase 3, one of the main executioners of apoptosis, revealed that cleaved caspase 3 is not present during treatment with GO (Fig 2.2B). This is in contrast to UV induced MEF cell death, where caspases mediate cell death, as seen by the inhibition of cell death upon treatment with zVAD-fmk and by the production of the active form of caspase 3 (Fig 2.2A-B).

Caspase independent MEF cell death induced by high levels of H_2O_2 occurs in a Poly(ADP-ribose) polymerase (PARP) dependent manner (Yu et al., 2002), which we were also able to confirm (Fig 2.3B). PARP, a nuclear enzyme involved in the DNA damage response and cell death, becomes activated in response to DNA damage and attaches ADP-ribose units (PAR polymer) to itself and nuclear proteins (Kraus and Lis, 2003). We next sought to evaluate the contribution of PARP in H_2O_2 induced caspase independent cell death. Upon GO addition, cells pretreated with PARP inhibitor, DPQ, showed significant resistance to membrane permeabilization, as opposed to cells treated without DPQ (Fig 2.3A). Given that PARP protein levels remained constant while PAR formation increased as verified by western blot against PARP and PAR, we concluded that PARP was activated within 15 min of stimulation with GO. PAR formation was then eliminated upon addition of DPQ (Fig 2.3B). Thus, treatment of MEFs with GO results in a caspase independent but PARP dependent cell death.

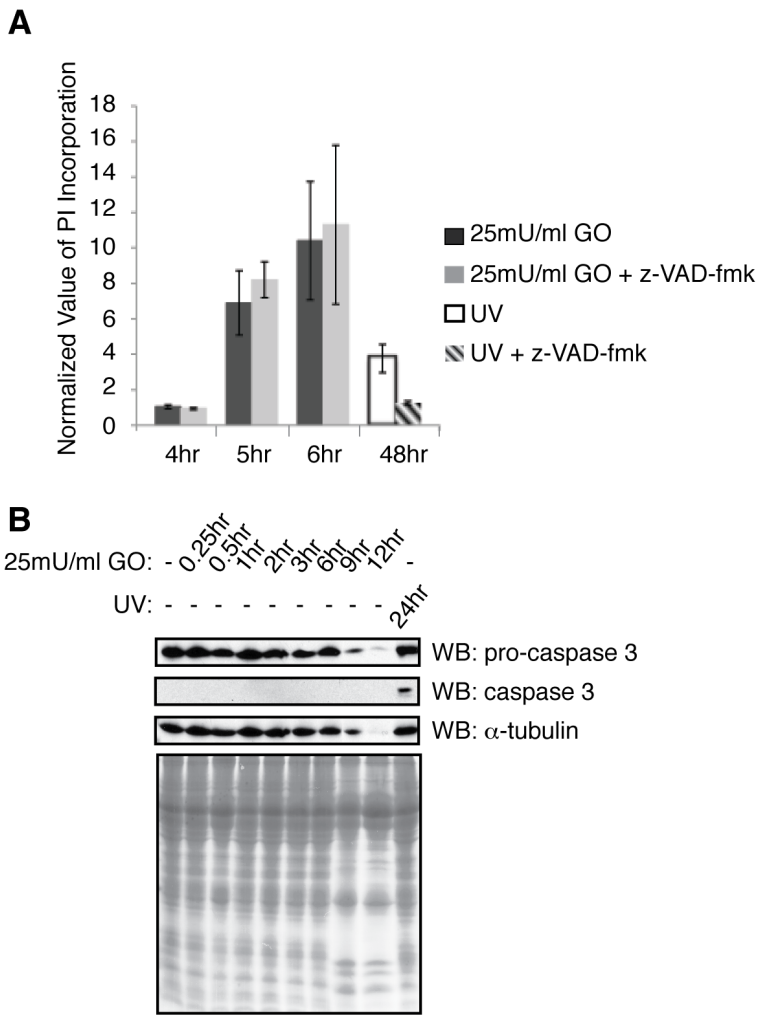

Figure 2.2: Continuous H_2O_2 exposure (via GO) to fibroblasts induces a caspase independent cell death

(A) Following pretreatment for 1 hr in the presence of 100 mM z-VAD-fmk or DMSO, MEFs were subsequently treated with 25 mU/ml GO or 200 J/m^2 UV and cell death was analyzed at the indicated time points. **(B)** Cell lysate was analyzed by western blotting against pro-caspase3, caspase3, and α-tubulin. The cell lysates were also stained by Coomassie Brilliant Blue to demonstrate equal loading. z-Vad-fmk was kept in the media following GO or UV stimulation. Cell death was determined as the normalized value of propidium iodide incorporation (see Methods). All results are presented as the average of triplicate experiments. Error bars signify ±s.e.m (standard error of mean).

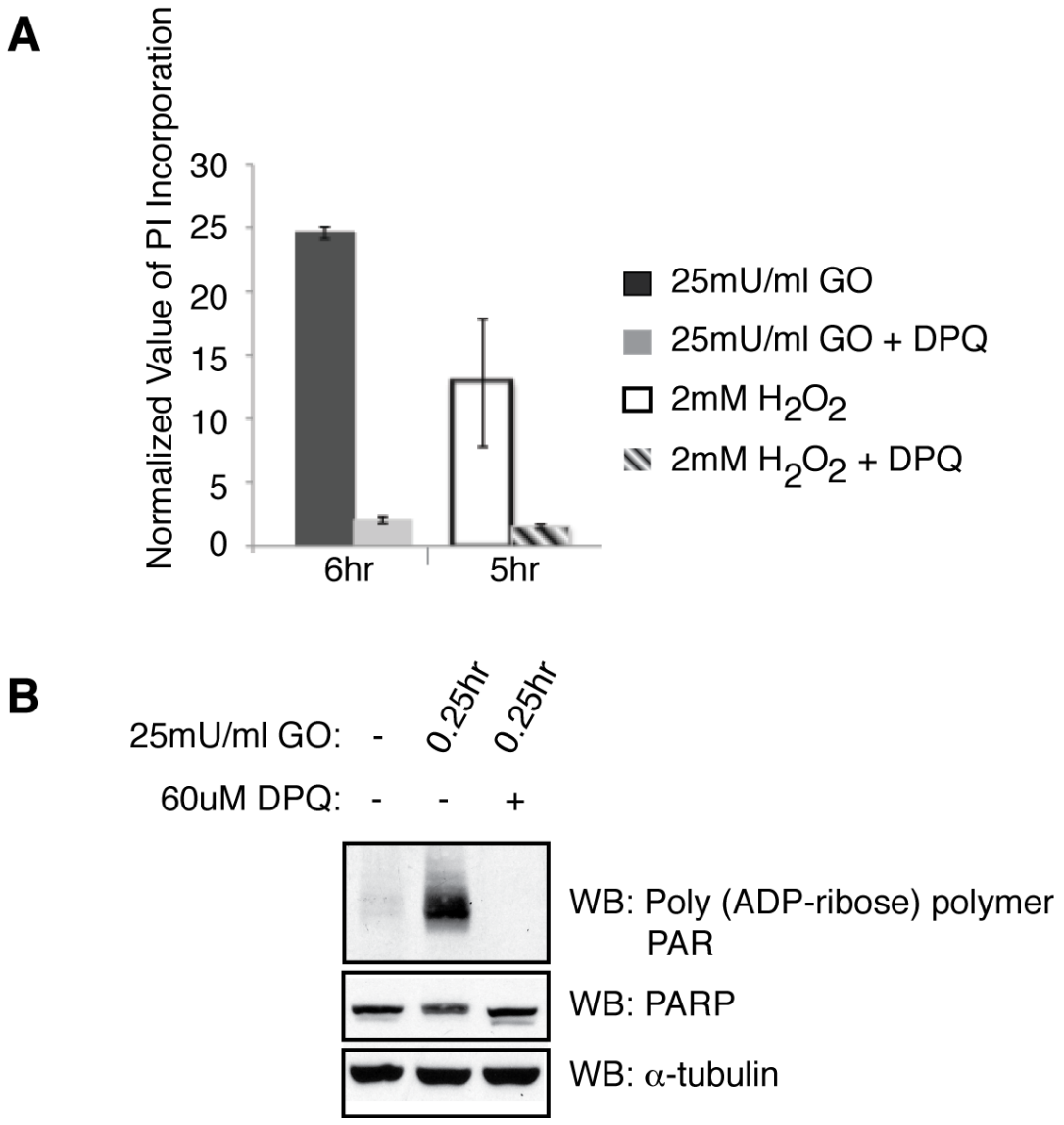

Figure 2.3: Continuous H_2O_2 exposure (via GO) to fibroblasts induces a Parp dependent cell death

(A) Following pretreatment for 1 hr in the presence of 60 mM of DPQ or DMSO, MEFs were subsequently treated with 25 mU/ml GO or 2 mM H_2O_2 and cell death was analyzed at the indicated time points. **(B)** Cell lysate was analyzed by western blotting against PAR (poly (ADP-ribose) polymer), PARP, and α-tubulin. DPQ was kept in the media following GO stimulation. All results are presented as the average of triplicate experiments. Error bars signify ±s.e.m (standard error of mean).

2.3.4 NF-κB potentiates H_2O_2 induced cell death

There have been extensive reports illustrating cooperativity between PARP and NF-κB. In response to DNA damaging agents such as ATM and ionizing radiation, PARP-1 has been shown to be an essential upstream mediator of NF-κB activation (Stilmann et al., 2009; Veuger et al., 2009). PARP-1 can also act as a direct co-activator of NF-κB (Hassa et al., 2001). Since we have shown that chronic insult with H_2O_2 induces a PARP dependent cell death, we next wanted to determine whether NF-κB also plays any role in H_2O_2 induced cell death. To examine this, we compared rates of cell death in wt and *nfkb*$^{-/-}$ (*nfkb1*$^{-/-}$*rela*$^{-/-}$*crel*$^{-/-}$) MEFs treated with 25 mU/ml GO. Although we expected that cell death would be enhanced in the absence of NF-κB due to its well established pro-survival activity, we found, to our surprise, that MEFs which lacked p50, RelA and c-Rel were more resistant to H_2O_2 induced cell death than wt cells (Fig 2.4A).

To directly address the involvement of NF-κB in the delay of cell death, *nfkb*$^{-/-}$ cells were reconstituted, using a retroviral transgenic system, with either *rela* transgene (Tg), which is the major transactivating subunit of NF-κB, or a DNA defective binding mutant of

rela (*R35AY36A* Tg). Both *rela* Tg and *R35AY36A* Tg reconstituted cells contained similar levels of RelA protein when compared to wt MEFs (Fig 2.4B). Upon treatment with GO, *rela* Tg cells displayed increased incorporation of PI as opposed to *nfkb*$^{-/-}$ cells reconstituted with either empty vector (pBabe) or *R35AY36A* Tg (Fig 2.4B). However the amount of PI incorporation in *rela* Tg cells was decreased compared to wt cells, indicating only partial rescue of the cell death phenotype. Our attempt to study cell death in *relA* Tg reconstituted in *rela*$^{-/-}$ cells was unsuccessful since reconstitution with *relA* did not rescue the cell death phenotype. This could be because of the transformation of the *rela*$^{-/-}$ cells with viral oncoproteins, which disrupts many transcriptional regulatory pathways, and resulted in the loss of this mechanism of modulating NF-κB function. Regardless, the lack of cell death in *R35AY36A* Tg in *nfkb*$^{-/-}$ cells indicates that NF-κB promoted cell death is dependent on NF-κB, in particular, RelA DNA binding activity.

To examine the reason for the partial rescue of the cell death phenotype in response to GO, the response of the *rela* reconstituted cells to TNFa induced cell death, as well as TNFa induced DNA binding was inspected. Since it has been shown that *de novo* synthesis prevents the occurrence of apoptotic death upon treatment with TNFa (Papa et

al., 2006), cells containing a transcriptionally active RelA should prevent cell death from occurring. Accordingly, upon TNFa stimulation, wt and *rela* Tg cells did not undergo cell death, as opposed to *R35AY36A* Tg and pBabe cells (Fig 2.5A). EMSA results also show that NF-κB was not activated in both pBabe and *R35AY36A* Tg cells, in contrast to wt and, to a lower extent, *rela* Tg cells (Fig 2.5B). The incomplete rescue of NF-κB activation in *rela* Tg cells might be due to the absence of NF-κB subunits, p50 and cRel. The p50:RelA heterodimer is the major NF-κB species, and both cRel and RelA homodimers have also been reported to play roles in the regulation of target gene expression (Gilmore, 2006). Therefore, the absence of these dimers and the presence of only RelA homodimer might result in only suboptimal activation of some NF-κB target genes, and explains the partially functionally rescued *relA* reconstituted cells.

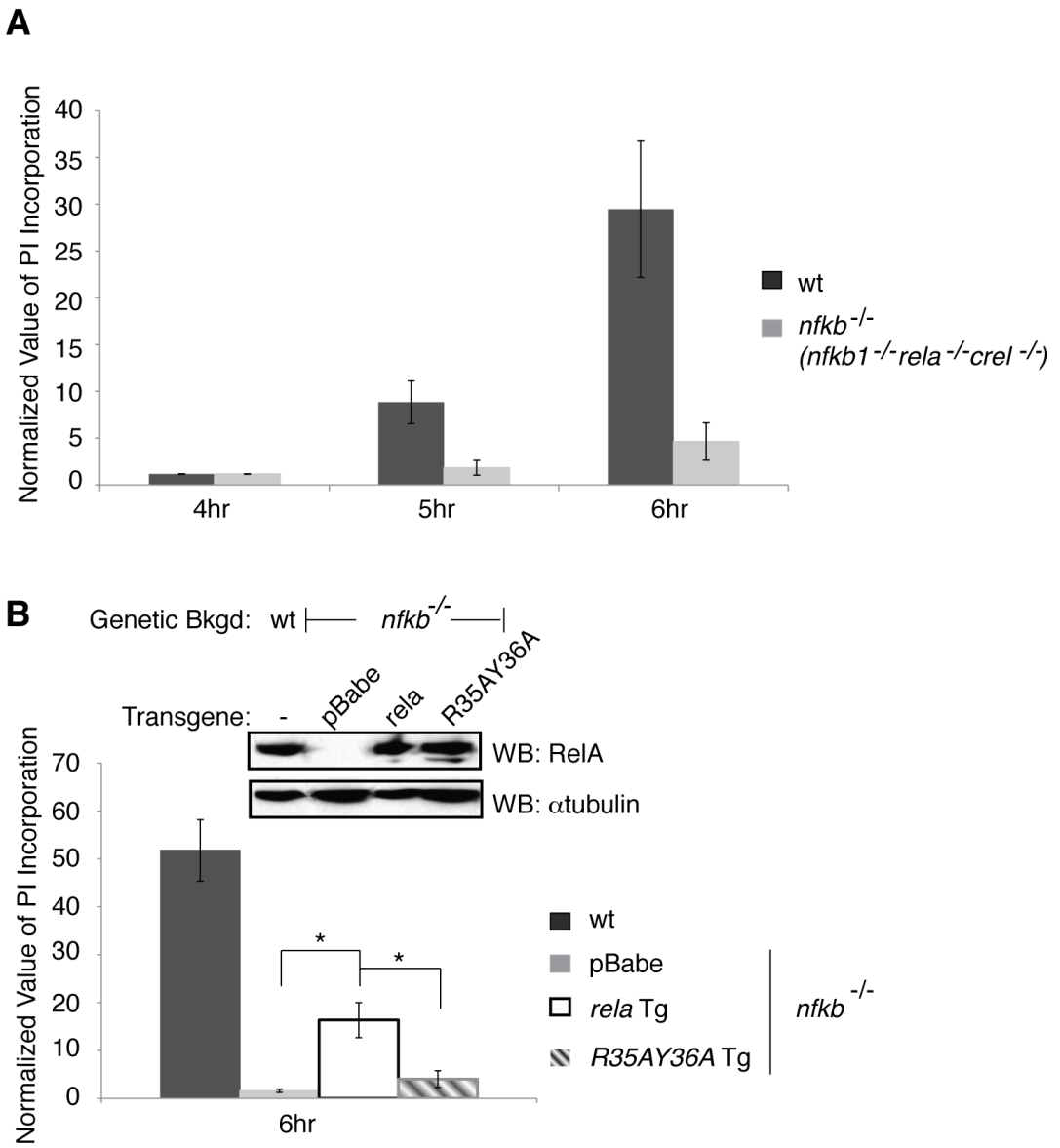

Figure 2.4: NF-κB augments cell death in H_2O_2 induced cell death

Cell death assays were performed on wt, *nfkb*$^{-/-}$ MEFs **(A)**, and *nfkb*$^{-/-}$ cells reconstituted with empty vector (pBabe), *rela* transgene (Tg), or *rela* mutant (*R35AY36A* Tg) **(B)** treated with 25 mU/ml GO for the indicated periods of time. RelA was verified by western blot. Results are presented as the average of 3 independent experiments. Error bars signify ±s.e.m. * denotes $p<0.05$.

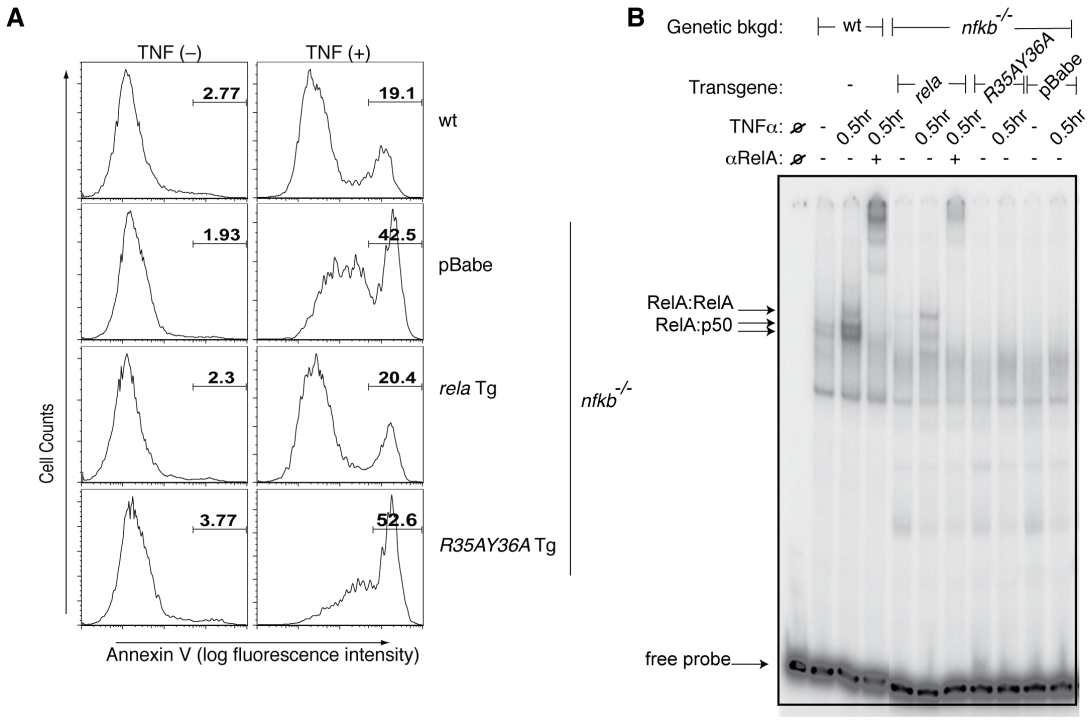

Figure 2.5: In response to TNFα, rela Tg cells are functionally rescued in their cell death phenotype but are only partially functionally rescued in their DNA binding response

(A-B) wt, *relA* Tg, *R35AY36A* Tg, and pBabe *nfkb*$^{-/-}$ cells were analyzed for cell death in terms of AnnexinV positive cells following 16 hrs of treatment with 10 ng/ml TNFα **(A)** and for nuclear localization and DNA binding by EMSA analysis following treatment with 1 ng/ml TNFα **(B)**. Supershift analysis was performed by adding RelA antibody to the EMSA reaction.

2.3.5 The canonical NF-κB activation pathway is required for the pro-cell death function of NF-κB in response to chronic exposure to H_2O_2

To further determine whether NF-κB acts as a promoter of cell death in response to H_2O_2, we compared the rates of cell death of *ikba*$^{-/-}$ MEFs which were reconstituted with either wt ikba (*wt ikba* Tg) or a mutant IκBα, where both Ser 32 and Ser36, which are the IKK phosphorylation sites, are mutated to alanine (*aa ikba* Tg), thus preventing NF-κB activation. Interestingly, in order to achieve cell death in a timely fashion, 50 mU/ml GO instead of 25 mU/ml GO was needed to induce cell death in both cell lines. This may be a reflection of cell line-specific characteristics or due to the over-expression of IkBa upon reconstitution in these cell lines (G.Ghosh, data not shown). Nevertheless, *wt ikba* Tg cells had a rapid rate of cell death compared to *aa ikba* Tg cells, where the canonical NF-κB activation pathway had been blocked (Fig 2.6A). As expected, NF-κB activation was completely blocked in *aa ikba* Tg cells as demonstrated by the lack of NF-κB activation upon TNFα stimulation by EMSA analysis (Fig 2.6B). These results further suggest that the resistance to death of *aa ikba* Tg cells is due to the lack of NF-κB activity. All together, these results strongly indicate that NF-κB plays a pro-cell death role in response to H_2O_2

induced caspase independent cell death, and that the canonical activation pathway is required in mediating NF-κB's pro-cell death role.

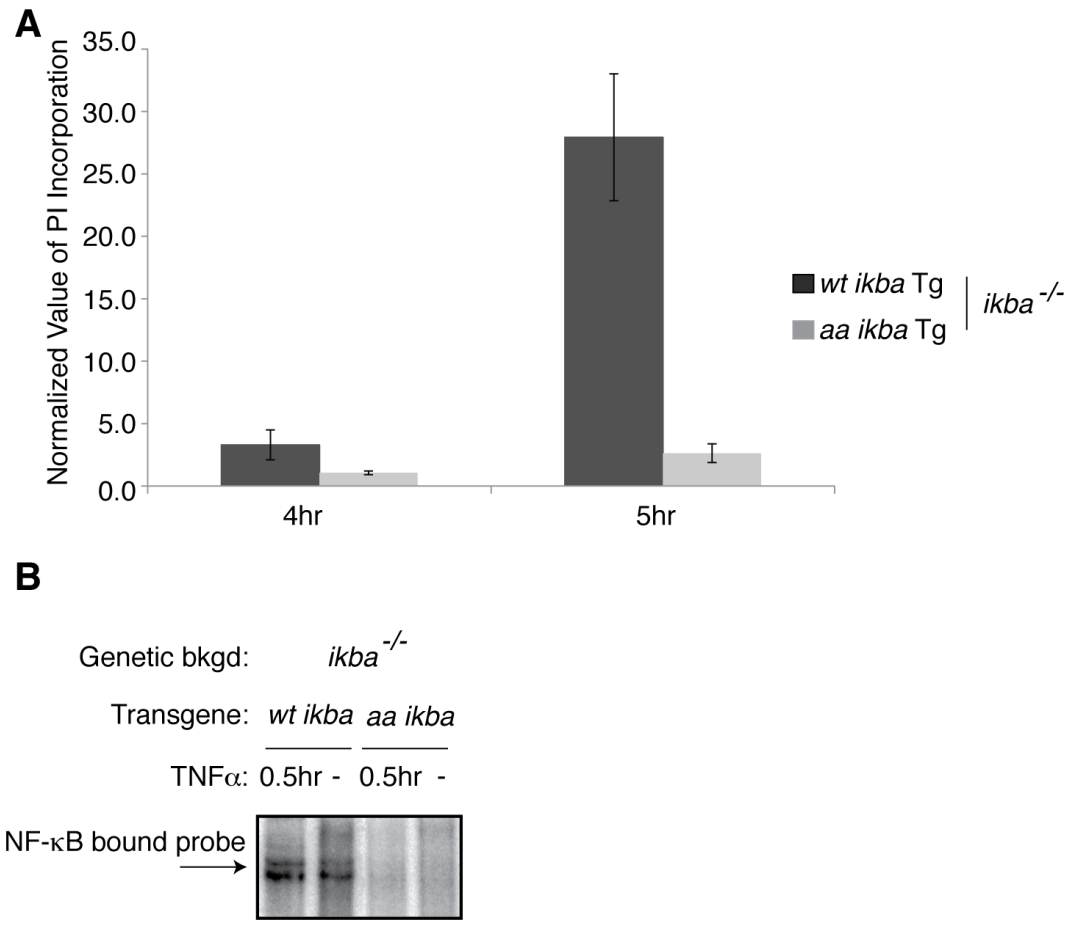

Figure 2.6: The canonical activation pathway is required for NF-κB's pro-cell death function

(A) Cell death assays were performed on *ikba*$^{-/-}$ MEFs reconstituted with either *wt ikba* Tg, or with *aa ikba* Tg treated with 50 mU/ml GO for the indicated periods. All results are presented as the average of 3 independent experiments. Error bars signify ±s.e.m. **(B)** *wt ikba* Tg and *aa ikba* Tg MEFs were treated with 1 ng/ml TNFα for 0.5 hr for EMSA analysis.

2.3.6 NF-κB is activated via the canonical pathway in response to chronic H_2O_2 insult

We next examined whether NF-κB was activated in response to chronic exposure to H_2O_2. Indeed, as seen by EMSA analysis, NF-κB was activated in a prolonged manner upon addition of GO in MEFs (Fig 2.7A). Given that NF-κB has been reported to be activated in both an IKK independent and dependent manner in response to H_2O_2, we then performed IKK activity assays, in which IKK was immunoprecipitated from GO treated MEFs followed by an *in vitro* kinase assay. IKK activity assays reveal that IKK is activated following one hour of treatment with GO (Fig 2.7B). Accordingly, there is also concomitant degradation of IκBα (Fig 2.7C). All together these results show that NF-κB is activated via the canonical pathway in MEFs in response to chronic exposure to H_2O_2.

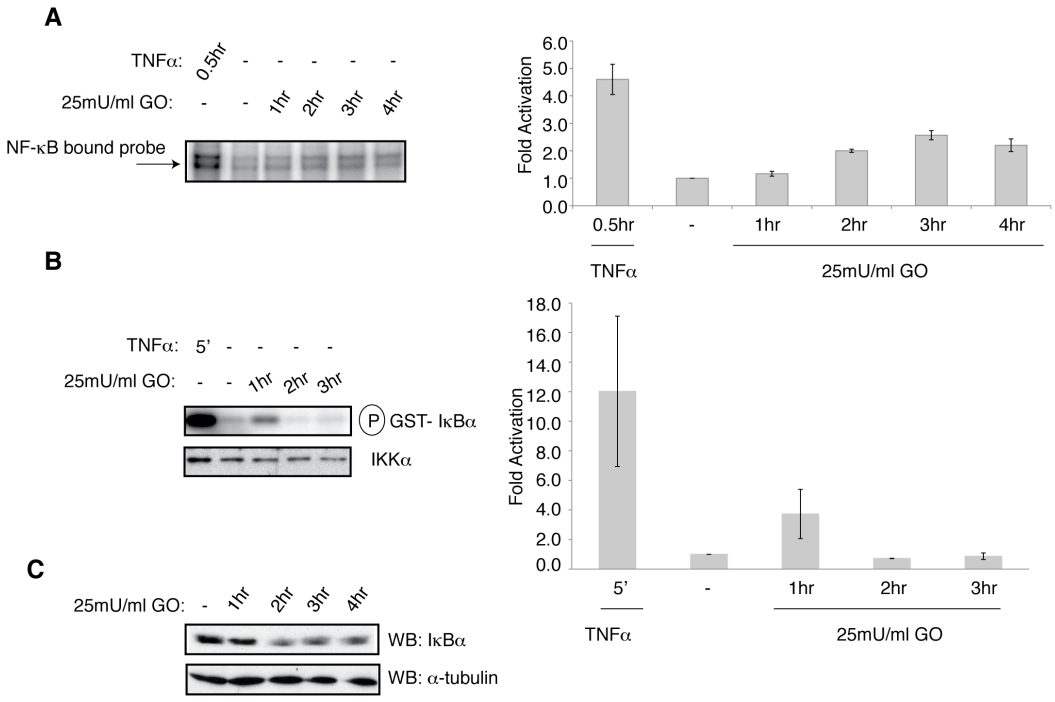

Figure 2.7: NF-κB is activated by IKK mediated IκBα degradation

wt MEFS were treated with either 1.0 ng/ml TNFα or 25 mU/ml GO for the indicated times, for EMSA **(A)** IKK activity **(B)** or IκBα degradation analysis **(C)**. Quantification of EMSA and IKK kinase assay experiments are shown. All results are presented as the average of 3 independent experiments. Error bars signify ±s.e.m.

2.3.7 NF-κB-dependent survival genes are repressed whereas death promoting genes are induced by H_2O_2

As a transcription factor, NF-κB's active participation in cell death is likely to be mediated through its target genes. Therefore, we set out to examine the expression pattern of several NF-κB target genes that are known to impact cell death or survival (Table 2.2). Using real time quantitative PCR (qPCR), we measured mRNA levels at 0 and 4 hrs after GO treatment in wt MEF and *nfkb*$^{-/-}$ cells reconstituted with empty vector (pBabe) or *relA* Tg. While the majority of these genes did not undergo changes in expression levels (Table 2.2), we identified 4 genes that underwent significant alterations: cell survival factors, Bcl-2 and XIAP, and cell death promoting factors, TNFα and Fas ligand (FasL). The significant reduction of Bcl-2 expression in both wt and *rela* Tg cells and not pBabe cells (Fig 2.9) implies that Bcl-2 repression is due to the presence of RelA. A similar trend is seen for inhibitor of apoptosis, XIAP. In contrast, TNFα expression was significantly induced in both wt and *relA Tg* cells, while not in pBabe cells. FasL was induced in only wt cells. These results suggest that TNFα, but not FasL, induction by H_2O_2 is RelA dependent. The lack of FasL induction in *rela* Tg cells could be attributed to the partial rescue phenotype of the *relA* Tg cells (Fig 2.9).

Table 2.2: Relative Changes in Gene Expression Levels in response to H_2O_2

Cell Death Genes:

	wt	pBabe	*rela* Tg
TNFα	6.5 ± 1.0 *	1.2 ± 0.2	2.6 ± 0.50 *
Fas Ligand	2.4 ± 0.5 *	0.8 ± 0.12	1.5 ± 0.90
Fas Receptor	1.1 ± 0.07	0.82 ± 0.04 *	0.85 ± 0.10
Bax	0.86 ± 0.27	0.91 ± 0.11	0.76 ± 0.08 *

Cell Survival Genes:

	wt	pBabe	*rela* Tg
XIAP	0.46 ± 0.03 *	0.8 ± 0.05	0.50 ± 0.07 *
Bcl-2	0.51 ± 0.13 *	0.83 ± 0.03 *	0.71 ± 0.08 *
Bcl-xL	0.79 ± 0.12	0.91 ± 0.11	0.67 ± 0.20
cIAP-1	0.89 ± 0.24	0.87 ± 0.03 *	0.69 ± 0.07 *
p53	1.01 ± 0.11	0.84 ± 0.08	0.90 ± 0.15

Relative gene expression levels of all the genes examined in wt and pBabe or *rela* Tg reconstituted *nfkb*$^{-/-}$ cells following 4 hrs of treatment with 25 mU/ml GO are given in the following table. Relative gene expression levels are presented as the average of triplicate experiments with the ± standard deviation given as well. * denotes $p<0.05$

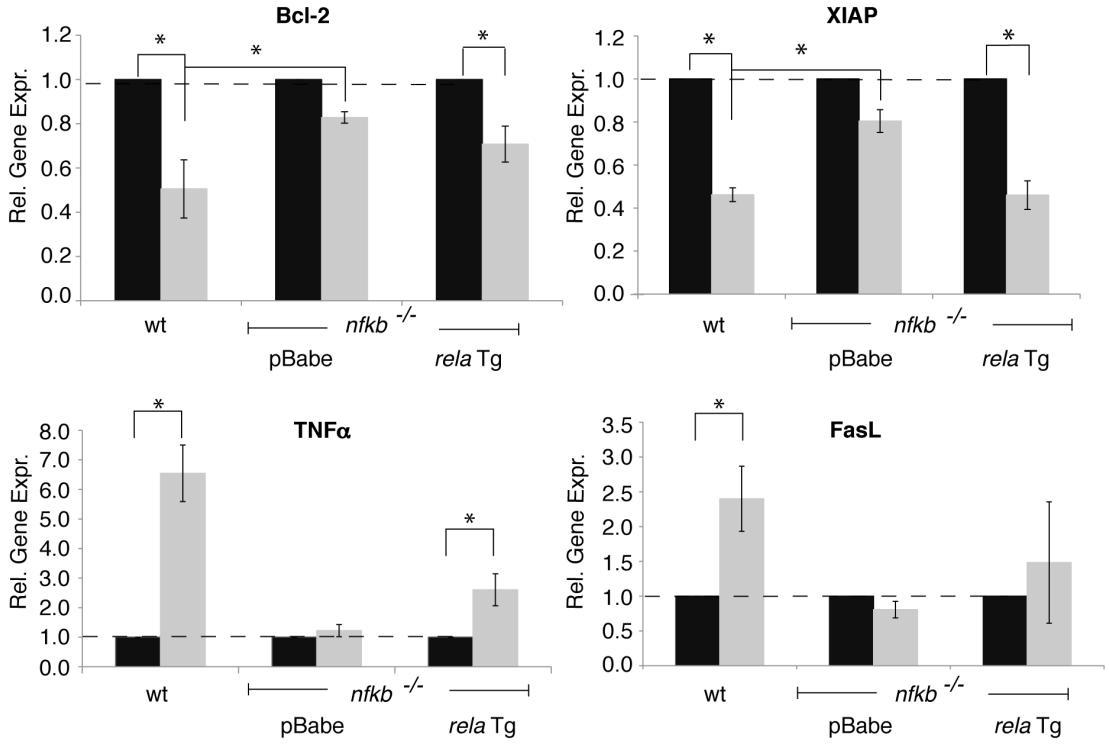

Figure 2.9: NF-κB dependent survival genes, Bcl-2 and XIAP, are repressed, while cell death genes, TNFα and FasL, are induced

Total RNA was isolated from wt and pBabe or *rela* reconstituted *nfkb*$^{-/-}$ MEFs without treatment (*black bars*) or following 4hrs of treatment with 25 mU/ml GO (*grey bars*). Relative gene expression (Rel. Gene. Expr.) levels were determined using real time RT-PCR and are presented as compared to untreated samples. Results are presented as the average of three triplicate experiments. Error bars signify ± standard deviation. * denotes $p<0.05$

2.4 Discussion

This study has discovered an unexpected function of NF-κB in that it promotes MEF cell death in response to chronic insult with H_2O_2. We have shown that intracellular H_2O_2 was continuously produced in MEFs treated with GO and that this unremitting exposure to H_2O_2 resulted in a caspase-independent but PARP dependent cell death. We also show that the pro-death activity of NF-κB is dependent on the DNA binding activity of RelA, which is induced through IKK-mediated IκBα degradation. The death promoting activity of NF-κB might be mediated by the down regulation of a subset of NF-κB dependent pro-survival factors and up-regulation of NF-κB dependent pro-death factors, as demonstrated by the repression of Bcl-2 and XIAP, and induction of TNFα and FasL.

Due to the repression of pro-survival factor Bcl-2 in wt and *rela* Tg cells, we propose that the pro-cell death function of NF-κB is primarily due to its transcriptional down regulation of Bcl-2, since it has been shown that in MNNG induced caspase independent but PARP-1 dependent MEF cell death, over-expression of Bcl-2 can delay cell death (Yu et al., 2002). Bcl-2 over-expression delays cell death due to its

ability to prevent translocation of apoptosis inducing factor, AIF, from the mitochondria to the nucleus. This translocation event is central in causing MNNG and H_2O_2 induced MEF cell death (Yu et al., 2002). The fact that Bcl-2 over-expression can only delay cell death fits with our proposed model, since *nfkb*$^{-/-}$ cells, which contain higher levels of Bcl-2 than either wt or *rela* Tg cells, eventually also succumb to cell death (J. Ho, data not shown). Additionally, our result, in which Bcl-2 is down-regulated in a seemingly NF-κB dependent manner to promote PARP dependent fibroblast cell death, suggests a novel level of cooperativity between PARP and NF-κB. This is because PARP and NF-κB cooperativity has only been shown in instances where PARP-1 can act as a direct co-activator for RelA and p50, or as an upstream mediator of NF-κB activation in response to various stimuli (Hassa et al., 2001; Stilmann et al., 2009; Veuger et al., 2009).

We have convincingly demonstrated that NF-κB has a pro-cell death function in response to chronic insult with H_2O_2 in MEFs. Although it was shown that in HeLa cells, NF-κB promotes cell survival in response to a single bolus addition of low nanomolar concentration of H_2O_2 (Storz and Toker, 2003), this variation can be attributed to differences in cell type, as well as differences in the application of H_2O_2, and thus amount

of intracellular H_2O_2, which, as previously stated, can switch the cell death mode. We propose that NF-κB can be anti-cell death in caspase dependent cell death induced by transient or low levels of H_2O_2, but that NF-κB has a pro-cell death function in caspase independent cell death induced by continuous or high levels of H_2O_2. Indeed, NF-κB's role in promoting cell survival and death is a complex event. This is demonstrated by genotoxic agent, VP16, induced cell death, in which both pro- and anti-apoptotic genes were induced in NF-κB dependent manner, such that the final outcome depended on a balance of the induction levels of pro- and anti-apoptotic genes (Wu and Miyamoto, 2008).

Our gene expression results are strongly supported by previous studies, which showed that cell death stimulation with daunorubicin, cisplatin, or $p14^{ARF}$ over-expression in U2OS osteosarcoma cells resulted in RelA mediated transcriptional repression of pro-survival genes, Bcl-xL or XIAP (Perkins and Gilmore, 2006). These previous reports also showed that RelA acts in a dominantly transcriptionally repressive manner. Interestingly, we observe selective activation and repression of certain death and survival genes, in that TNFα was induced while Bcl-2 and XIAP were repressed in a seemingly NF-κB dependent manner (Fig 4).

There are currently more reports addressing NF-κB's singular transcriptional response in promoting cell death (either complete repression or induction of survival or death genes, respectively) (Campbell et al., 2004; Campbell et al., 2006; Ho et al., 2005) and significantly fewer reports describing NF-κB's mixed transcriptional response in promoting cell death (repression and induction of survival and death genes) (Liu et al., 2006b). This is the first report suggesting that NF-κB uses a mixture of transcriptional responses in promoting cell death upon ROS stimulation. It is unclear at this stage as to how NF-κB mediates repression of some target promoters and activation of others. However, given that oxidative stress is known to inactivate the cysteine active sites of cellular phosphatases, this would change the cellular phospho-protein state (Gloire et al., 2006b) and could potentially inhibit or enhance the recruitment of coactivators and corepressors. Additionally, RelA mediated repression of pro-survival genes has been reported to involve Thr505 phosphorylation of RelA, which can enhance the interaction between RelA and HDAC1 (Perkins and Gilmore, 2006). Further studies are still required to fully unravel this mechanism.

The induction and repression of cell death and survival genes, respectively, in response to H_2O_2 also suggests that activation of NF-κB is

required for mediating its pro-cell death response. Previous reports of NF-κB's pro-cell death function have been shown to depend on either basal (Lin et al., 1998; Liu et al., 2006b) or activated NF-κB (Perkins and Gilmore, 2006). However, we cannot fully conclude that NF-κB activation is solely required to mediate the pro-cell death response, since pBabe reconstituted cells contain lower levels of basal NF-κB (Fig 2D).

Our studies have also clearly shown that NF-κB is activated via the canonical pathway in MEFs, which is in contrast to reports where NF-κB activated in response to oxidative stress occurred via an atypical mechanism, involving an IKK independent mechanism and IkBa Tyr42 phosphorylation. The presence of SHIP1 has been reported to revert the mechanism of NF-κB activation from atypical to canonical in response to H_2O_2 (Gloire et al., 2006b). Thus, the presence of SHIP2 in MEFs, which is functionally similar to SHIP1 (Wang et al., 2004), supports our observed NF-κB activation mechanism.

Unremitting exposure of tissues to ROS can lead to pathophysiological conditions, such as neurodegenerative disorders and chronic obstructive pulmonary disease (Behl and Moosmann, 2002;

Carnevali et al., 2003; Trachootham et al., 2008). Our result that NF-κB might play a role in promoting cell death adds another layer of complexity to therapeutic drug design and should be taken into consideration when NF-κB inhibitor pharmaceutical targets are used in treatment. Overall, this study shows that NF-κB dependent transcription is responsible for promoting H_2O_2 induced cell death. Further experiments will be done to explore the detailed molecular mechanism.

2.5 Acknowledgments

I would like to thank Erika Mathes for *wt ikba* Tg and *aa ikba* Tg cells; Masataka Asagiri for performing the Facs analysis for Figure 2.5; Dong Wang and Vincent Shih for qPCR technical assistance; Dennis Otero, Xiang-Yang Zhong and Anthony Farina for valuable discussions; and Olga Savinova, Sulakshana Mukherjee, Zhihua Tao, and Smarajit Polley for their critical reading of this manuscript. GG was supported by NIH Grant GM071862; GG and AH were supported by GM085490. JH is supported by the Ruth L. Kirschstein National Research Service Award NIH/NCI T32 CA009523.

Chapter 2, has been submitted for publication as it may appear in PLoS One, 2010. Ho, Jessica Q.; Asagiri, Masataka; Hoffmann, Alexander; Ghosh, Gourisankar. "NF-κB potentiates caspase independent hydrogen peroxide induced cell death". The dissertation author was the primary author of this paper.

Chapter 3: Oxidation of the 20S proteasome potentially enhances its proteolytic activity in ubiquitin independent degradation

3.1 Introduction

The proteasome is a multicatalytic complex involved in many cellular processes in eukaryotes, such as protein and RNA turnover, cell division, signal transduction, transcription, and translation (Glickman and Ciechanover, 2002; Hershko and Ciechanover, 1992, 1998). The catalytic component of the proteasome is a cylindrical shaped 20S complex, which is referred to as the 20S proteasome. The 20S proteasome contains 3 different proteolytic activities: a peptidyl glutamyl hydrolyzing (PGH) like, trypsin like, and chymotrypsin like, such that cleavage occurs after acidic residues, basic residues, and hydrophobic residues, respectively (Murata et al., 2009). The eukaryotic 20S proteasome is comprised of four stacked rings in a cylindrical arrangement (Bochtler et al., 1999; Groll et al., 1997). Two identical outer rings are formed by seven α subunits (α 1-7), whereas the identical inner rings are formed by seven different β subunits (β1-7). The active sites are located inside the cylindrical chamber and the gates into the chamber are closed by the N-terminal tails of three specific α subunits. Such a structural organization allows the proteasome to avoid indiscriminate protein degradation, resulting in the formation of an inactive or latent 20S proteasome (Bochtler et al., 1999; Groll et al.,

1999). Four known activators, PA7000 (19S), PA28α/ β, PA28γ and PA200, regulate gate opening by directly binding to the outer ring of the catalytic core (Rechsteiner and Hill, 2005).

The major active proteasomal component in cells is the 26S proteasome, which is formed by the association between the 20S and 19S regulatory particle (RP). Substrates of the 26S proteasome are most commonly covalently linked to a polymer composed of the 76 amino acid protein known as ubiquitin (Ub) (Hershko and Ciechanover, 1998). The 19S RP, also known as PA700, specifically recognizes and unfolds the poly-Ub tagged proteins for degradation by the 20S. The 19S RP from budding yeast contains a total of 17 subunits, 6 which are ATPase subunits (Rpt) and 11 which are non ATPase subunits (Rpn). Sub-complexes of the 19S RP are the base, which directly interacts with the 20S, and the peripheral lid. The base is composed of Rpn subunits 1, 2, 10, and the 6 Rpt subunits. The peripheral lid is composed of Rpn subunits 3, 5-9, 11, 12. The exact subunits which are involved in substrate recognition have not been identified. However, *in vitro* studies show that highly conserved Rpn 10 is able to bind poly-Ub chains, suggesting that it is one of the subunits involved in recognition of Ub proteins. Rpn 11 also shares high sequence homology to a de-Ub enzyme, suggesting

that it is involved in de-ubiquitinylation of the ubiquitinylated substrates(Bailly and Reed, 1999; Fu et al., 2001a).

The 19S RP, specifically recognizes and unfolds the poly-Ub tagged proteins for degradation by the 20S proteasome in an ATP dependent manner. Three distinct classes of Ub carrier proteins and ligases, E1 (ubiquitin activating), E2 (ubiquitin conjugating), and E3 (ubiquitin-protein ligase), are required for signal-dependent attachment of Ub to target proteins (Glickman and Ciechanover, 2002; Hershko and Ciechanover, 1992, 1998).

Immuno affinity pull down and biochemical purification have revealed that the 20S is associated with a variety of regulatory particles: PA700, PA28, or both PA700 and PA28 as a hybrid proteasome (Fig3.1.1) (Rechsteiner and Hill, 2005). PA28 activators form a homo- or hetero-oligomeric ring structure to interact with the 20S proteasome. X-ray structures of PA28 bound to 20S CP revealed the molecular details of the gate opening mechanism (Rechsteiner and Hill, 2005; Whitby et al., 2000). While biological functions of this activator are not yet entirely clear, it has long been proposed that PA28 proteasomes generate immuno active peptides from larger peptides generated by the 26S proteasome (Li et al., 2006). Despite the many activators that are known to associate with the 20S proteasome, an estimated 30% of total

20S remains free (Tanahashi et al., 2000). This free pool could be 'truly' free or bound to unknown inhibitors or activators. The function of this free 20S, if any, is controversial.

Recent studies, using temperature sensitive cell lines and mutational analysis, have reported an emerging group of natively unfolded substrates that were degraded without prior ubiquitination, as in the cases of p21, ornithine decarboxylase (ODC), p53, c-Fos, c-Jun, and steroid receptor coactivator-3 (Src-3). In support of their ability to be degraded in a Ub-independent manner, many of these substrates were also degraded by the 20S proteasome, without the 19S RP, Ub, or ATP in the reaction mix, *in vitro*. It is important to note that, like p21, most of these proteins are degraded by the 26S proteasome via ubiquitination when they are bound to their respective binding partners. Thus, it is generally thought these proteins have alternative degradation pathways. When these proteins are unbound, they exist in an unfolded or loosely folded state, which allows them to be degraded in a Ub-independent manner. However, these proteins become stably folded once bound to their binding partners, and thus require Ub-dependent/ 26S proteasome mediated degradation. (Bossis et al., 2003; Jariel-Encontre et al., 1995; Kriwacki et al., 1996; Salvat et al., 1999).

Interestingly, we have also made similar observations when examining both the degradation of the NF-κB inhibitor molecule, IκBα, in resting cells and the processing of p105, an IκB- like precursor of the NF-κB p50 subunit. The Ub- dependent 26S proteasome mediated degradation of IκBα bound to NF-κB has been extensively demonstrated. However, unbound IκBα is notoriously unstructured and the degradation rate of IκBαL12R, where all potential internal ubiquitinylation sites in unbound IκBα have been mutated, is identical to wild type unbound IκBα. This suggests that unbound IκBα is degraded in a Ub-independent manner. Furthermore, *in vitro* degradation assays show that the 20S proteasome can discriminately degrade recombinant IκBα in the absence of Ub and ATP. Similarly, in the case of p105 processing, a mixture of only 20S proteasome and p105 in an *in vitro* degradation assay results in the degradation of the C-terminal portion of p105, known as IκBγ, to produce the processed product, p50. Recombinant IκBγ can also be degraded by the 20S proteasome *in vitro*. Finally, using temperature sensitive cell lines where the 26S/Ub system is drastically impaired at the restrictive temperature, the processing of p105 to p50 remained at the same level at both the restrictive and permissive temperatures (Mathes et al., 2008; Moorthy et al., 2006).

Based on the reports of numerous proteins degraded in a Ub-independent manner by the 20S proteasome *in vitro* and evidence that a large pool of free cellular 20S proteasome exists, we speculate that a specific form of 20S proteasome exists in cells to degrade natively unfolded substrates in a Ub-independent manner, which we call "active" 20S. This active 20S could potentially differ from latent 20S due to binding of yet unknown activators or inhibitors, post-translational modifications, or different subunit composition. Thus, we set out to examine the mechanism of Ub- independent degradation of NF-κB inhibitor molecules IκBα and IκBγ by isolating and biochemically characterizing the 20S proteasome involved in their Ub- independent degradation. To isolate this pool of "active" 20S, we took the following approach: purify the 20S through a series of careful chromatographic steps, and characterize "active" and "latent" 20S pools through activity assays against the NF-κB inhibitor molecules. Then, following separation of the active and inactive pools, the differences would be identified through mass spectrometry (MS).

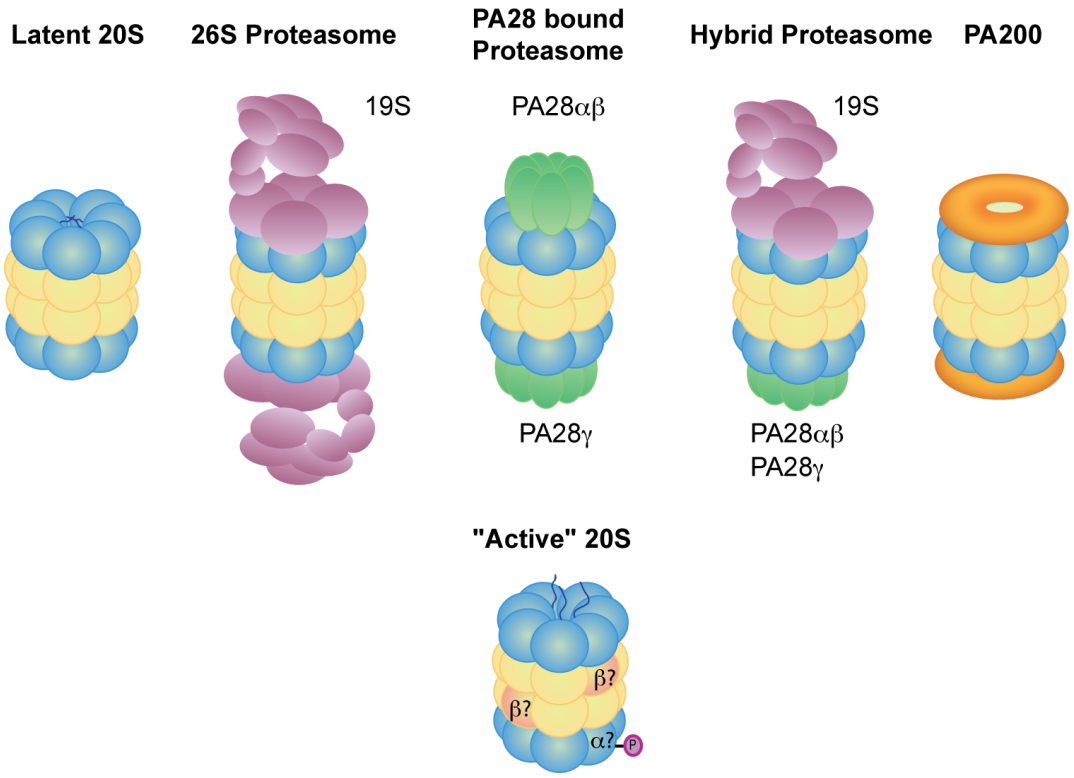

Figure 3.1.1: Different cellular pools of the proteasome.

A schematic showing the known types of regulatory particles (19S, PA28αβ, PA28γ, PA200) with the 20S proteasome on the top row and a speculative form of 20S proteasome, which we refer to as the active 20S, shown on the bottom row. This active 20S proteaseome could be responsible for Ub-independent degradation due to different subunit composition or a post-translational modification.

3.2 Materials and Methods

3.2.1 Purification of 20S Proteasome

20S proteasome complexes were purified from 500ml of bovine blood containing anticoagulant citrate (*Innovative Research*). Cells were washed four times by adding 600ml of wash buffer (5mM Tris-HCl, pH 7.5, 150mM NaCl) followed by a spin at 4959 x g (5300 rpm) for 20minutes. Cells were then lysed with 500ml of lysis buffer (5mM Tris-Hcl, pH 7.0, 5mM BME) which contained protease inhibitor cocktail (*Sigma*) and the lysed cells were then spun down at 4959 x g for 1.5hrs. The supernatant then underwent ammonium sulfate precipitation (50-75%), and was dialyzed against five changes of 11L of dialysis buffer (5mM Tris-HCl pH7.5, 5mM BME). After dialysis, half of the dialyzed protein (by volume) was flash frozen and stored in -80° for future usage. The other half was further diluted 3.6 fold with the dialysis buffer for loading onto the Q Sepharose Fast Flow column (anion exchange) (*Amersham Biosciences*). Following two 150ml washes, the first one with dialysis buffer and the second one containing 200mM NaCl, the bound proteins were eluted with a linear gradient from 200-600mM NaCl over ten column volumes. The proteasome containing fractions were then

loaded onto a size exclusion column (Sephacryl S-300, *Amersham Biosciences*), pre-equilibrated with gel filtration buffer (50mM Tris, pH 7.5, 5mM BME). Proteasome containing fractions were pooled and diluted two fold with 4M ammonium sulfate so that the final concentration of the solution was 2M ammonium sulfate. The proteasome was then loaded onto a high performance (HP) phenyl sepharose column (hydrophobic interaction column) (*Amersham Biosciences*), which had been pre-equilibrated with gel filtration buffer containing 2M ammonium sulfate. Bound proteins were then eluted with a linear gradient of 2M- 0M ammonium sulfate over 20 column volumes. Finally, the pooled proteasome was further diluted ten to twenty fold with gel filtration buffer and loaded onto a Mono Q column (anion exchange) (*Amersham Biosciences*), which was also pre-equilibrated with gel filtration buffer. Proteins were eluted with a linear gradient from 350-376mM NaCl over 10 column volumes. An average of one to three milligrams of protein was recovered after the Mono Q column. All purification steps before the phenyl sepharose step were done at 4°C, and all following purification steps were performed at room temperature. Proteasome containing fractions were pooled based on visual verification with 1D SDS gel analysis.

3.2.2 Purification of GST-IκBγ

Bacterial expression vector, pGEX- 4T2, containing the gene construct for p105 (435- 971), also known as IκBγ, was a kind gift from Dr. Moorthy. The expression plasmid was introduced to BL21 (DE3) cells and the transformed bacterial cells were then cultured at 37 °C in two liters of LB media with 100ug/ml of ampicillin. Upon induction at an OD600 of 0.3 to 0.4 with 0.1mM IPTG, the culture was then grown for an additional 12- 18 hours at 25°C. After spinning at 6300rpm for twenty minutes, the collected cells were lysed in lysis buffer (20mM Tris, pH 7.5, 50mM NaCl, 1mM DTT, 0.5mM EDTA pH 8.0) containing 0.5mM PMSF and protease inhibitor cocktail (sigma). Insoluble material was then cleared by centrifugation at 13K rpm for 45 minutes and the resulting supernatant was loaded onto a Fast Flow Q column (Amersham), pre-equilibrated with lysis buffer. Proteins were then eluted over ten column volumes with a linear gradient from 50mM -1M NaCl. GST- IκBγ containing fractions were pooled and then underwent affinity purification, where the proteins were loaded onto a GST column (Amersham). GST containing proteins were eluted over 20 column volumes using lysis buffer containing 10mM L-Glutathione reduced (Sigma), where the pH was adjusted to 7-7.5. Elutions containing GST- IκBγ were then pooled and

concentrated using a centri-prep YM30 concentrator (Millipore). The concentrated proteins were finally loaded onto a Superdex S200 gel filtration column (Amersham), pre- equilibrated in gel filtration buffer (20mM Tris, pH 7.5, 50mM NaCl, 1mM DTT), for the separation of contaminating GST molecules and aggregates. The resulting protein was judged to be 90% pure by 1D SDS gel analysis. All purification steps preceding the size exclusion chromatography step were done at 4°C, whereas the steps following it were done at room temperature.

3.2.3 *In vitro* degradation assay (proteasome activity assay)

Recombinant proteins, GST-IκBγ and His- IκBα, were used as substrates for the activity assays used to determine the activity of the proteasome. Recombinant His- IκBα was a kind gift from Erika Mathes. In the assay, the substrate is mixed in a varying molar ratio with purified proteasome in a reaction buffer containing 200 mM NaCl, 20 mM Tris HCl, pH 7.1, 10mM $MgCl_2$ and 1 mM DTT. The mixture is incubated for 1 hour at 37°C. The reaction is quenched upon the addition of 4X SDS dye and boiling for one minute at 95°C. The products are then separated by SDS-PAGE followed by visualization by coomassie staining. One tenth the amount of the same sample was used for

visualization by western blot using either GST antibody (Santa Cruz, sc-138) or IκBa antibody (Santa Cruz, sc-371).

3.2.4 Creation of oxidative stress in cells

Cells were oxidatively stressed using glucose oxidase, as previously stated in chapter 2.2.

3.2.5 Immunoprecipitation (IP) of 20S proteasome

20S was immunoprecipitated from either glucose oxidase treated or untreated mouse 3T3 cells. Following treatment, cells were washed two times with D-PBS (Gibco), and then lysed in RIPA buffer (20mM Tris pH7.5, 200mM NaCl, 1% Triton-X 100, 2mM DTT, 5mM p- nitrophenyl phosphate, 2mM sodium orthovanadate, 1X protease inhibitor cocktail (Sigma)). After the insoluble material was cleared upon centrifugation at 13k rpm for 10min at 4°C, each IP reaction was normalized with RIPA buffer to 1mg/ml, where each reaction contained a total protein concentration of 500ug. Each reaction was then pre-cleared by adding protein G agarose (Upstate) for one hour at 4°C. Ten micrograms of mouse 20S α3 (C9) subunit antibody (Biomol, PW8115)

was added to the pre-cleared lysate at 4°C for 12- 14 hours. Protein G agarose was then added to the reaction for an additional 2 hours at 4°C. The beads were collected after centrifugation at 3.3xg for 3 minutes, and washed 4xs (1ml/wash) with wash buffer (20mM Tris pH 7.5, 150mM NaCl, 0.5% Triton X 100). Following the last wash, 7ul of 4X SDS dye was added to the beads and the samples were boiled for 5minutes at 95°C. The 20S proteasome was visualized by separating the samples on a 12.5% SDS gel and immunoblotting against 20S subunit α3 (Biomol, PW8115). IP of 20S from HeLa cells followed the protocol given above, with the following exception: the 20S β7 subunit antibody (Biomol, PW9150) was used to immunoprecipitate the 20S core particle.

3.2.6 Activity Assay using immunoprecipitated 20S proteasome

The 20S proteasome was immunoprecipitated from both glucose oxidase treated and untreated HeLa cells, following the protocol given above. However, after the last wash, the wash solution was completely aspirated, leaving only the beads. Eighty microliters of reaction buffer, which contained 0.14 ug of recombinant His-IκBα and 200 mM NaCl, 20 mM Tris HCl, pH 7.1, and 10mM $MgCl_2$, was then added to the beads. The reaction mixture was rotated for one hour at 37°C. The reaction

was quenched upon the addition of 4X SDS dye and boiling for 5 minutes at 95°C. The results of the degradation assay were visualized on a 10% SDS gel and immunoblotting against IκBα (Santa Cruz, sc371). The results of the immunoprecipitation reaction were visualized on a 12.5% SDS gel and immunoblotting against 20S core particle α3.

3.3 Results

3.3.1 Purification summary of the 20S proteasome from bovine blood

The protein isolation protocol for the 20S proteasome from bovine blood was achieved following this series of chromatographic steps: Ammonium Sulfate precipitation, Q Fast Flow column (anion exchange chromatography), Sephacryl S-300 column (size exclusion chromatography), Phenyl Sepharose column (hydrophobic interaction chromatography), and MonoQ column (high resolution anion exchange chromatography). SDS gels and chromatograms characteristic of each step are shown in Fig 3.3.1. Given that the native proteasome was isolated from tissue, the initial ammonium sulfate precipitation and Q column steps were used to isolate fractions containing primarily proteasome (Fig 3.3.1A). Following size exclusion chromatography, the phenyl sepharose column was used to separate tightly associated chaperone, Hsp90, from the 20S. Elution off the phenyl sepharose column showed that the 20S eluted in a single sharp peak, indicating a seemingly homogenous species (Fig 3.3.1B). However, further separation on the MonoQ column, an ion exchange

column which is known to have high resolution capabilities, showed a heterogeneous species. These differences in elution volume could not be distinguished by separation on a 1D SDS gel, where the 20S proteasome banding pattern appeared identical in each fraction (Fig 3.3.1C).

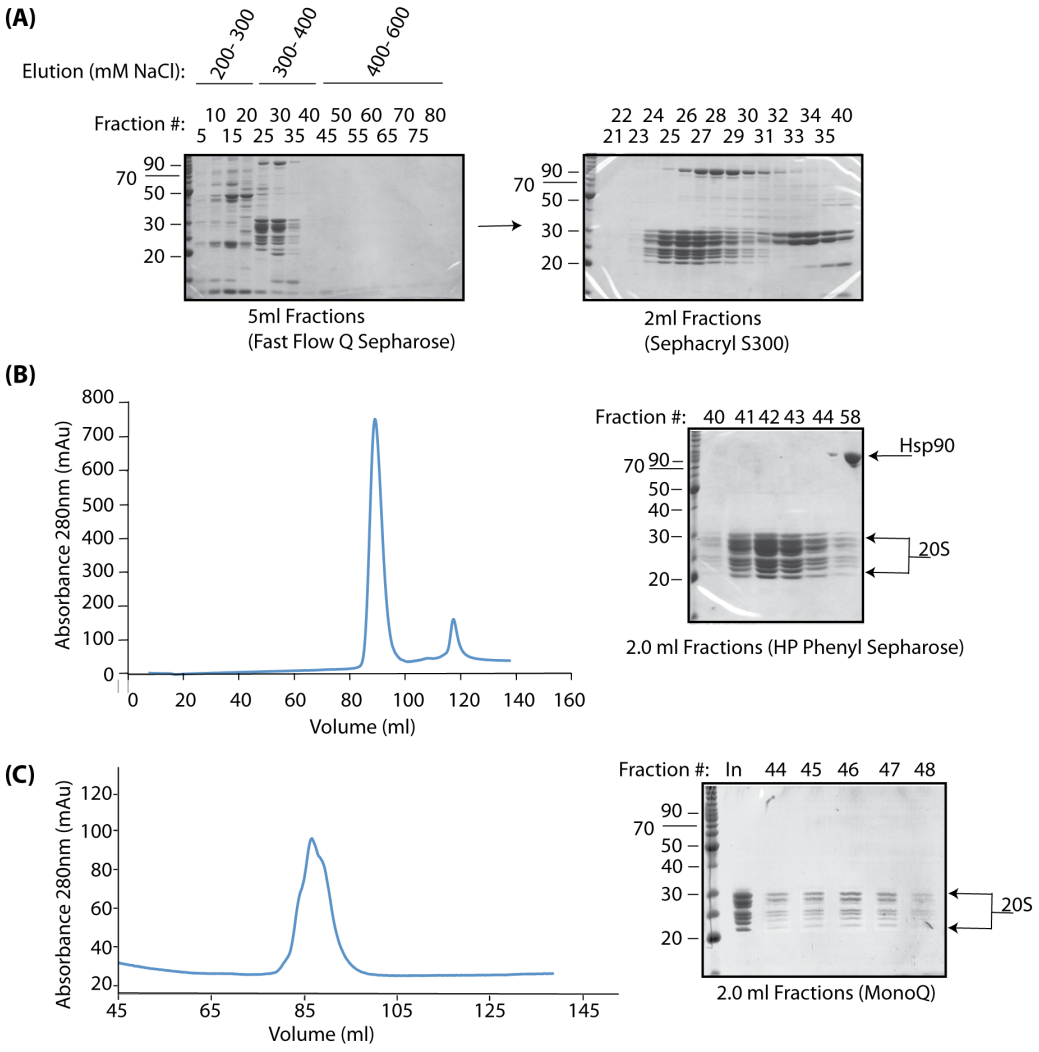

Figure3.3.1: Purification summary for 20S proteasome from bovine blood.

(A to B) Following ammonium sulphate precipitation, the precipitated pellet was separated on a Q fast flow column using a salt gradient. 20S containing fractions were pooled and further purified by fractionation on the Sephacryl S300. **(C)** Contaminating protein, Hsp90, was then separated from the 20S using the phenyl sepharose column. **(D)** 20S containing fractions were then pooled and fractionated on a MonoQ column, using a steep salt gradient. Coomassie stained 1D SDS gels are shown for each step, where 20S proteasome subunits migrate between 20 to 30kDa. Chromatograms are shown for the phenyl sepharose and mono Q steps. In= input.

3.3.2 20S proteasome fractionated by MonoQ chromatography produces inconsistent activity, whereas further fractionation by MiniQ chromatography produces active 20S proteasome

Given that we had optimized the protocol for isolating 20 proteasome, we now wanted to characterize inactive and active 20S proteasome fractions. To do so, we took individual fractions following MonoQ elution, since elution by MonoQ chromatography produced an uneven profile, and tested the activity of each fraction for its ability to degrade N terminally tagged GST-tagged IκBγ (GST- IκBγ). When the activity of the fractions following MonoQ fraction were initially performed, the fractions that eluted in the higher salt fractions showed enhanced ability to degrade GST- IκBγ (Fig 3.3.2A). However, this proved to be irreproducible as 20S proteasome isolated following MonoQ fractionation in later purification trials were largely inactive (Fig 3.3.2B). 20S purified in these later purification trials was eluted off the MonoQ using a near isocratic gradient (350- 376mM NaCl), as opposed to earlier trials where steeper gradients were used (300-500mM NaCl) (compare Fig. 3.3.2B to A). This result was puzzling since elution using a near isocratic gradient, such as to finely separate subtle differences in charge, generally improves separation between different species.

We also attempted to roughly determine whether differences in elution volume from the MonoQ were due to differences in subunit composition, post- translational modification, or association with another protein by 1D SDS gel analysis. However, in agreement with earlier purfication trials, proteasome isolated following the MonoQ column did not have differences in banding pattern, despite having different elution volumes (Fig 3.3.2B middle). Due to the overloading of the protein on the SDS gel, a minor contaminating band, which ran at 50kDa, was identified in the majority of the fractions. LC-MS/MS results indicate that this band is in fact proteasome subunits (data not shown).

Since proteasome fractions following MonoQ chromatography were unable to degrade GST- IκBγ, the fractions were combined and separated on the MiniQ column, another anion exchange column, which is known to have higher resolution capabilities than the MonoQ column. Surprisingly, all the proteasomes eluted off this column were able to rapidly degrade GST- IκBγ in an *in vitro* degradation assay (Fig 3.3.3A). When the activity of these "miniQ fractions" were compared to pooled fractions from the previous mono Q step, the miniQ 20S proteasome fractions were noticeably more active than the "monoQ fractions" (Fig 3.3.3Bi). Additionally, the active 20S "miniQ fractions" were missing a protein band located above the 30kDa marker in

comparison to the "monoQ fractions" upon SDS gel analysis (Fig 3.3.3Bii).

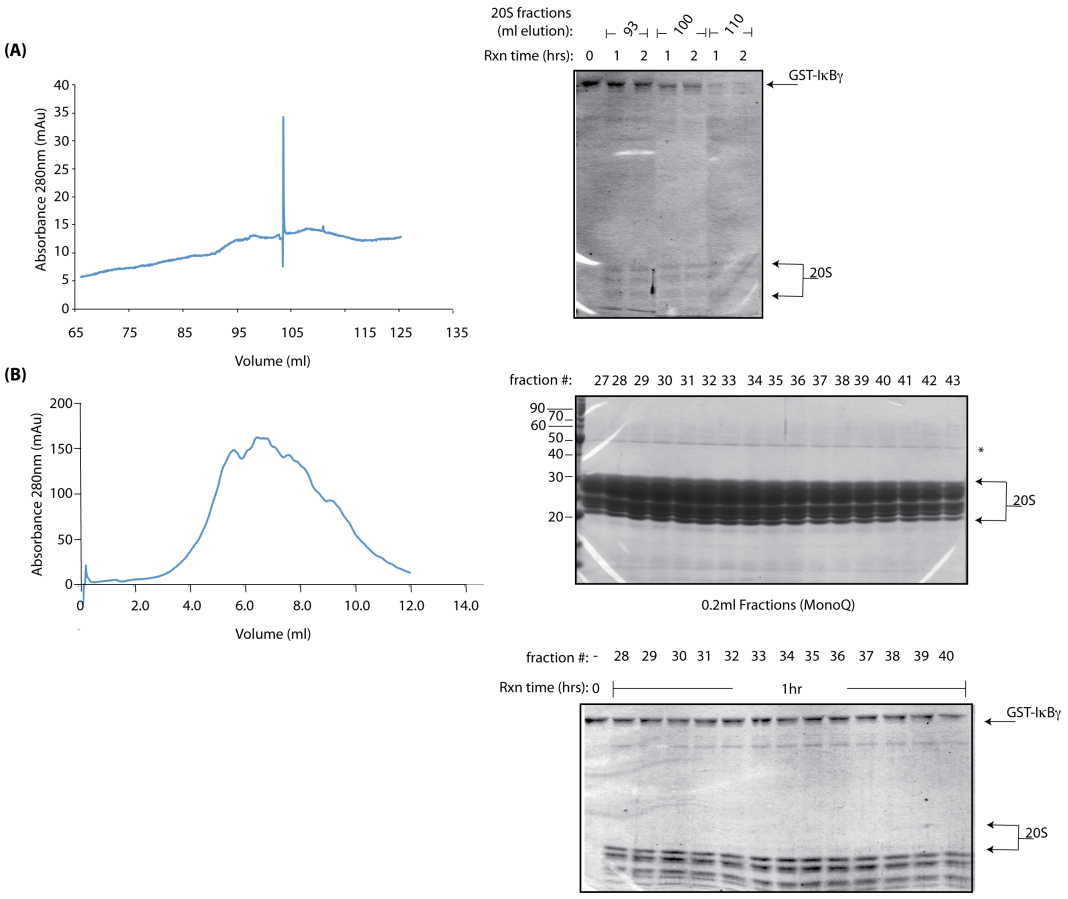

Figure 3.3.2: Separation of 20S proteasome by Mono Q chromatography produces inconsistent 20S activity.

Chromatograms of 20S proteasome fractionation from the MonoQ column, from an earlier purification trial, which used a 300-400mM NaCl gradient **(A)** or from a current purification trial, which used a 350-376mM NaCl gradient **(B)** are shown on the left hand side. In order to test the ability of the proteasome to degrade GST-IκBγ, an activity assay was performed using the 20S fractions from the chromatogram in **(A)**, where the results were visualized by coomassie staining on a SDS gel (top right). The peak fractions from the chromatogram in **(B)** were visualized on a coomasie stained SDS gel (right, middle). 20S fractions from chromatogram **(B)** were then tested for their ability to degrade GST- IκBγ (bottom right).

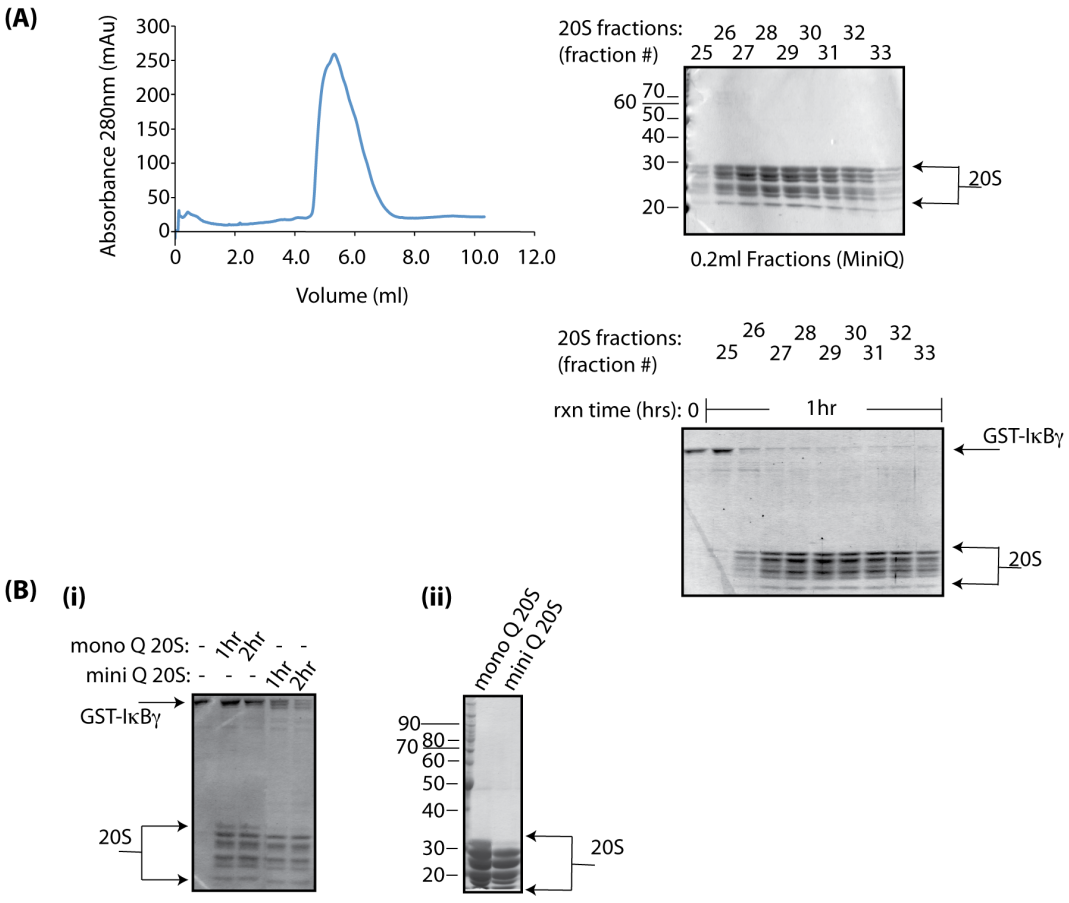

Figure3.3.3: Separation of 20S proteasome by Mini Q chromatography produces active 20S.

(A) Following MonoQ ion exchange chromatography, 20S fractions were pooled and separated on a MiniQ column. The elution profile is shown on the top left and the chromatogram fractions were analyzed by 1D SDS gel analysis (top right). An activity assay of the 20S fractions from the chromatogram in **(A)** was then performed (middle right). **(B)** An activity assay of 20S proteasome and 1D SDS gel analysis of the 20S following monoQ fractionation or miniQ fractionation is presented in Bi and Bii, respectively.

3.3.3 LC-MS/MS analysis of 20S samples reveal that active MiniQ proteasome contains higher amounts of cysteic acid modification than inactive MonoQ proteasome

In order to identify the differences between these pools of active and inactive 20S proteasome, the active "miniQ fractions" and the inactive "monoQ fractions" were separated on 1D 10% and 12% SDS gels, respectively. The resulting protein bands were individually excised, subjected to an in-gel tryptic digest, and analyzed by LC-MS/MS on a hybrid quadrupole-quadrupole time of flight instrument (QqTOF). The data were then analyzed by searching against a bovine database. While 1D SDS gel analysis failed to completely separate proteasome subunits, LC-MS/MS results indicate that all 7 α subunits and 7 β subunits were present in both active and inactive subunits, with an average sequence coverage of 65% (Table 3.3.1). Each gel band was identified to contain multiple subunits, and identical proteasome subunits were also found to be distributed amongst multiple gel bands (Figure 3.3.4). In addition, LC-MS/MS results show the absence of contaminating bands. All together these results indicate that the absence of the 30kDa migrating band in the active "mini Q" fractions was not due differences in subunit composition. Thus the focus shifted to post-translational

modifications, which also cause shifts in protein migration. The Mascot database search included the following post-translational modifications: phosphorylation, protein N-terminal acetylation, deamidation, oxidation, propionamide, and pyro-glu. Search results indicate that several subunits were found to be N terminally acetylated (β 4, α 6, α 3, β3, α 2). Additionally, serine phosphorylation of subunit α3 on its highly acidic C-terminal peptide was also found. Interestingly, a refined Mascot database search including cysteine sulfonic acid, also known as cysteic acid (-SO_3H), and methionine sulfone, revealed that thiol oxidation was indeed present within the samples. In particular, methionine sulfoxides and methionine sulfones were found, as well as 16 distinct peptides containing cysteic acid modifications. The earlier forms/stages of cysteic acid formation, cysteine sulfenic (-SOH) or cystein sulfinic (-SO_2H) acid containing peptides, were not found. However, most strikingly, the active "MiniQ fractions" were found to contain a higher degree of cysteic acid modifications compared to the inactive "MonoQ fractions". This is most convincingly shown in the a1 subunit, where there is equal sequence coverage between the inactive and active 20S samples, but where two more cysteic acid modifications were found in the active MiniQ fractions (Table3.3.1). This particular post-translational modification has been shown to modulate

the activity of proteins, such as in the case of peroxiredoxin (Bozonet et al., 2005; Veal et al., 2004; Woo et al., 2003a). Given that more cysteic acid modifications were found to occur in the active 20S samples, we hypothesized that the increase in 20S activity was due to an increase in its oxidation state. All together, these results demonstrate that 20S proteasome isolated from bovine blood is subjected to many post-translational modifications, which effect its elution from the MonoQ and MiniQ ion exchange columns.

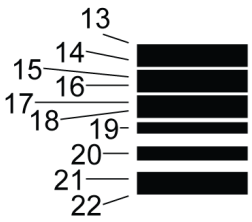

band	Subunits
13	α6/α4
14	α4/α6
15	α7/α3/α4
16	α7/α3/α1
17	α7/α1/α3
18	α1/α5/β2
19	α2/α1/α5
20	β6/β3/β7
21	β3/β5/β6/β4
22	β4/β5/β3/β1

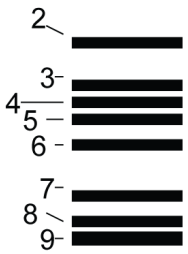

band	Subunits
2	α4/α6
3	α3/α7
4	α1/β2/α7
5	α1/α5/β2
6	α2/α5
7	β7/β6
8	β3/β4/β6
9	β5/β4/β3/β1

Figure 3.3.4: Schematic of LC-MS/MS proteasome subunit analysis of active MiniQ and inactive MonoQ 20S samples

Two 20S proteasome complexes with different activities are partially purified by 1-D SDS-PAGE. Since none of the 14 subunits are completely separated, each band contains a mixture of subunits. Different percentage gels were run in order to optimize the separation of a contaminating band at 50kDa. These bands were identified as cross-linked 20S subunits (data not shown).

Table 3.1: Cysteic Acid modifications in active MiniQ vs inactive MonoQ 20S samples

			10% GEL		12% GEL	
Protein	*Accession*	*#AA*	*%Seq Cov*	*#Cysteic*	*%Seq Cov*	*#Cysteic*
α1	XP_583783	246	65	3	63	1
α2	NP_001029834	234	79	0	44	0
α3	NP_001029407	255	65	1	47	0
α4	NP_001029553	261	67	1	47	0
α5	NP_001015566	241	65	1	41	0
α6	NP_001030387	263	66	1	68	0
α7	NP_001029405	248	87	3	42	0
β1	NP_001029541	239	36	1	19	0
β2	NP_001033616	277	57	2	19	0
β3	NP_001029768	205	63	1	51	1
β4	NP_001015615	201	80	1	45	1
β5	NP_001032701	263	55	0	56	0
β6	NP_001033628	241	56	0	37	0
β7	NP_001029438	264	42	1	34	0

The subunit sequence coverage following LC-MS/MS analysis of two functionally distinct 20S proteasome complexes is shown **(red)**. Accession numbers are included for clarity. A major difference between the two complexes is the greater number of cysteic acids **(blue)** found in the active complex (10% gel).

3.3.4 Purification of 20S proteasome from oxidizing condition produces inconsistent 20S activity

To test more thoroughly whether differences in oxidation do in fact effect 20S activity, bovine blood from the same source vial was divided in half, where each half of the batch was purified either in the presence or absence of reducing agent, followed by an activity assay using GST-IκBγ. The results from the purification trials remain contradictory. While 20S proteasome purified in the presence of 5mM βME was inactive and 20S proteasome purified in the absence of βME was active towards IκBγ, and is in agreement with our hypothesis, 20S purified in the presence and absence of 2mM TCEP had comparable activities (Fig 3.3.5A and B). This result is surprising because TCEP is supposedly a more stable reducing agent than βME. When the proteasome banding pattern was compared after each step of purification in the presence or absence of 2mM TCEP, 20S samples purified in the absence of reducing agent contained a fainter amount of the 30kDa band, which is similar to the banding pattern of active MiniQ fractions (Fig 3.3.5C). However, there was no enhanced degradation activity of 20S proteasome purified in the absence of reducing agent. Further analysis by MS was also inconclusive. While 20S

purified in the presence of TCEP was analyzed using LC- MS/MS, 20S samples purified in the absence of TCEP were analyzed by TORP, another MS method, which resulted in poor sequence coverage (data not shown). Thus, we were unable to conclude whether or not either samples had more or less cysteic acid modification.

Given the inconsistency of the activity of 20S purified in the presence and absence of reducing agent, it seemed to suggest that within tissue, the 20S proteasome exists as a heterogeneous pool. This could further increase the heterogeneity of the 20S pool and could mask the increased activation upon oxidation effect. It has been shown that 20S purified from aged rat skeletal muscle differs in activity than 20S isolated from young rat skeletal muscle. This difference in activity has been shown to be due to differences in the oxidation state of the proteasome (Ferrington et al., 2005). Additionally, 20S purified from untreated and sugar starved maize roots revealed oxidation of the proteasome from the starved roots (Basset et al., 2002). Thus, the source of the blood used for purification, as in whether the blood was drawn from an older or younger cow or from a well-nourished or malnourished cow, could affect the results. Thus, this led us to go to cells where we could better control the homogeneity of 20S.

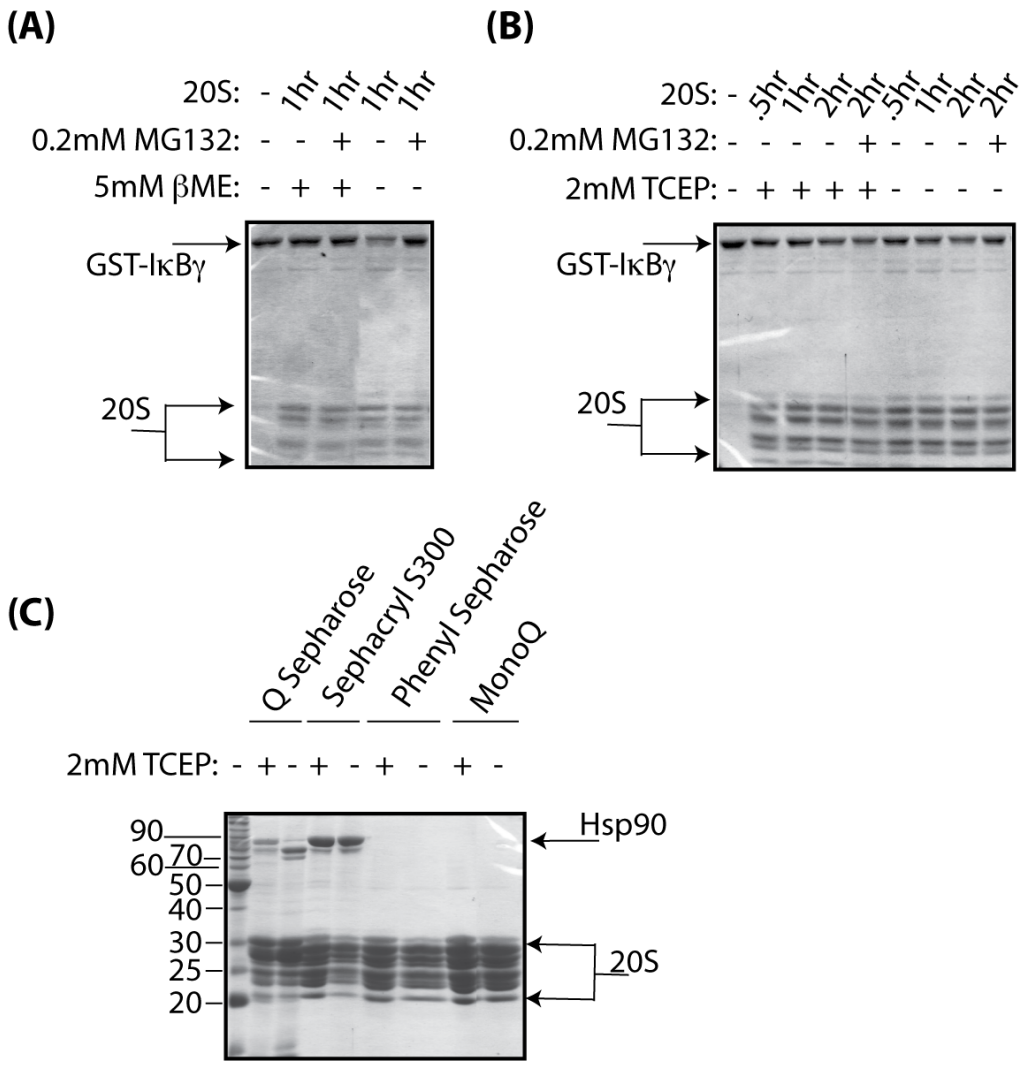

Figure3.3.5: 20S purified in reduced and oxidizing conditions produced inconsistent differences in activity.

(A to B) Activity assays were performed using 20S proteasome isolated from bovine blood in the presence or absence of 5mM βME **(A)** or 2mM TCEP **(B)**. The degradation of recombinant GST- IκBγ was monitored by coomassie gel analysis. Proteasome inhibitor, MG132, was used to verify that IκBg degradation was due completely to the activity of the proteasome. **(C)** To determine whether 20S proteasome purified in the presence or absence of 2mM TCEP contained different protein banding patterns, similar to the "inactive MonoQ" and "active MiniQ" 20S fractions, the 20S isolated after each chromatography step was visualized by coomassie staining.

3.3.5 20S proteasome isolated from oxidatively stressed cells has comparable activity to 20S proteasome isolated from control cells

In order to create a more uniformly oxidized proteasome, HeLa cells were treated with 200mU/ml of glucose oxidase (GO), a reagent which creates chronic levels of intracellular hydrogen peroxide. The cells were treated for 3, 4, or 5 hours with GO and subsequently, 20S proteasome was immunoprecipitated (IP'd) from the cells. The activity of IP'd 20S between treated and untreated cells was then compared, by determining the rate of degradation of recombinant His tagged IκBa (His-IκBα)(Fig 3.3.6A). The intensity of the IκBα band remained the same after degradation by the 20S IP'd from oxidatively stressed to untreated cells, where equal levels of 20S were present in each immunoprecipitation (IP) reaction, as verified by immunoblotting against 20S subunit α3 (Figure 3.3.6B).

To further ensure that the degradative ability of the proteasome was not impaired by the IP reaction and to more fully dilute out the protease inhibitor cocktail present in the cell lysate buffer, 20S was isolated from 200mU/ml GO treated MEF cells by gel filtration (Superose6), followed by anion exchange chromatography (HiTrapQ).

The presence of 20S proteasome was verified by silver stain analysis (Figure 3.3.6D). An activity assay was then performed testing the ability of 20S isolated under oxidizing conditions to degrade His- IκBα, under different temperatures, as well as with different enzyme to substrate ratios (Figure3.3.6C). However, in all conditions, 20S isolated from oxidized cells did not display any enhanced activity.

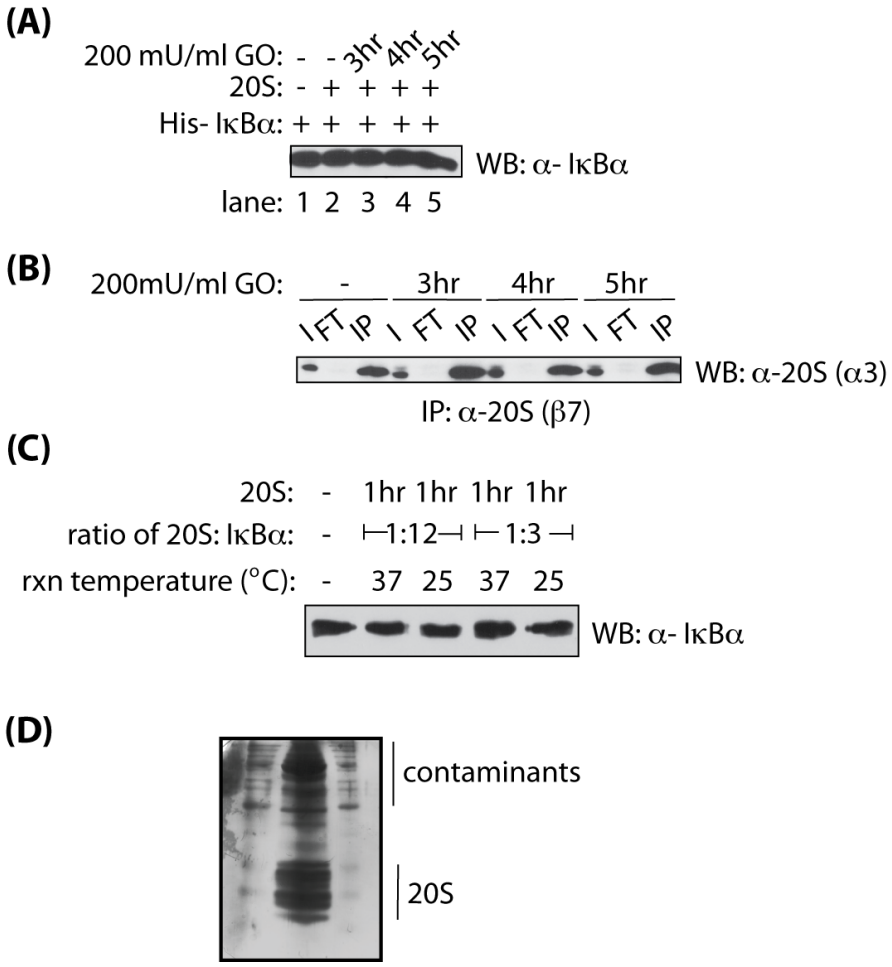

Figure3.3.6: 20S isolated from oxidatively stressed cells does not have enhanced degradation activity

(A to B) HeLa cells were treated with 200mU/ml of glucose oxidase (GO) for the indicated times. Following IP of 20S from the cell lysate, an activity assay was performed by adding recombinant His- IκBα to the isolated proteasome **(A).** To ensure equal amounts of 20S proteasome were present in each IP reaction, a western blot against 20S subunit α3 was performed **(B)**. **(C to D)** MEFs were treated for 3hrs with 200 mU/ml GO. 20S proteasome was then isolated and analyzed for purity by silver stain analysis **(D)**. An activity assay was then performed using recombinant His- IκBα **(C)**. The reaction was done at different temperatures (25°C or 37°C) and at varying ratios of enzyme (20S) to substrate (IκBα). IκBα degradation was monitored by western blot using an antibody against the C-terminus of IκBα. In= input, FT= flow through

3.4 Discussion

LC-MS/MS analysis indicates that the proteasome contains several post-translational modifications (PTMs): acetylation, phosphorylation, and thiol oxidation, in particular methionine sulfoxide and cysteic acid modifications. The identification of these modifications is supported by the fact that these types of modifications have also been reported in the literature (Schmidt et al., 2010; Zong et al., 2006; Zong et al., 2008). For example, our MS analysis reveals phosphorylation on the α3 peptide (ESLKEEDESDDDNM), which was also identified in the murine cardiac 20S proteasome (Zong et al., 2006). We also observed cysteic acid modifications. In general, cysteic acid modifications arise from reaction with cysteine thiolates with H_2O_2, that are then converted to Cys-SOH, which can be further oxidized to Cys-SO_2H or Cys-SO_3H depending on the level of oxidative stress in the environment (Poole et al., 2004). Although we have not clearly established that the cysteic acid modifications arise solely from biological events and not from artificial modifications that come from sample preparation, such as air oxidation, we can, in the future, use chemical agents that bind to the primary oxidation event. The primary oxidation event would then be in a chemically distinct form from the latter artificial oxidation events

(Zong et al., 2008). However, recent reports stating that cysteic acid modifications were found in 20S proteasome isolated from mouse and Jurkat T cells, support our finding that the proteasome is susceptible to cysteic acid modification (Schmidt et al., 2010; Schmidt et al., 2006). Moreover, our finding that the 20S has a tendency to be oxidized is also supported by another aspect in our studies, where LC-MS/MS identified proteasome subunits as the contaminating 50kDa band seen in the 1D SDS gel analysis of purified proteasome (Fig3.3.2B middle). Since all proteasome subunits are known to migrate roughly between 20 to 30kDa, the slower migration of this band on an SDS gel strongly suggest potential cross-linking ability of these subunits. All together, these results suggest that the 20S undergoes cysteic acid modification.

Most strikingly from our results, we observed a disproportionate amount of cysteic acid modifications present in the "active MiniQ" 20S samples as opposed to the "inactive MonoQ" 20S samples (Table 3.3.1). However, because there is less sequence coverage of the inactive MonoQ samples, we cannot firmly conclude that the MiniQ 20S samples are more oxidized. To more directly quantitate the differences in redox state between samples, further MS analysis, which compares the PTM signal on identical peptides from both samples, can be done by using differential alkylation with stable isotopic labeling reagents

[$^{12}C_2$]-iodoacetic acid and [$^{13}C_2$]-bromoacetic acid (Atsriku et al., 2007). However, despite lacking such analysis, the active and inactive 20S samples serve as internal controls for each other, in that they were prepared similarly, and thus, imply that the MiniQ 20S samples contain a higher level of oxidation than MonoQ 20S samples.

Based on our LC-MS/MS results, we suggest that PTMs affect the activity of the 20S proteasome. Although we were unable to determine whether the α3 phosphorylation event was present in the active or inactive 20S samples, phosphorylation on α3 by PKA has been reported to activate murine 20S proteasome *in vitro* (Zong et al., 2006). Further experiments would need to be done to determine whether this phosphorylation event does indeed regulate the differences in the rate of degradation of NF-κB inhibitor molecule, IκBγ.

Our observation that active MiniQ 20S proteasome fractions contained more cysteic acid modifications than inactive MonoQ 20S fractions suggest that oxidation of the 20S proteasome increases its hydrolyzing activity (Table 3.3.1). While it is known that oxidation of the proteasome changes it activity, there are conflicting reports as to whether oxidation enhances or decreases the activity of the proteasome. 20S proteasome isolated from Alzheimer's disease subjects and aged rat muscle have decreased chymotrypsin-like activity

compared to control subjects and muscle, respectively. However, the chymotrypsin-like activity was regained once the 20S was treated with reducing agent, DTT (Cecarini et al., 2007; Ferrington et al., 2005). These results indicate that oxidation of the 20S decreases its activity, whereas reduction of the proteasome increases its activity. In contrast, 20S isolated from chicken erythrocytes and plants exposed to either H_20_2 or metal catalyzed oxidation, respectively, displayed increased activity, suggesting that oxidation of the 20S increases its activity (Strack et al., 1996). Our attempts to fully demonstrate that oxidation of the 20S increases its proteolytic activity were inconclusive. We first tried to determine whether the activity of 20S purified from bovine blood in the absence of reducing agent was enhanced compared to 20S purified from the same source of bovine blood in the presence of reducing agents, βME and TCEP. However, whereas purification in the absence of βME produced 20S that was significantly more active than 20S purified in the presence of 5mM βME, purification of 20S in the absence or presence of 2mM TCEP produced 20S with comparable activities (Fig3.3.5). When we then attempted to more uniformly oxidize 20S by oxidatively stressing mammalian cells, isolation of 20S from oxidatively stressed HeLa and MEF cells produced overall inactive 20S (Fig3.3.6). However, due to the inconsistency of these results, we cannot firmly

conclude that oxidation of the 20S proteasome does not enhance its activity. Additionally, other lines of evidence suggest that oxidation enhances its proteolytic activity. For example, the dramatic difference in activity before and after MiniQ is puzzling given that the MonoQ and MiniQ are fundamentally not different, both are ion exchange columns and differ only in resin bed bead size. This then brings up the question, what does cause the dramatic shift in 20S activity? A plausible explanation could be the amount of time between MonoQ and MiniQ fractionation, in that MonoQ fractions were left at 4°C for several days before MiniQ fractionation. This would allow for the reducing agent to break down leading to the oxidization of the MiniQ fractions, which is in agreement with LC-MS/MS results indicating oxidation of the MiniQ samples. Additionally, oxidation studies done with liver epithelial 20S proteasome provide a plausible explanation as to why the activity of mammalian 20S was not enhanced upon its isolation from oxidatively stressed cells. In the case of liver epithelial 20S, treatment with 1mM H_20_2 leads to a 50% decrease in activity against short lived cellular proteins, as opposed to 20uM to 400uM H_20_2 which increased its activity (Basset et al., 2002; Grune et al., 1995). These results indicate that proteasome activity is dependent on the level of oxidative modification and that mild oxidation can lead to increases in activity but that over-oxidation

can inactivate the enzyme. Since we now know that treatment of cells with 200mU/ml GO produces well over 250uM H_2O_2 consistently in the cell (Chapter 2), treatment of the cells with 200mU/ml GO could over-oxidize the proteasome, rendering it inactive. In order to conclusively demonstrate that mild oxidation of the mammalian 20S proteasome enhances its activity, future experiments can be done where we would titrate amounts of GO and then test the activity of the 20S. Furthermore, if LC-MS/MS can pinpoint sites that are undergoing oxidation, we can perform mutational analysis and over-express these mutant subunits in cells and test the activity of the proteasome. All together, we have shown that we can isolate 20S proteasome from bovine blood to 99% purity, as determined by LC-MS/MS. This 20S proteasome is susceptible to a variety of PTMs, including phosphroylation and thiol oxidation. We also demonstrated that the 20S proteasome degrades NF-κB inhibitor molecule, IκBγ, in a ubiquitin and ATP independent manner, an event which may depend on mild oxidation of the 20S proteasome's cysteine residues.

3.5 Acknowledgments

I would like to thank Justin Torpey for performing all of the mass spec analysis and valuable discussions; Erika Mathes for the His- IκBα protein; Yidan Li for her critical reading of this chapter. JH is supported by the Ruth L. Kirschstein National Research Service Award NIH/NCI T32 CA009523.

Parts of Chapter 3 are adapted from a manuscript in preparation, 2010. Ho, Jessica Q.; Hyunh, Kim; Mathes, Erika; Ghosh, Gourisankar. "PA28αβ bound 20S is responsible for the degradation of free IκBα". The dissertation author is the primary author. I designed and performed all of the experiments, except for the mass spec analysis, which Justin Torpey performed. I also analyzed the data and wrote the manuscript. Gourisankar Ghosh is the corresponding author.

Chapter 4: PA28αβ mediates the ubiquitin independent degradation of free IκBα

4.1 Introduction

The most well known activators of the 20S proteasome are the 19S regulatory particle (RP) and the PA28 family of RPs. The 20S proteasome can be gated on the top and bottom by 19S RPs, to form the 26S proteasome, a 2.5MDa complex. The19S RP consists of the lid, which binds and de-ubiquitinates protein substrates, and a base, which contains ATPases. In order for globular proteins to be degraded, the protein interacts with the 19S base, undergoes protein unfolding by the ATPases, and translocation into the 20S catalytic core (Voges et al., 1999). It has been shown that, while ATP hydrolysis is required for protein unfolding, ATP binding alone to the 19S ATPase subunits causes association to the 20S proteasome, gate opening, and translocation of unfolded proteins (Smith et al., 2005).

There are 3 family members in the PA28 activator complexes: PA28α, PA28β, and PA28γ. PA28α and β form a heteroheptamer, PA28$\alpha\beta$, whereas PA28γ exists as a homoheptamer. Although PA28α and β share 50% amino acid homology, PA28γ only shares 25% amino acid homology with PA28α and β. However, the overall secondary structure, which is composed of 4 α helices with a linker sequence between helix 2 and 3, is similar between all PA28 family members (Li

and Rechsteiner, 2001). The linker region is called the activation loop, and mutation within the loop results in the inability of the PA28 RP to activate the proteasome. Chimera studies also reveal that the N terminus region in combination with the activation loop assist in PA28 oligomerization, but that the C terminus region helps the stability of the PA28 complex in binding to the 20S (Zhang et al., 1998). Binding of PA28αβ to the 20S enhances the proteolyitc activity of all 20S active sites (trypsin like, chymotrypsin like, and PGPH like), while binding of PA28γ only enhances the trypsin like activity (Mao et al., 2008; Realini et al., 1997).

PA28αβ subunits are expressed in many organs, are abundant in immune tissues, are primarily expressed in the cytosol, and are induced by interferon (IFN)-γ and infection. The primary role of PA28αβ is the generation of antigens for presentation by class I molecules in the acquired immune response (Schwarz et al., 2000). It is thought to enhance the production of MHC class I epitopes either by altering the specificity of the cleavage or facilitating peptide diffusion from the 20S core to produce longer peptides (Rechsteiner and Hill, 2005). In contrast, PA28γ is primarily expressed in the brain, is present primarily in the nucleus of cells, and is not upregulated by IFNγ (Mao et al., 2008; Rechsteiner and Hill, 2005). Since PA28γ deficient mice have reduced

body size and *pa28g*$^{-/-}$ MEFs have slower transition from the G to S phase in cell cycle, PA28γ is thought to be involved in cell proliferation and cell cycle transition (Barton et al., 2004; Murata et al., 1999). This is further illustrated by the recently identified cellular targets of PA28γ (Chen et al., 2007; Li et al., 2007; Li et al., 2006).

The 26S proteasome and PA28γ bound to 20S can both degrade protein substrates in a ubiquitin (Ub) and ATP independent manner. All of these substrates are loosely unfolded in their native states. For example, 26S proteasome was able to degrade both the insulinB chain and β-casein in a cell- free proteolysis assay in the presence of a non-hydrolyzable form of ATP, ATPγS, and without prior ubiquitination of either substrate (Smith et al., 2005). Cell cycle inhibitor p21 can also be degraded *in vitro* in the absence of Ub and ATP by both the 26S proteasome and PA28γ (Li et al., 2007; Liu et al., 2006a). RNAi, gain of function experiments, and analysis of *pa28*$^{-/-}$ MEFs together reveal that PA28γ degrades oncogene steroid co-activator-3 (Src-3), as well as cell cycle inhibitors, p21, p16, and p19, in an ATP and Ub independent manner. The degradation of p21 by PA28γ bound 20S is thought to be facilitated by direct interaction between PA28γ and p21. In the cell, p21 is known to either be bound to one of many different interacting partners, such as CDK2/cyclin complexes and PCNA, or to be in a free

unstructured state. *In vitro* degradation assays revealed that PA28γ degraded free p21 at a faster rate than p21 incubated with its binding partner, Cdk2/cyclin E, indicating that PA28γ only mediates the Ub-independent degradation of the free form of p21. This is similar to Src3, which is only degraded in its free unstructured state(Chen et al., 2007; Li et al., 2007; Li et al., 2006).

NF-κB inhibitor molecule, IκBα, also exists in bound and free states. IκBα can bind to NF-κB transcription factors to inhibit their translocation to the nucleus. Upon stimulation of the cell, bound IκBα undergoes ubiquitination, which then leads to its degradation by the 26S proteasome. Unbound or free IκBα is rapidly synthesized and degraded in resting cells (Frankenberger et al., 1994; Scott et al., 1993). Its purpose is to ensure the complete inhibition of NF-κB, thus preventing leaky NF-κB activity at the basal level. This free pool of IκBα is also required for the stimulus- induced NF-κB response, given that stabilization of free IκBα dampens the NF-κB response. Free IκBα is known to be unstructured and only becomes stabilized upon binding to NF-κB. Turnover of free IκBα has been shown to be independent of internal lysine ubiquitination, and can be degraded *in vitro* by the 20S proteasome (Mathes et al., 2008; O'Dea et al., 2007).

Based on the results presented in chapter 3, where we were unable to determine whether an active pool of 20S is solely responsible for the degradation of free IκBα, we set out to determine if the 26S and/or PA28 bound 20S proteasomes are involved in the Ub-independent turn- over of free IκBα. To this end, we used a combination of *in vitro* and *in vivo* approaches.

4.2 Materials and Methods

4.2.1 Purification of PA28α

Recombinant PA28α was purified as described in (Gao et al., 2004; Masters et al., 2005) with minor modifications. BL21 cells expressing human PA28α were a kind gift from Dr. Gregory Pratt's laboratory. Glycerol stocks of BL21 cells expressing PA28α were streaked onto an ampicillin plate and individual colonies were used to culture two liters of LB media containing 100ug/ml of ampicillin. The PA28α culture was grown at 30°C and induced with 0.6mM IPTG at an OD_{600} of 0.3. Two hours post- induction, the cells were collected after spinning at 6300rpm for twenty minutes. Cells were then lysed with 120ml of lysis buffer (10mM Tris, pH 7.0, 25mM KCl, 10mM NaCl, 1.1mM MgCl2, 0.5mM PMSF) for each 2L pellet. After addition of protease inhibitor cocktail (sigma), the cells were sonicated and insoluble cell material was cleared after centrifugation for 45 minutes at 13K rpm. The crude soluble lysate was then loaded onto a Q Sepharose Fast Flow column (Amersham), which had been pre-equilibrated with lysis buffer, and proteins were eluted over 10 column volumes, with a linear gradient from 10mM to 500mM NaCl. PA28α containing fractions, as verified by 1D SDS gel analysis, were then pooled and loaded onto a HP High Trap Q column (anion

exchange) (Amersham), which had been pre-equilibrated in lysis buffer. Bound proteins were eluted over ten column volumes using a linear gradient from 10mM to 250mM NaCl. PA28α containing fractions were pooled based on the absence of higher molecular weight contaminating migrating proteins (50-60kDa). Pooled fractions were then loaded onto a Superdex200 size exclusion column (Amersham), which had been pre-equilibrated with gel filtration buffer (10mM Tris pH 7.0, 190mM KCl, 10mM NaCl, 1.1 mM MgCl2, 0.1mM EDTA, 1mM DTT). Homogenous PA28α protein was pooled based on its migration off size exclusion chromatography as a heptamer as well as its overall purity. The resulting protein was judged to more than 99% pure by SDS PAGE analysis. The purification steps preceding the HP High trap Q step were carried out at 4°C, and all following steps were carried out at room temperature.

4.2.2 Purification of PA28β

PA28β was purified as described in (Gao et al., 2004), with the following modifications. BL21 cells expressing human PA28β were a kind gift from Dr. Gregory Pratt. PA28β was cultured from LB broth containing kanamycin, in a manner identical to PA28α, where the only the time

frame of induction was altered (cells were induced at an OD_{600} of 0.2). The cells were then collected and lysed in lysis buffer (10mM Tris pH 8.8, 25mM KCl, 10mM NaCl, 1.1mM MgCl2, 10mM BME, 0.5mM PMSF) containing protease inhibitor cocktail. After removal of insoluble material, the supernatant underwent a 40% ammonium sulfate precipitation, and the precipitated pellet was then dissolved in dialysis buffer A (10mM Tris pH8.8, 0.5mM PMSF, 20mM BME) where each 35 mL of precipitated supernatant pellet was dissolved in 3 mL of dialysis buffer. The re-dissolved pellet was then dialyzed against two liters of dialysis buffer A for three to four hours at 4°C. The dialyzed protein was then spun down for 15 minutes at 13k rpm to clear precipitated material. The crude protein was further diluted 24 fold with dialysis buffer and loaded onto Q Sepharose Fast Flow column, and PA28β containing fractions were eluted over 10 column volumes with a linear gradient from 100 to 300mM KCl. PA28β containing fractions were pooled and dialyzed against four liters of dialysis buffer B (5mM potassium phosphate pH 6.7, 10mM BME) for four hours at 4°C. The dialyzed fractions were then loaded onto a freshly prepared hydroxyapatite column, pre-equilibrated in dialysis buffer B. Bound proteins were eluted over 10 column volumes with a linear gradient from 50 to 300mM potassium phosphate pH 6.7. PA28β was then pooled

based on its overall purity, where the protein was judged to be greater than 80% pure. Since PA28β was prone to be proteolytically cleaved, all purification steps were carried out at 4°C.

4.2.3 PA28αβ complex formation

PA28αβ complex was purified, loosely following the protocol given in (Song et al., 1997). PA28αβ was first purified as individual components, given that recombinant PA28α purifies as a hetero-heptamer and that PA28β purifies as monomer (Realini et al., 1997). The following protocol was performed at room temperature. The two purified proteins were combined with an 14 fold molar excess of PA28β relative to PA28α. The proteins were diluted in refolding buffer (190mM KCl, 10mM NaCl, 1.1mM MgCl2, 0.1mM EDTA, 10mM Tris pH7.5, 10mM BME, 5% glycerol) such that the final concentration of each protein was less than 0.1mg/ml. The mixture was incubated at room temperature for two hours with constant rotation. After concentration with a YM30 concentrator (Amicon), the mixture was then loaded onto a Superdex200 size exclusion column, pre-equilibrated in gel filtration buffer, which was refolding buffer without glycerol. Purified complex

was pooled based on its migration as a hetero-heptamer. The presence of both components was verified by immunoblotting against the individual components, and equal stoichiometric amounts of each protein component were then verified by 1D SDS gel analysis. The resulting protein was judged to more than 90% pure by SDS gel analysis.

4.2.4 Purification of PA28γ

PA28γ was purified following the protocol as stated above for PA28α, with the following minor modifications. BL21 cells expressing human PA28γ were a kind gift from Dr. Gregory Pratt. Glycerol stocks of BL21 cells expressing PA28γ were streaked onto a kanamycin plate and individual colonies were used to culture two liters of LB media containing 25ug/ml of kanamycin. Cell lysate was loaded onto a Fast Flow Q sepharose column, pre- equilibrated with lysis buffer, and crude PA28γ fractions were eluted using a linear gradient of 10-500mM NaCl. Fractions containing the highest percentage of PA28γ protein in comparison to contaminating bands were pooled and loaded onto a HP HiTrap Q column. Proteins were then eluted with a linear gradient from 150- 300mM NaCl, where PA28γ containing fractions were pooled

based on the absence or lower amounts of higher molecular weight contaminating bands. Finally, the pooled proteins were loaded onto a SuperdexS200 size exclusion column (Amersham), pre-equilibrated with lysis buffer containing 1mM DTT, and purified PA28γ was obtained upon pooling of only PA28γ fractions which migrated as a heptamer and contained the least amount of co-migrating higher molecular weight (50-100kDa) contaminating bands. The resulting protein was judged to be more than 90% pure by SDS gel analysis.

4.2.5 Purification of His tagged IκBα WT and IκBα Δ288

Bacterial expression plasmid, pet15b, containing gene constructs for either IκBα WT or IκBα Δ288 were introduced into BL21(DE3) cells. Transformed bacterial cells were cultured in 2 liters of LB Media with 100ug/ml ampicillin at 37°C. Once the OD_{600} reached 0.3, the cultures were induced with 0.1mM IPTG, and grown for 12-14 hours at 25°C. The cells were then collected by centrifugation at 5000rpm for 20min at 4°C. Cells were lysed with lysis buffer (20mM Tris-HCl pH 7.5, 100mM NaCl, 5mM βME, 1x protease inhibitor cocktail), followed by removal of insoluble material by centrifugation at 13k rpm 4°C. The remaining

soluble portion was loaded onto a Fast Flow Q column and eluted over 10 column volumes using a salt gradient from 200mM to 500mM NaCl. Fractions containing the protein of interest were verified by SDS page analysis and pooled together based on overall purity. Pooled fractions were then loaded onto a Nickel column, washed with Buffer A (20mM Tris pH 7.5, 200mM NaCl, 5mM Imidazole), and eluted with Buffer A containing 200mM Imidazole. Eluted proteins were then pooled, diluted 10 fold with buffer B (20mM Tris pH 7.5 and 1mM DTT), and loaded onto a HiTrap Q column, pre-equilibrated with buffer B. Proteins were eluted over 16 column volumes using a gradient from 100mM to 400mM NaCl. Pooled proteins were then further purified on an SD75 gel filtration column, pre-equilibrated with gel filtration buffer (10mM Tris pH 7.5, 150mM NaCl, 1mM DTT). Pooled proteins were judged to be 90% pure based on SDS page analysis.

4.2.6 *In vitro* degradation assays

Recombinant His- tagged IκBα WT or IκBα Δ288 was used as a substrate for the activity assays used to determine the activity of the proteasome. In the assay, substrate was mixed in a varying molar ratio with purified proteasome in a reaction buffer containing 200 mM NaCl,

20 mM Tris HCl, pH 7.1, 10mM $MgCl_2$ and 1 mM DTT. The mixture was incubated for the indicated periods of time at 25°C. The reaction was quenched upon the addition of 4X SDS dye and boiling for one minute at 95°C. The products were then separated by SDS-PAGE followed by visualization by coomassie staining. One tenth the amount of the same sample was used for visualization by western blot using IκBα antibody, specific against full length IκBα (Santa Cruz, sc-847).

4.2.7 Culturing of *nfkb*$^{-/-}$ cells

nfkb$^{-/-}$ cells were cultured as described in materials and methods from chapter 2.

4.2.8 Immunoprecipitation (IP) of regulatory particles (RP) to free IκBα

N-terminal Flag tagged IκBα was immunoprecipitated either from mouse p65$^{-/-}$p50$^{-/-}$crel$^{-/-}$ 3T3 cells or IκBa$^{-/-}$ 3T3 cells expressing transgene, Flag IκBα. These reconstituted cell lines were a kind gift from Dr. Erika Mathes. Following treatment, cells were washed two times with D-PBS (Gibco), and then lysed in RIPA buffer (20mM Tris pH7.5, 200mM NaCl, 1% Triton-X 100, 2mM DTT, 5mM p- nitrophenyl phosphate, 2mM sodium

orthovanadate, 1X protease inhibitor cocktail (sigma)). After the insoluble material was cleared upon centrifugation at 13k rpm for 10min at 4°C, each IP reaction was normalized with RIPA buffer to 1mg/ml, where each reaction contained a total protein amount of 500ug. Each reaction was then pre-cleared by adding protein G agarose (Upstate) for one hour at 4°C. To immunoprecipitate Flag- IκBα, 1ul of ten- fold-diluted monoclonal Flag antibody (Sigma, F3165) was added to the pre-cleared lysate at 4°C for 12-14 hours. Protein G agarose was then added to the reaction for an additional 2 hours at 4°C. The beads were collected after centrifugation at 3.3xg for 3 minutes, and washed 4xs (1ml/wash) with wash buffer (20mM Tris pH 7.5, 150mM NaCl, 0.5% Triton X 100). Following the last wash, 7ul of 4X SDS dye was added to the beads and the samples were boiled for 5 minutes at 95°C. 19S RP was visualized by separating the samples on a 10% SDS gel and immunoblotting against 19S subunit, Rpt6 (Biomol, PW9265). The 20S and PA28 regulatory particles were visualized by separating the samples on a 12.5% SDS gel and immunoblotting against 20S subunit α3 (Biomol, PW8115) and respective PA28 subunit (Biomol, PW 8185, 8240, 8190).

4.3 Results

4.3.1 Involvement of the 26S proteasome in ubiquitin (Ub) independent degradation

We first set out to investigate the involvement of the 26S proteasomes in the Ub-independent degradation of IκBα. Human 26S proteasome was purchased from Boston Biochemical and an *in vitro* degradation assay was performed, using recombinant His tagged IκBα as the substrate. In these assays, the rate of IκBα degradation is significantly slower when 26S proteasome is used compared to that of 20S proteasome alone, suggesting that, at least *in vitro*, the 26S proteasome is not primarily responsible for the Ub- independent degradation of free IκBα (Fig 4.3.1).

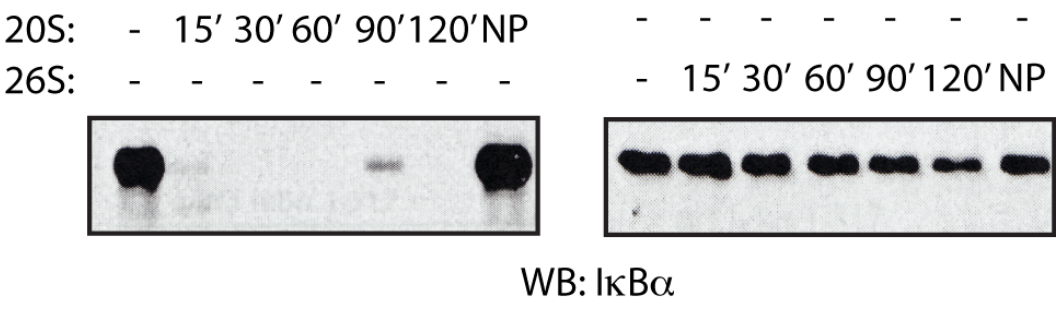

Figure 4.3.1: 26S proteasome degrades free IκBα at a slower rate than 20S proteasome *in vitro*

Recombinant full length IκBα was incubated with either 20S (left panel) or 26S (right panel) proteasome in a 1:10 ratio for the indicated periods of time at 25°C. IκBα was used for the degradation assay immediately after its elution from the Superdex200 (gel filtration) column. Degradation of free IκBα was visualized by western blotting against IκBα, using an antibody specific against the entire IκBα protein. NP= IκBα incubated for 120' at 25°C without proteasome. This experiment was done by Erika Mathes.

4.3.2 Involvement of PA28 regulatory particles (RPs) in ubiquitin (Ub) independent degradation

Next we set out to investigate whether other RPs, in particular the PA28 RPs, are involved in Ub-independent degradation of NF-κB inhibitor molecules, IκBγ and IκBα. To do so, we recombinately expressed and purified to homogeneity each of the different RPs, which make up the PA28 RPs: PA28αβ and PA28γ (Fig 4.3.2). While both PA28α and PA28γ are known to express as a heptamer, PA28β has been shown to express as a monomer. In order to form the PA28 αβ heptamer, this required that the components be purified separately and then mixed together, with PA28β being added in 14 fold molar excess to PA28α. Once the complexes were isolated, they were incubated with bovine 20S proteasome, which had been purified as previously stated in materials and methods (2.2.1). Following formation of the PA28 bound 20S proteasome complexes, each complex was tested for its ability to degrade both recombinant N-terminal GST tagged IκBγ (GST- IκBγ) and His tagged IκBα proteins (His-IκBα). While 20S alone can degrade both substrates without the addition of Ub or ATP, the addition of PA28α, PA28γ, and PA28αβ slightly enhances the degradation of IκBγ and IκBα (Fig 4.3.3A and B). This is most clearly seen at the 2hr time point

(compare lanes 8, 11, and 14 to lane 5 for both Fig 4.3.3A and B). In comparison to the other PA28 complexes, PA28αβ showed the most enhanced degradation of the substrates.

To more clearly determine if binding of PA28αβ to 20S enhanced the degradation of IκBα, we decided to use freshly purified recombinant His- IκBα for the *in vitro* degradation assays, since the Komives group has shown that recombinant IκBα is prone to aggregation upon storage at -80°C (personal communication). Immediately following elution from the Superdex 200 column (gel filtration), IκBα was mixed with either 20S alone or PA28αβ bound 20S in a degradation assay (Fig 4.3.3C). Addition of PA28αβ led to a significant increase in the rate of degradation of IκBα (compare Fig 4.3.3C lanes 4 and 5 to 10 and 11). To enhance the differences in degradation rate, 20S proteasome was added to IκBα in a 1:100 ratio (Fig 4.3.3C), as opposed to the other assays where the degradation assay was performed in a 1:12.5 ratio (Fig 4.3.3A and B). Addition of proteasome inhibitor, MG132, inhibited protein degradation, demonstrating that degradation was due solely to the activities of the proteasome. In summary, these results indicate that the *in vitro* degradation of NF-κB inhibitor molecules, IκBγ and IκBα, occurs in a Ub and ATP independent

manner and that PA28, especially PA28αβ RP's, bound 20S enhances the degradation of the these inhibitor molecules *in vitro*.

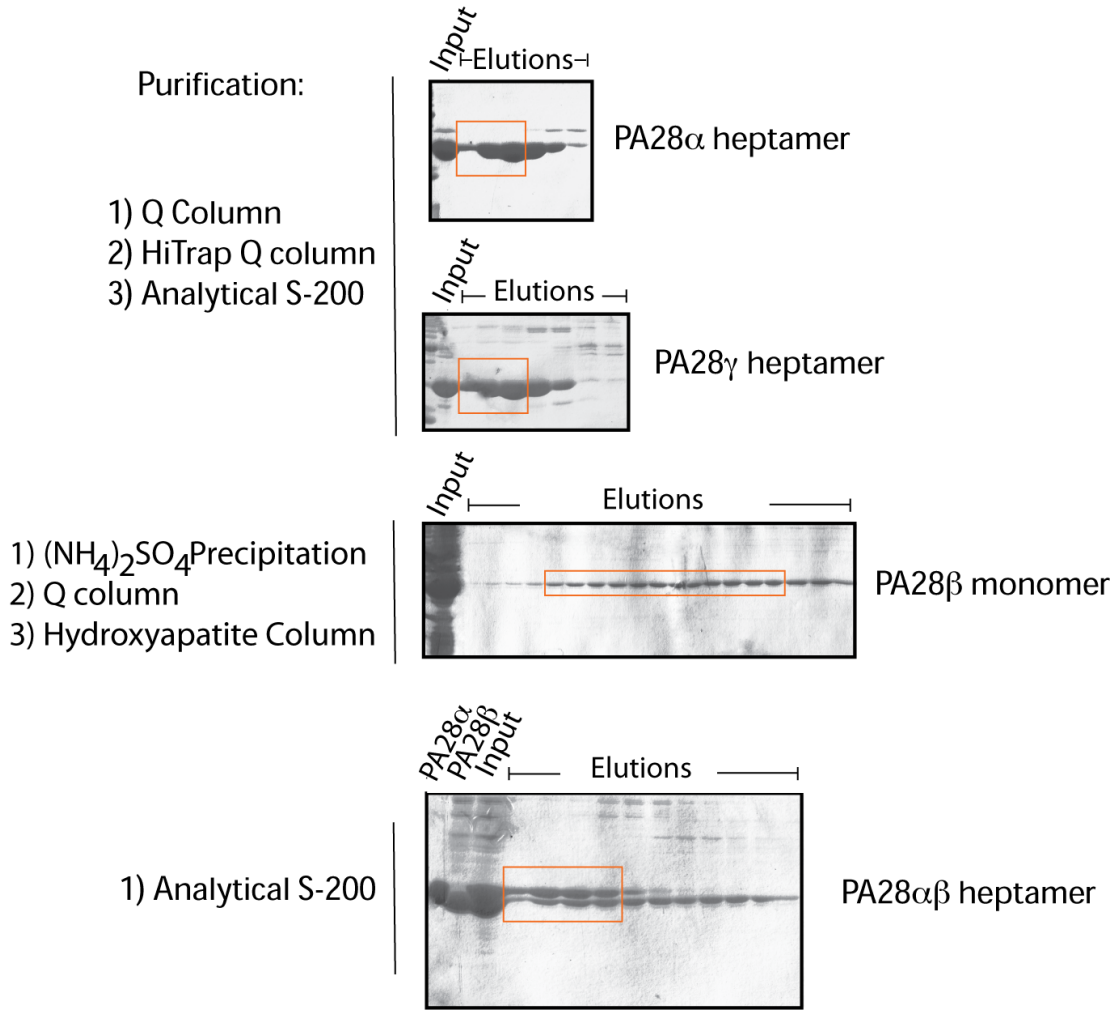

Figure 4.3.2: Purification summary for PA28 regulatory particles.

The purification of each PA28 subunit, as detailed in materials and methods, is summarized on the left side of the figure. Following the last step of purification, elution fractions are analyzed by coomassie stained SDS gels for homogeneity. Pooled elution fractions are indicated by orange boxes.

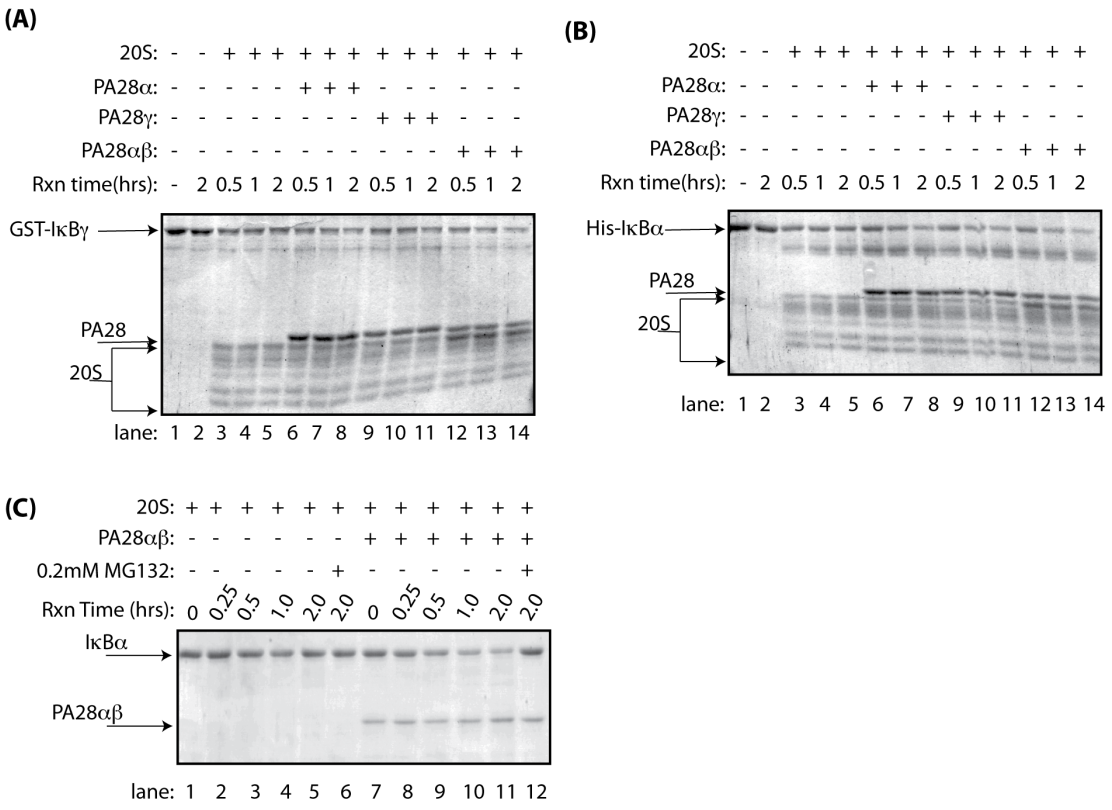

Figure 4.3.3: *In vitro* degradation of both IκBγ and IκBα is enhanced by binding of PA28 regulatory particles to 20S proteasome.

(A,B) Degradation assay of recombinant GST-IκBγ **(A)** or His-IκBα **(B)** by either 20S alone or the 20S bound to the indicated PA28 regulatory particle (RP). The indicated PA28 RP was mixed in 1.5 fold molar excess with 20S at 25°C, and the resulting proteasome complex was incubated with recombinant GST- IκBγ or His- IκBα in a 1:12.5 ratio, respectively. **(C)** PA28αβ RP was mixed in 4 fold molar excess with 20S at 25°C, and the resulting proteasome complex was incubated with untagged IκBα in a 1:100 ratio, respectively. Untagged IκBα was used for the degradation assay immediately following its elution from the Superdex 200 column. Degradation of each substrate was visualized by Coomassie stained SDS gels.

4.3.3 Interaction of 26S and PA28 regulatory particles (RPs) with free IκBα

There are two possibilities explaining the enhanced *in vitro* degradation of IκBα when PA28 RPs were present in the reaction mixture: one, PA28 RPs interact with and recruit IκBα to the 20S proteasome or two, PA28 RP enhances 20S protease activity. To test the first possibility, we performed immunoprecipitation (IP) reactions to see whether these regulatory particles do in fact interact with IκBα. We chose to focus interaction studies primarily on IκBα since our lab already had an established cell system in place to test the interaction. In the *nfkb1*$^{-/-}$*rela*$^{-/-}$*crel*$^{-/-}$ (named *nfkb*$^{-/-}$) cells, Flag- IκBα had been reconstituted and existed only as the free form, given that all of IκBα's interacting partners were absent. In agreement with the *in vitro* degradation assays, we were unable to detect interaction of the 19S RP to free IκBα, further illustrating that the 26S proteasome is not involved in the Ub- independent degradation of free IκBα (Fig 4.3.4). However, we were also unable to detect any interaction with any PA28 regulatory particles, as well as the 20S CP (Fig 4.3.4). To ensure that the IP conditions were favorable for protein protein interactions, we

determined that Flag- IκBα could interact with its known binding partner, RelA, as seen in the *ikba*$^{-/-}$ cells reconstituted with Flag- IκBα (Fig4.3.4). Interaction between any of the regulatory particles with IκBα was also undetectable when the IP reactions were performed in the presence of proteasome inhibitor, MG132, and cross- linking reagent, DSP (data not shown).

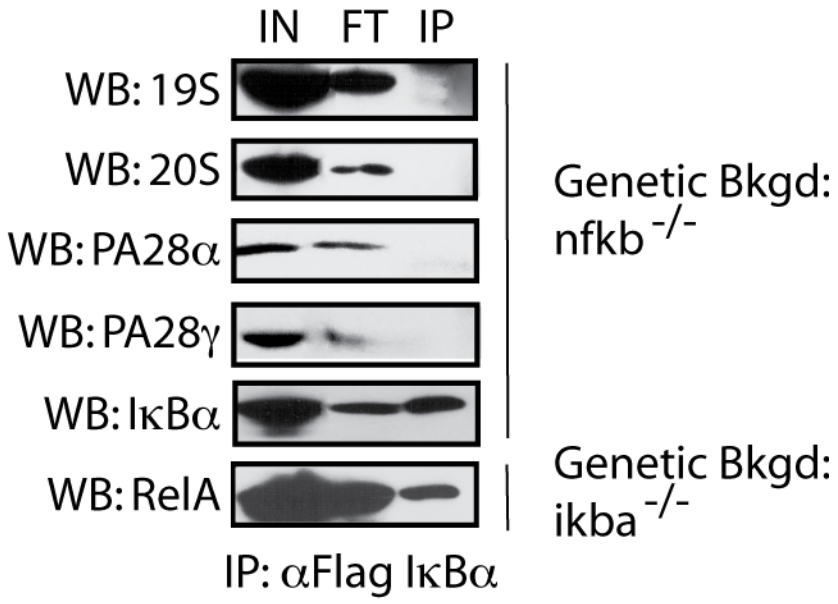

Figure 4.3.4: Proteasome regulatory particles fail to interact with the free form of FLAG tagged IκBα.

Immunoprecipitation (IP) and western blot (WB) analysis of the interaction of proteasome regulatory particles or 20S core particle with Flag tagged IκBα in $p65^{-/-}p50^{-/-}crel^{-/-}$ 3T3 cells. Data is representative of at least three independent experiments. To ensure IP conditions were favorable for protein/protein interactions, interaction of Flag- IκBα to p65 in Ikba-/- 3T3 cells was detected. IN= input, FT= flow through.

4.3.4 *In vivo* involvement of PA28αβ regulatory particles in the turnover of free IκBα

Although we were unable to detect interaction with free IκBα to PA28αβ RP by IP, PA28αβ still enhanced the *in vitro* degradation of free IκBα. To more fully determine whether PA28αβ is involved in the turnover of free IκBα, either PA28α or β was over-expressed in *nfkb*$^{-/-}$ cells where IκBα is present only in the free form (Fig 4.3.5A). Over-expression of PA28α or PA28β led to a significant decrease in basal free IκBα protein levels (Fig 4.3.5A).

In stimulated cells, the NF-κB activation response depends on both the bound and free IκBα degradation pathways, given that stabilization of free IκBα is known to decrease NF-κB activation upon stimulation. Thus, we set out to more fully address whether PA28αβ was involved in the turnover of free IκBα by determining whether stabilization of free IκBα by knocking out of the PA28 RPs, led to a decrease in NF-κB activation. Stimulation of MEFs lacking PA28 α, β, and γ subunits (*pa28*$^{-/-}$) showed significant decrease in both basal NF-κB activation (0hr time points) and thapsigarin stimulated NF-κB activation (1,2, 4hrs time points), compared to cells containing all PA28 RPs (*pa28*$^{+/+}$) (Fig 4.3.5B).

All together, these results strongly suggest that PA28αβ bound to 20S is the form of proteasome responsible for the turnover of free IκBα.

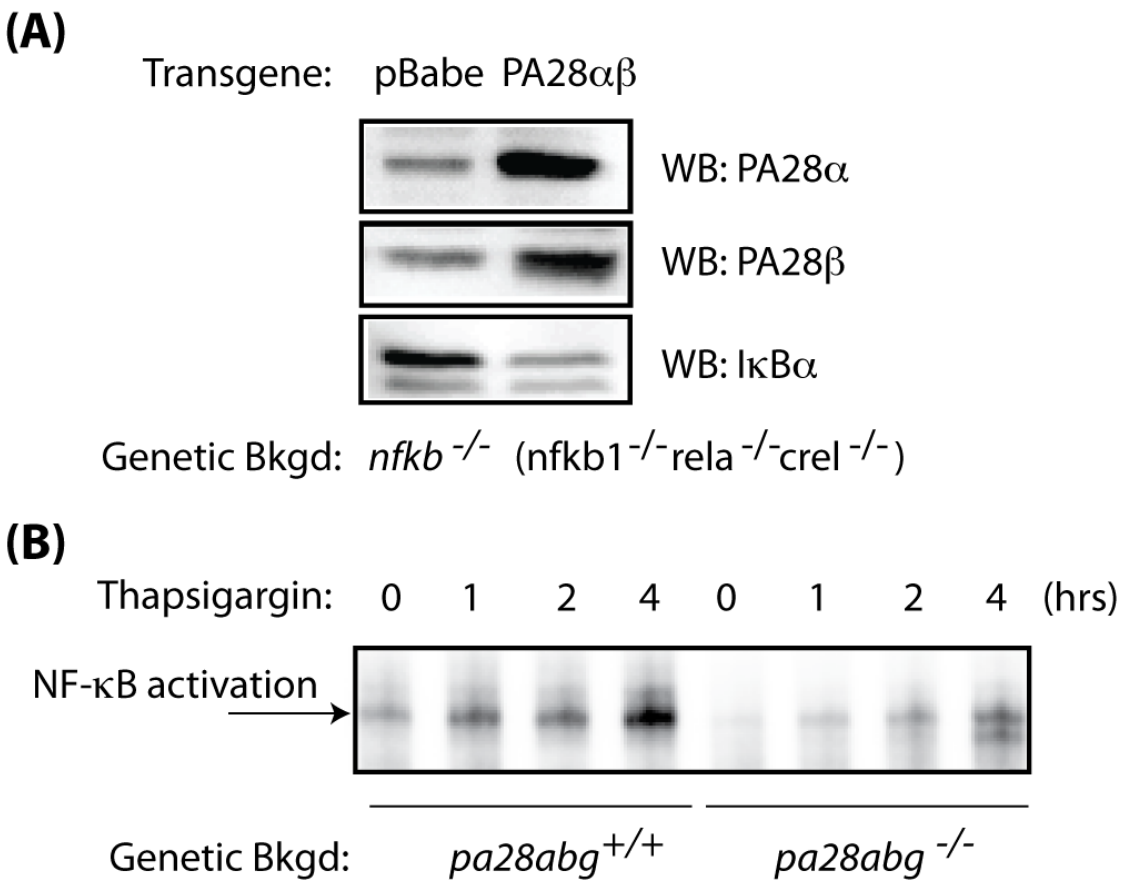

Figure 4.3.5: PA28 αβ associated 20S is responsible for the turnover of free IκBα *in vivo*.

(A) Either PA28 α or β was over-expressed in *nfkb*$^{-/-}$ cells and the resulting changes in basal IκBa levels were determined. As a negative control, empty vector (pBabe) was also expressed. PA28α (PW8185), β (sc-23642), and IκBα (sc-371) were detected by western blot. **(B)** To determine whether the increase in free IκBα half-life affected NF-κB activation, *pa28*$^{+/+}$ and *pa28*$^{-/-}$ cells were treated with known NF-κB activator, thapsigargin, for the indicated periods of time, and NF-κB activation was detected by EMSA. These experiments were performed by Ellen O'Dea from Alex Hoffman's laboratory.

4.3.5 Discriminatory activity of the PA28αβ regulatory particles for free IκBα

The degradation signal for the ubiquitin (Ub) independent turnover of free IκBα lies within the C-terminal region of IκBα and deletion of this region significantly enhances the half-life of free IκBα *in vivo*. Thus, to more fully demonstrate that PA28αβ is responsible for the turnover of free IκBα, *in vitro* degradation assays were done using full length (FL) IκBα or a truncated mutant of IκBα containing only residues 1-287 (IκBαΔ288), which lacks the degradation signal. PA28αβ bound 20S degraded free IκBα FL at a faster rate than IκBαΔ288, in that there is still IκBα Δ288 protein remaining at 2hrs compared to IκBαFL(Fig 4.3.6A). To ensure the specificity of the *in vitro* reaction, a degradation reaction was performed using GST tagged to two ubiquitin molecules (GST-diUb), which is known to be a stably folded, globular protein. Both 20S alone and PA28αβ bound 20S were unable to degrade GST-diUb (Fig 4.3.6B). Given that the truncated mutant of IκBα was degraded significantly slower than FL IκBα, and that this result follows the same trend as seen *in vivo*, it is strongly suggestive that PA28αβ bound 20S is involved in the turnover of free IκBα.

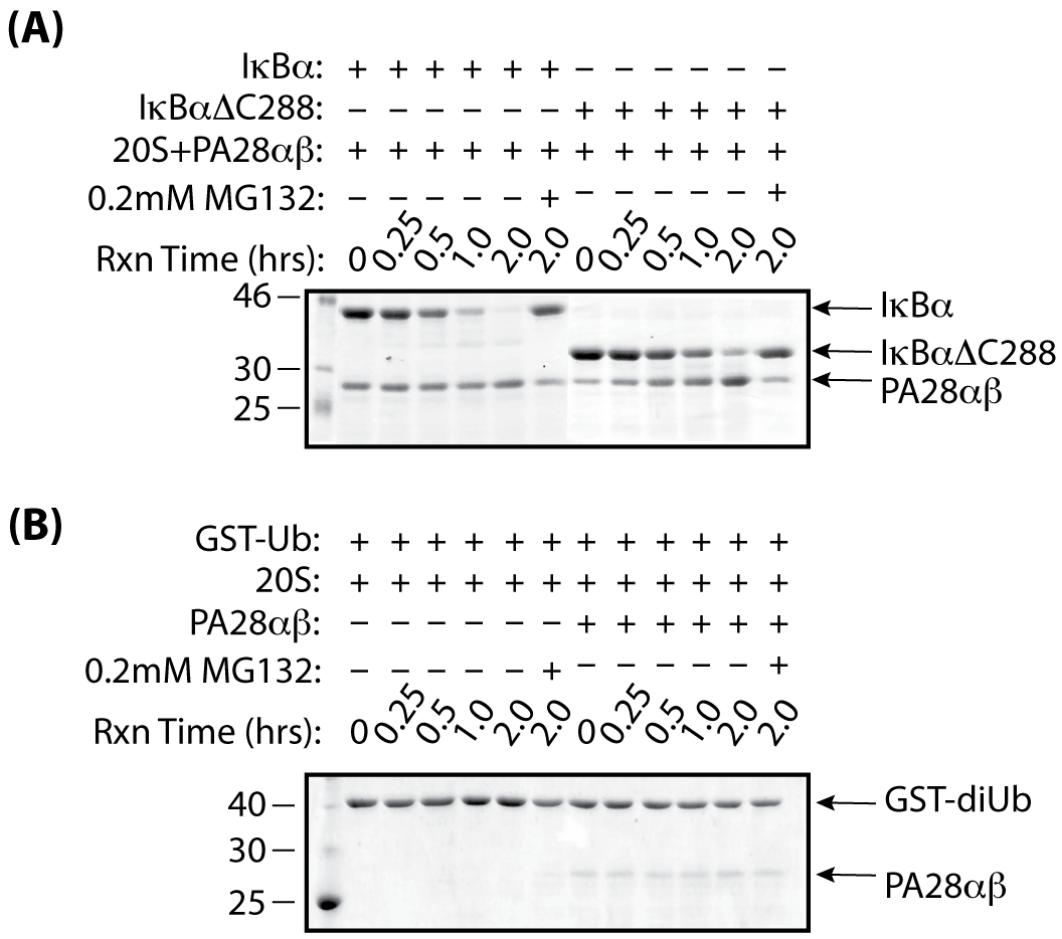

Figure 4.3.6: PA28αβ bound 20S is able to discriminate between wild type and a stabilized mutant of free IκBα *in vitro*

(A) PA28αβ bound 20S proteasome degrades recombinant full length (FL) IκBα at a faster rate than a truncated mutant of IκBα containing only residues 1-287 (IκBα ΔC288). PA28αβ RP was mixed in 4 fold molar excess with 20S at 25°C, and the resulting proteasome complex was incubated with the indicated IκBα molecule in a 1:100 ratio, respectively. Both FL and truncated IκBα was used for the degradation assay immediately following its elution from the Superdex 200 column. **(B)** To ensure the specificity of the degradative activity of the proteasome, a degradation assay was performed using stably folded GST tagged di-ubiquitin (GST-diUb). Degradation of each substrate was visualized by Coomassie stained SDS gels.

4.4 Discussion

We have shown that, while 26S proteasome cannot degrade free IκBα *in vitro*, both PA28αβ and PA28γ bound 20S are both able to enhance the degradation of IκBα *in vitro*. These results are consistent with conclusions inferred from the crystal structure of PA28 *Trypanosoma brucei* homologue, PA26, bound to yeast 20S, where binding of PA26 caused gate opening of the latent 20S (Whitby et al., 2000). Because PA28 RPs do not have ATPase or ubiquitin recognition motifs, degradation of their substrates does not require ATP or ubiquitination, as we saw in the case of IκBα *in vitro*(Hill et al., 2002; Rechsteiner and Hill, 2005). More importantly, the degradation of free IκBα by PA28αβ bound 20S seen *in vitro* occurs in a specific and discriminatory manner, as demonstrated by the lack of degradation of both GST-diUb and the *in vivo* stabilized mutant of IκBα (IκBαΔ288)

Although IκBα has been reported to interact with 20S proteasomal subunit α3, we were unable to detect this interaction, as well as interaction of PA28αβ to free IκBα in Flag- IκBα reconstituted *nfkb*$^{-/-}$ cells (Petropoulos and Hiscott, 1998). Other protein substrates involved in Ub-independent degradation have been shown to interact with either the

20S proteasome or the RPs using a variety of techniques. For example, p21 was recently shown to interact with PA28γ, using recombinant proteins, an over-expression system, and between endogenous proteins (Chen et al., 2007; Li et al., 2007). Interestingly, in order to detect interaction between the endogenous proteins, the cells were treated with proteasome inhibitor MG132, for 4 to 6 hours (Chen et al., 2007). In our attempt to detect interaction between endogenous IκBα and endogenous 20S or any RP, cells were only treated with MG132 for 1hour prior to lysis. Prolonged treatment could potentially assist in prolonging the interaction. We also attempted to determine interaction between IκBα and PA28αβ using recombinant proteins (data not shown). However, PA28 RPs proved to have significant non-specific binding properties *in vitro* and bound to both the resin and IgG, thus masking any interaction with IκBα. However, although we were unable to detect an interaction between PA28αβ and IκBα, we cannot conclude that they do not interact in cells, given that over-expression of PA28α or β in *nfkb*$^{-/-}$ cells led to a substantial decrease in the level of basal free IκBα (Fig 4.3.5A). Knock- out of PA28 α,β, and γ also showed lower levels of basal NF-κB activation and induced NF-κB activity, which indicates that more free IκBα is present to inhibit NF-κB translocation (Fig

4.3.5B). All together, these results strongly indicate that PA28 αβ plays a role in IκBα turnover.

We also noticed that both PA28αβ and PA28γ bound 20S displayed enhanced degradation of free IκBα *in vitro*, albeit PA28 αβ bound 20S was more efficient than PA28γ bound 20S in degrading IκBα. Based on our results, we cannot conclusively rule out that PA28γ is not involved in the turn over of free IκBα, since delayed NF-κB activation was seen in *pa28*$^{-/-}$ (*pa28a*$^{-/-}$*b*$^{-/-}$*g*$^{-/-}$) cells. While PA28αβ has more of an immune function and PA28γ has a role in cell growth, NF-κB, and thus IκBα turnover, plays a central role in both of these cellular responses. It is tempting to speculate that both of these RPs are involved in the Ub independent turnover of free IκBα, and that the type of PA28 RP involved in free IκBα turnover is dependent on the cell type and whether the cellular stimuli leads to an immune or cell growth response. In support of this model, stimulation of cells with IFNγ is known to induce an inflammatory response, which involves the up-regulation of PA28αβ and cause NF-κB activation. Preliminary data by the Alex Hoffmann laboratory shows that IFNγ stimulation also enhances the Ub-independent degradation of free IκBα. It would be interesting to see whether cell growth stimuli, which induce NF-κB activation, also causes

the Ub-independent turnover of free IκBα by PA28γ bound 20S proteasome.

4.5 Acknowledgments

I would like to thank Dr. Gregory Pratt for the BL21 cells expressing PA28 α,β, and γ; Kim Hyunh for her experimental assistance; Erika Mathes for the His-IκBα FL and His- IκBαΔC288 clones; Xiang-Yang Zhong for Gst-diUb protein; Ellen O'Dea for performing the EMSA and PA28 over-expression and western blot analysis for Figure 4.3.5; Yidan Li for her critical reading of this chapter;. JH is supported by the Ruth L. Kirschstein National Research Service Award NIH/NCI T32 CA009523.

Parts of Chapter 4 are adapted from a manuscript in preparation, 2010. Ho, Jessica Q.; Hyunh, Kim; Mathes, Erika; Ghosh, Gourisankar. "PA28αβ bound 20S proteasome is responsible for the degradation of free IκBα". The dissertation author the primary author. Kim Hyunh performed the purification of His- IκBα FL and His- IκBα ΔC288 as well as the degradation assay of IκBα with PA28αβ (Figure 4.3.3C and 4.3.6), using the purified 20S proteasome and PA28αβ regulatory particles that the dissertation author purified and the degradation assay that the dissertation author designed; Erika Mathes performed the experiment in Figure 4.3.1. Both Kim Hyunh and Eirka Mathes are co-authors.

Chapter 5: Discussion

NF-κB is a pleiotropic transcription factor that is present in a multitude of species and is integral in regulating diverse cellular processes such as inflammation, the innate and adaptive immune response, and cell survival. Mis-regulation of NF-κB is known to lead to many diseases, such as cancer, neurodegenerative disorders, and diseases associated with chronic inflammation (arthritis, Crohn's disease) (Courtois and Gilmore, 2006; Gerondakis et al., 2006). Since NF-κB is involved in regulating such a diverse array of cellular processes, its activity must be tightly regulated as well. Thus, this study characterizes NF-κB on two fronts, where we examine NF-κB's role in regulating the cellular stress response to oxidative stress as well as the degradation system which regulates NF-κB activity.

5.1 NF-κB's role in mediating cellular stress response to oxidative stress

From our research, we have convincingly shown that NF-κB promotes a caspase independent but PARP dependent fibroblast cell death, which is induced by chronic insult with H_2O_2. This result is surprising given NF-κB's well- established pro-survival activity (Beg and Baltimore, 1996; Beg et al., 1995; Kucharczak et al., 2003; Papa et al., 2006). However, there have been a few scattered reports in the

literature, which also show that, in certain cell types, NF-κB can have a pro-cell death function in response to atypical stimuli of NF-κB (Campbell et al., 2004; Campbell et al., 2006; Liu et al., 2006b; Perkins and Gilmore, 2006). Thus the pro-survival or death function of NF-κB appears to be both stimulus and cell context dependent. Fully understanding how NF-κB dictates the cell fate response is necessary to improve the efficacy of therapeutics in which NF-κB inhibitors are predominantly used. This is especially seen in the case of anti-cancer therapeutics (Campbell et al., 2004; Ho et al., 2005). Indeed, while it is generally thought that inhibiting NF-κB activation sensitizes cancer cells to chemotherapy, a recent report convincingly demonstrates that the effectiveness of antimitotic drugs in inducing apoptosis in prostate cancer cells is contingent on whether NF-κB is activated (Parrondo et al., 2010). Specifically, treatment of an aggressive, castration-resistant prostate cancer cells with anti-mitotic drugs is only effective when there is also co-treatment with BA, a drug that induces NF-κB activity.

Additionally, using real time quantitative PCR (qPCR), we were able to show that NF-κB dependent pro-survival genes, Bcl-2 and XIAP, were down-regulated while the NF-κB dependent, pro-death gene (TNFα) was up-regulated in response to H_2O_2. Given that these changes in mRNA levels only occurred in cells that contained NF-κB family

member, RelA, we suggested that NF-κB is involved in changing the expression levels of these genes. If NF-κB is indeed responsible for these subsequent changes in mRNA levels, this would be the first report showing that activated NF-κB can simultaneously up-regulate and down-regulate genes in response to oxidative stress. It is intriguing to speculate the possible mechanisms by which this can occur. Since oxidative stress is known to inactivate phosphatases, this can lead to a change in the overall cellular phosphorylation state (Gloire et al., 2006b; Papa et al., 2006), which can then affect the recruitment of potential co-activators, repressors, and HDACs. Additionally, given that PARP is also an important mediator of H_2O_2 induced cell death (Yu et al., 2002) and that PARP is a known co-activator of NF-κB (Hassa et al., 2001; Stilmann et al., 2009; Veuger et al., 2009), it would be interesting to explore more fully whether the co-activating function of PARP or PARylation of NF-κB by PARP contributes to the simulataneous up- and down-regulation of genes by NF-κB.

5.2 Regulation of NF-κB by the oxidized 20S proteasome and PA28αβ bound 20S proteasome

The other area of my work has focused on how NF-κB activity is regulated, in particular by the ubiquitin-independent degradation of both IκBγ and free IκBα. From *in vitro* degradation assays we were able to show that the 20S proteasome is able to degrade IκBγ in an ATP and ubiquitin independent manner. LC-MS/MS results showed that 20S proteasome with enhanced ability to degrade IκBγ actually contains higher levels of cysteic acid modifications. We suggest that mild oxidation of the 20S proteasome can enhance its proteolytic activity, but severe oxidation can inhibit its activity. This oxidative effect on the ubiquitin independent degradation activity has important potential implications for cellular adaption to stress. Under oxidative stress, protein oxidation can lead to an increase in unfolded and misfolded proteins (Davies and Shringarpure, 2006). Thus, since 20S proteasome is only able to degrade partially unfolded proteins and if its activity is indeed enhanced, oxidized 20S proteasome would be able to help the cell effectively adapt to oxidative stress (Trachootham et al., 2008). Our result that IκBγ is degraded in a ubiqutin independent manner by oxidized 20S proteasome potentially suggests that an there would be an increase the amount of p105 processing and thus increase NF-κB activation upon oxidative stress. Given that NF-κB also plays an important role in the cellular stress response, an increase in the amount

of activated NF-κB could also affect how well the cell adapts to cellular stress.

With regards to free IκBα, using *in vitro* degradation assays, we were able to show that PA28αβ bound 20S proteasome was able to efficiently degrade free IκBα in an ubiquitin independent manner, as opposed to the 26S proteasome, the 20S alone, or PA28γ bound 20S proteasome. Additional *in vitro* degradation assays showed that degradation of free IκBα *in vitro* occurs in a specific and discriminatory manner. Furthermore, genetic experiments revealed that over-expression of PA28αβ significantly decreased the level of intracellular free IκBα. Additionally, both basal and activated NF-κB activation in pa28 $a^{-/-}b^{-/-}g^{-/-}$ cells is significantly dampened, indicating an excess of free IκBα levels. All together, these results strongly indicate that the ubiquitin independent degradation is mediated by PA28αβ bound 20S proteasome. This finding is significant because this is the first example of a physiological substrate for the PA28αβ bound 20S proteasome.

While previous studies have focused on the sequences and regions in free IκBα that can act as a degradation signal (Mathes et al., 2008; Mathes et al., 2010), this study has focused primarily on the form of the proteasome that specifically degrades free IκBα. Insight gained from degron studies of free IκBα only provide an explanation for why

free IκBα is an optimal substrate for ubiquitin independent degradation, where it was shown to be due to its loosely folded nature (Mathes et al., 2010). However, these studies do not explain why free IκBα is specifically degraded by the PA28αβ bound 20S proteasome and less efficiently by the 26S proteasome, PA28γ bound 20S proteasome, and 20S proteasome alone. Perhaps the highly negatively charged tail of free IκBα, which has been shown to be required for the ubiquitin-independent degradation of free IκBα (Mathes et al., 2008), can facilitate a specific docking interaction for IκBα to PA28αβ through electrostatic interactions. This could subsequently assist in the substrate recognition of IκBα to the PA28αβ regulatory particle.

References

Atsriku, C., Benz, C.C., Scott, G.K., Gibson, B.W., and Baldwin, M.A. (2007). Quantification of cysteine oxidation in human estrogen receptor by mass spectrometry. Anal Chem *79*, 3083-3090.

Bader, N., and Grune, T. (2006). Protein oxidation and proteolysis. Biol Chem *387*, 1351-1355.

Bader, N., Jung, T., and Grune, T. (2007). The proteasome and its role in nuclear protein maintenance. Exp Gerontol *42*, 864-870.

Baeuerle, P.A., and Baltimore, D. (1988). I kappa B: a specific inhibitor of the NF-kappa B transcription factor. Science *242*, 540-546.

Bafana, A., Dutt, S., Kumar, S., and Ahuja, P.S. (2010). Superoxide dismutase: an industrial perspective. Crit Rev Biotechnol.

Bailly, E., and Reed, S.I. (1999). Functional characterization of rpn3 uncovers a distinct 19S proteasomal subunit requirement for ubiquitin-dependent proteolysis of cell cycle regulatory proteins in budding yeast. Mol Cell Biol *19*, 6872-6890.

Bakkar, N., and Guttridge, D.C. (2010). NF-kappaB signaling: a tale of two pathways in skeletal myogenesis. Physiol Rev *90*, 495-511.

Baldwin, A.S., Jr. (1996). The NF-kappa B and I kappa B proteins: new discoveries and insights. Annu Rev Immunol *14*, 649-683.

Barkett, M., and Gilmore, T.D. (1999). Control of apoptosis by Rel/NF-kappaB transcription factors. Oncogene *18*, 6910-6924.

Barton, L.F., Runnels, H.A., Schell, T.D., Cho, Y., Gibbons, R., Tevethia, S.S., Deepe, G.S., Jr., and Monaco, J.J. (2004). Immune defects in 28-kDa

proteasome activator gamma-deficient mice. J Immunol *172*, 3948-3954.

Basak, S., Kim, H., Kearns, J.D., Tergaonkar, V., O'Dea, E., Werner, S.L., Benedict, C.A., Ware, C.F., Ghosh, G., Verma, I.M.*, et al.* (2007). A fourth IkappaB protein within the NF-kappaB signaling module. Cell *128*, 369-381.

Basset, G., Raymond, P., Malek, L., and Brouquisse, R. (2002). Changes in the expression and the enzymic properties of the 20S proteasome in sugar-starved maize roots. evidence for an in vivo oxidation of the proteasome. Plant Physiol *128*, 1149-1162.

Beg, A.A., and Baltimore, D. (1996). An essential role for NF-kappaB in preventing TNF-alpha-induced cell death. Science *274*, 782-784.

Beg, A.A., Sha, W.C., Bronson, R.T., Ghosh, S., and Baltimore, D. (1995). Embryonic lethality and liver degeneration in mice lacking the RelA component of NF-kappa B. Nature *376*, 167-170.

Behl, C., and Moosmann, B. (2002). Oxidative nerve cell death in Alzheimer's disease and stroke: antioxidants as neuroprotective compounds. Biol Chem *383*, 521-536.

Beinke, S., Belich, M.P., and Ley, S.C. (2002). The death domain of NF-kappa B1 p105 is essential for signal-induced p105 proteolysis. J Biol Chem *277*, 24162-24168.

Bochtler, M., Ditzel, L., Groll, M., Hartmann, C., and Huber, R. (1999). The proteasome. Annu Rev Biophys Biomol Struct *28*, 295-317.

Bossis, G., Ferrara, P., Acquaviva, C., Jariel-Encontre, I., and Piechaczyk, M. (2003). c-Fos proto-oncoprotein is degraded by the proteasome independently of its own ubiquitinylation in vivo. Mol Cell Biol *23*, 7425-7436.

Bozonet, S.M., Findlay, V.J., Day, A.M., Cameron, J., Veal, E.A., and Morgan, B.A. (2005). Oxidation of a eukaryotic 2-Cys peroxiredoxin is a molecular switch controlling the transcriptional response to increasing levels of hydrogen peroxide. J Biol Chem *280*, 23319-23327.

Cadenas, E. (1989). Biochemistry of oxygen toxicity. Annu Rev Biochem *58*, 79-110.

Campbell, K.J., Rocha, S., and Perkins, N.D. (2004). Active repression of antiapoptotic gene expression by RelA(p65) NF-kappa B. Mol Cell *13*, 853-865.

Campbell, K.J., Witty, J.M., Rocha, S., and Perkins, N.D. (2006). Cisplatin mimics ARF tumor suppressor regulation of RelA (p65) nuclear factor-kappaB transactivation. Cancer Res *66*, 929-935.

Carnevali, S., Petruzzelli, S., Longoni, B., Vanacore, R., Barale, R., Cipollini, M., Scatena, F., Paggiaro, P., Celi, A., and Giuntini, C. (2003). Cigarette smoke extract induces oxidative stress and apoptosis in human lung fibroblasts. Am J Physiol Lung Cell Mol Physiol *284*, L955-963.

Casagrande, S., Bonetto, V., Fratelli, M., Gianazza, E., Eberini, I., Massignan, T., Salmona, M., Chang, G., Holmgren, A., and Ghezzi, P. (2002). Glutathionylation of human thioredoxin: a possible crosstalk between the glutathione and thioredoxin systems. Proc Natl Acad Sci U S A *99*, 9745-9749.

Cecarini, V., Ding, Q., and Keller, J.N. (2007). Oxidative inactivation of the proteasome in Alzheimer's disease. Free Radic Res *41*, 673-680.

Chance, B., Sies, H., and Boveris, A. (1979). Hydroperoxide metabolism in mammalian organs. Physiol Rev *59*, 527-605.

Chang, T.S., Jeong, W., Woo, H.A., Lee, S.M., Park, S., and Rhee, S.G. (2004). Characterization of mammalian sulfiredoxin and its reactivation of hyperoxidized peroxiredoxin through reduction of cysteine sulfinic acid in the active site to cysteine. J Biol Chem *279*, 50994-51001.

Chen, X., Barton, L.F., Chi, Y., Clurman, B.E., and Roberts, J.M. (2007). Ubiquitin-independent degradation of cell-cycle inhibitors by the REGgamma proteasome. Mol Cell *26*, 843-852.

Chevallet, M., Wagner, E., Luche, S., van Dorsselaer, A., Leize-Wagner, E., and Rabilloud, T. (2003). Regeneration of peroxiredoxins during recovery after oxidative stress: only some overoxidized peroxiredoxins can be reduced during recovery after oxidative stress. J Biol Chem *278*, 37146-37153.

Cooke, M.S., Evans, M.D., Dizdaroglu, M., and Lunec, J. (2003). Oxidative DNA damage: mechanisms, mutation, and disease. FASEB J *17*, 1195-1214.

Courtois, G., and Gilmore, T.D. (2006). Mutations in the NF-kappaB signaling pathway: implications for human disease. Oncogene *25*, 6831-6843.

Davies, K.J. (2001). Degradation of oxidized proteins by the 20S proteasome. Biochimie *83*, 301-310.

Davies, K.J., and Shringarpure, R. (2006). Preferential degradation of oxidized proteins by the 20S proteasome may be inhibited in aging and in inflammatory neuromuscular diseases. Neurology *66*, S93-96.

de Oliveira-Marques, V., Cyrne, L., Marinho, H.S., and Antunes, F. (2007). A quantitative study of NF-kappaB activation by H2O2: relevance in inflammation and synergy with TNF-alpha. J Immunol *178*, 3893-3902.

Dobrzanski, P., Ryseck, R.P., and Bravo, R. (1993). Both N- and C-terminal domains of RelB are required for full transactivation: role of the N-terminal leucine zipper-like motif. Mol Cell Biol *13*, 1572-1582.

Engelhardt, J.F. (1999). Redox-mediated gene therapies for environmental injury: approaches and concepts. Antioxid Redox Signal *1*, 5-27.

Ferrington, D.A., Husom, A.D., and Thompson, L.V. (2005). Altered proteasome structure, function, and oxidation in aged muscle. FASEB J *19*, 644-646.

Frankenberger, M., Pforte, A., Sternsdorf, T., Passlick, B., Baeuerle, P.A., and Ziegler-Heitbrock, H.W. (1994). Constitutive nuclear NF-kappa B in cells of the monocyte lineage. Biochem J *304 (Pt 1)*, 87-94.

Franzoso, G., Bours, V., Park, S., Tomita-Yamaguchi, M., Kelly, K., and Siebenlist, U. (1992). The candidate oncoprotein Bcl-3 is an antagonist of p50/NF-kappa B-mediated inhibition. Nature *359*, 339-342.

Fu, H., Reis, N., Lee, Y., Glickman, M.H., and Vierstra, R.D. (2001a). Subunit interaction maps for the regulatory particle of the 26S proteasome and the COP9 signalosome. Embo J *20*, 7096-7107.

Fu, X., Kassim, S.Y., Parks, W.C., and Heinecke, J.W. (2001b). Hypochlorous acid oxygenates the cysteine switch domain of pro-matrilysin (MMP-7). A mechanism for matrix metalloproteinase activation and atherosclerotic plaque rupture by myeloperoxidase. J Biol Chem *276*, 41279-41287.

Gao, X., Li, J., Pratt, G., Wilk, S., and Rechsteiner, M. (2004). Purification procedures determine the proteasome activation properties of REG gamma (PA28 gamma). Arch Biochem Biophys *425*, 158-164.

Gardner, A.M., Xu, F.H., Fady, C., Jacoby, F.J., Duffey, D.C., Tu, Y., and Lichtenstein, A. (1997). Apoptotic vs. nonapoptotic cytotoxicity induced by hydrogen peroxide. Free Radic Biol Med *22*, 73-83.

Geiszt, M., and Leto, T.L. (2004). The Nox family of NAD(P)H oxidases: host defense and beyond. J Biol Chem *279*, 51715-51718.

Gerondakis, S., Grumont, R., Gugasyan, R., Wong, L., Isomura, I., Ho, W., and Banerjee, A. (2006). Unravelling the complexities of the NF-kappaB signalling pathway using mouse knockout and transgenic models. Oncogene *25*, 6781-6799.

Ghafourifar, P., and Cadenas, E. (2005). Mitochondrial nitric oxide synthase. Trends Pharmacol Sci *26*, 190-195.

Ghisletti, S., Huang, W., Jepsen, K., Benner, C., Hardiman, G., Rosenfeld, M.G., and Glass, C.K. (2009). Cooperative NCoR/SMRT interactions establish a corepressor-based strategy for integration of inflammatory and anti-inflammatory signaling pathways. Genes Dev *23*, 681-693.

Ghisletti, S., Huang, W., Ogawa, S., Pascual, G., Lin, M.E., Willson, T.M., Rosenfeld, M.G., and Glass, C.K. (2007). Parallel SUMOylation-dependent pathways mediate gene- and signal-specific transrepression by LXRs and PPARgamma. Mol Cell *25*, 57-70.

Ghosh, S., May, M.J., and Kopp, E.B. (1998). NF-kappa B and Rel proteins: evolutionarily conserved mediators of immune responses. Annu Rev Immunol *16*, 225-260.

Gilmore, T.D. (2006). Introduction to NF-kappaB: players, pathways, perspectives. Oncogene *25*, 6680-6684.

Gilmore, T.D., Cormier, C., Jean-Jacques, J., and Gapuzan, M.E. (2001). Malignant transformation of primary chicken spleen cells by human transcription factor c-Rel. Oncogene *20*, 7098-7103.

Gilmore, T.D., Kalaitzidis, D., Liang, M.C., and Starczynowski, D.T. (2004). The c-Rel transcription factor and B-cell proliferation: a deal with the devil. Oncogene *23*, 2275-2286.

Glickman, M.H., and Ciechanover, A. (2002). The ubiquitin-proteasome proteolytic pathway: destruction for the sake of construction. Physiol Rev *82*, 373-428.

Gloire, G., Charlier, E., Rahmouni, S., Volanti, C., Chariot, A., Erneux, C., and Piette, J. (2006a). Restoration of SHIP-1 activity in human leukemic cells modifies NF-kappaB activation pathway and cellular survival upon oxidative stress. Oncogene *25*, 5485-5494.

Gloire, G., Legrand-Poels, S., and Piette, J. (2006b). NF-kappaB activation by reactive oxygen species: fifteen years later. Biochem Pharmacol *72*, 1493-1505.

Gloire, G., and Piette, J. (2009). Redox regulation of nuclear post-translational modifications during NF-kappaB activation. Antioxid Redox Signal *11*, 2209-2222.

Groll, M., Ditzel, L., Lowe, J., Stock, D., Bochtler, M., Bartunik, H.D., and Huber, R. (1997). Structure of 20S proteasome from yeast at 2.4 A resolution. Nature *386*, 463-471.

Groll, M., Heinemeyer, W., Jager, S., Ullrich, T., Bochtler, M., Wolf, D.H., and Huber, R. (1999). The catalytic sites of 20S proteasomes and their role in subunit maturation: a mutational and crystallographic study. Proc Natl Acad Sci U S A 96, 10976-10983.

Grune, T., Merker, K., Sandig, G., and Davies, K.J. (2003). Selective degradation of oxidatively modified protein substrates by the proteasome. Biochem Biophys Res Commun *305*, 709-718.

Grune, T., Reinheckel, T., Joshi, M., and Davies, K.J. (1995). Proteolysis in cultured liver epithelial cells during oxidative stress. Role of the multicatalytic proteinase complex, proteasome. J Biol Chem *270*, 2344-2351.

Hacker, H., and Karin, M. (2002). Is NF-kappaB2/p100 a direct activator of programmed cell death? Cancer Cell *2*, 431-433.

Hassa, P.O., Covic, M., Hasan, S., Imhof, R., and Hottiger, M.O. (2001). The enzymatic and DNA binding activity of PARP-1 are not required for NF-kappa B coactivator function. J Biol Chem *276*, 45588-45597.

Hayakawa, M., Miyashita, H., Sakamoto, I., Kitagawa, M., Tanaka, H., Yasuda, H., Karin, M., and Kikugawa, K. (2003). Evidence that reactive oxygen species do not mediate NF-kappaB activation. EMBO J *22*, 3356-3366.

Hensley, K., Robinson, K.A., Gabbita, S.P., Salsman, S., and Floyd, R.A. (2000). Reactive oxygen species, cell signaling, and cell injury. Free Radic Biol Med *28*, 1456-1462.

Hershko, A., and Ciechanover, A. (1992). The ubiquitin system for protein degradation. Annu Rev Biochem *61*, 761-807.

Hershko, A., and Ciechanover, A. (1998). The ubiquitin system. Annu Rev Biochem *67*, 425-479.

Hill, C.P., Masters, E.I., and Whitby, F.G. (2002). The 11S regulators of 20S proteasome activity. Curr Top Microbiol Immunol *268*, 73-89.

Hinz, M., Loser, P., Mathas, S., Krappmann, D., Dorken, B., and Scheidereit, C. (2001). Constitutive NF-kappaB maintains high expression of a characteristic gene network, including CD40, CD86, and a set of antiapoptotic genes in Hodgkin/Reed-Sternberg cells. Blood *97*, 2798-2807.

Ho, W.C., Dickson, K.M., and Barker, P.A. (2005). Nuclear factor-kappaB induced by doxorubicin is deficient in phosphorylation and acetylation and represses nuclear factor-kappaB-dependent transcription in cancer cells. Cancer Res *65*, 4273-4281.

Hoffmann, A., Natoli, G., and Ghosh, G. (2006). Transcriptional regulation via the NF-kappaB signaling module. Oncogene *25*, 6706-6716.

Huxford, T., Huang, D.B., Malek, S., and Ghosh, G. (1998). The crystal structure of the IkappaBalpha/NF-kappaB complex reveals mechanisms of NF-kappaB inactivation. Cell *95*, 759-770.

Huxford, T., Malek, S., and Ghosh, G. (1999). Structure and mechanism in NF-kappa B/I kappa B signaling. Cold Spring Harb Symp Quant Biol *64*, 533-540.

Jacobs, M.D., and Harrison, S.C. (1998). Structure of an IkappaBalpha/NF-kappaB complex. Cell *95*, 749-758.

Jariel-Encontre, I., Pariat, M., Martin, F., Carillo, S., Salvat, C., and Piechaczyk, M. (1995). Ubiquitinylation is not an absolute requirement for degradation of c-Jun protein by the 26 S proteasome. J Biol Chem *270*, 11623-11627.

Kamata, H., Honda, S., Maeda, S., Chang, L., Hirata, H., and Karin, M. (2005). Reactive oxygen species promote TNFalpha-induced death and sustained JNK activation by inhibiting MAP kinase phosphatases. Cell *120*, 649-661.

Karin, M., and Ben-Neriah, Y. (2000). Phosphorylation meets ubiquitination: the control of NF-[kappa]B activity. Annu Rev Immunol *18*, 621-663.

Kearns, J.D., Basak, S., Werner, S.L., Huang, C.S., and Hoffmann, A. (2006). IkappaBepsilon provides negative feedback to control NF-kappaB oscillations, signaling dynamics, and inflammatory gene expression. J Cell Biol *173*, 659-664.

Kraus, W.L., and Lis, J.T. (2003). PARP goes transcription. Cell *113*, 677-683.

Kriwacki, R.W., Hengst, L., Tennant, L., Reed, S.I., and Wright, P.E. (1996). Structural studies of p21Waf1/Cip1/Sdi1 in the free and Cdk2-bound state: conformational disorder mediates binding diversity. Proc Natl Acad Sci U S A *93*, 11504-11509.

Kucharczak, J., Simmons, M.J., Fan, Y., and Gelinas, C. (2003). To be, or not to be: NF-kappaB is the answer--role of Rel/NF-kappaB in the regulation of apoptosis. Oncogene *22*, 8961-8982.

Lander, H.M. (1997). An essential role for free radicals and derived species in signal transduction. FASEB J *11*, 118-124.

Li, J., and Rechsteiner, M. (2001). Molecular dissection of the 11S REG (PA28) proteasome activators. Biochimie *83*, 373-383.

Li, X., Amazit, L., Long, W., Lonard, D.M., Monaco, J.J., and O'Malley, B.W. (2007). Ubiquitin- and ATP-independent proteolytic turnover of p21 by the REGgamma-proteasome pathway. Mol Cell *26*, 831-842.

Li, X., Lonard, D.M., Jung, S.Y., Malovannaya, A., Feng, Q., Qin, J., Tsai, S.Y., Tsai, M.J., and O'Malley, B.W. (2006). The SRC-3/AIB1 coactivator is degraded in a ubiquitin- and ATP-independent manner by the REGgamma proteasome. Cell *124*, 381-392.

Lim, J.C., Choi, H.I., Park, Y.S., Nam, H.W., Woo, H.A., Kwon, K.S., Kim, Y.S., Rhee, S.G., Kim, K., and Chae, H.Z. (2008). Irreversible oxidation of the active-site cysteine of peroxiredoxin to cysteine sulfonic acid for enhanced molecular chaperone activity. J Biol Chem *283*, 28873-28880.

Lin, K.I., DiDonato, J.A., Hoffmann, A., Hardwick, J.M., and Ratan, R.R. (1998). Suppression of steady-state, but not stimulus-induced NF-kappaB activity inhibits alphavirus-induced apoptosis. J Cell Biol *141*, 1479-1487.

Liu, C.W., Li, X., Thompson, D., Wooding, K., Chang, T.L., Tang, Z., Yu, H., Thomas, P.J., and DeMartino, G.N. (2006a). ATP binding and ATP hydrolysis play distinct roles in the function of 26S proteasome. Mol Cell *24*, 39-50.

Liu, J., Yang, D., Minemoto, Y., Leitges, M., Rosner, M.R., and Lin, A. (2006b). NF-kappaB is required for UV-induced JNK activation via induction of PKCdelta. Mol Cell *21*, 467-480.

Livak, K.J., and Schmittgen, T.D. (2001). Analysis of relative gene expression data using real-time quantitative PCR and the 2(-Delta Delta C(T)) Method. Methods *25*, 402-408.

Livolsi, A., Busuttil, V., Imbert, V., Abraham, R.T., and Peyron, J.F. (2001). Tyrosine phosphorylation-dependent activation of NF-kappa B.

Requirement for p56 LCK and ZAP-70 protein tyrosine kinases. Eur J Biochem *268*, 1508-1515.

Malek, S., Huang, D.B., Huxford, T., Ghosh, S., and Ghosh, G. (2003). X-ray crystal structure of an IkappaBbeta x NF-kappaB p65 homodimer complex. J Biol Chem *278*, 23094-23100.

Mankan, A.K., Lawless, M.W., Gray, S.G., Kelleher, D., and McManus, R. (2009). NF-kappaB regulation: the nuclear response. J Cell Mol Med *13*, 631-643.

Mao, I., Liu, J., Li, X., and Luo, H. (2008). REGgamma, a proteasome activator and beyond? Cell Mol Life Sci *65*, 3971-3980.

Marnett, L.J. (1999). Lipid peroxidation-DNA damage by malondialdehyde. Mutat Res *424*, 83-95.

Marnett, L.J. (2000). Oxyradicals and DNA damage. Carcinogenesis *21*, 361-370.

Masters, E.I., Pratt, G., Forster, A., and Hill, C.P. (2005). Purification and analysis of recombinant 11S activators of the 20S proteasome: Trypanosoma brucei PA26 and human PA28 alpha, PA28 beta, and PA28 gamma. Methods Enzymol *398*, 306-321.

Mathes, E., O'Dea, E.L., Hoffmann, A., and Ghosh, G. (2008). NF-kappaB dictates the degradation pathway of IkappaBalpha. EMBO J *27*, 1357-1367.

Mathes, E., Wang, L., Komives, E., and Ghosh, G. (2010). Flexible regions within I{kappa}B{alpha} create the ubiquitin-independent degradation signal. J Biol Chem *285*, 32927-32936.

Michel, F., Soler-Lopez, M., Petosa, C., Cramer, P., Siebenlist, U., and Muller, C.W. (2001). Crystal structure of the ankyrin repeat domain of Bcl-3: a unique member of the IkappaB protein family. EMBO J *20*, 6180-6190.

Moorthy, A.K., Savinova, O.V., Ho, J.Q., Wang, V.Y., Vu, D., and Ghosh, G. (2006). The 20S proteasome processes NF-kappaB1 p105 into p50 in a translation-independent manner. Embo J *25*, 1945-1956.

Murata, S., Kawahara, H., Tohma, S., Yamamoto, K., Kasahara, M., Nabeshima, Y., Tanaka, K., and Chiba, T. (1999). Growth retardation in mice lacking the proteasome activator PA28gamma. J Biol Chem *274*, 38211-38215.

Murata, S., Yashiroda, H., and Tanaka, K. (2009). Molecular mechanisms of proteasome assembly. Nat Rev Mol Cell Biol *10*, 104-115.

Nakamura, Y., Romberger, D.J., Tate, L., Ertl, R.F., Kawamoto, M., Adachi, Y., Mio, T., Sisson, J.H., Spurzem, J.R., and Rennard, S.I. (1995). Cigarette smoke inhibits lung fibroblast proliferation and chemotaxis. American journal of respiratory and critical care medicine *151*, 1497-1503.

Nishi, T., Shimizu, N., Hiramoto, M., Sato, I., Yamaguchi, Y., Hasegawa, M., Aizawa, S., Tanaka, H., Kataoka, K., Watanabe, H*., et al.* (2002). Spatial redox regulation of a critical cysteine residue of NF-kappa B in vivo. J Biol Chem *277*, 44548-44556.

O'Dea, E., and Hoffmann, A. (2009). NF-kappaB signaling. Wiley Interdiscip Rev Syst Biol Med *1*, 107.

O'Dea, E.L., Barken, D., Peralta, R.Q., Tran, K.T., Werner, S.L., Kearns, J.D., Levchenko, A., and Hoffmann, A. (2007). A homeostatic model of IkappaB metabolism to control constitutive NF-kappaB activity. Mol Syst Biol *3*, 111.

Oliveira-Marques, V., Marinho, H.S., Cyrne, L., and Antunes, F. (2009). Role of hydrogen peroxide in NF-kappaB activation: from inducer to modulator. Antioxid Redox Signal *11*, 2223-2243.

Papa, S., Bubici, C., Zazzeroni, F., Pham, C.G., Kuntzen, C., Knabb, J.R., Dean, K., and Franzoso, G. (2006). The NF-kappaB-mediated control of

the JNK cascade in the antagonism of programmed cell death in health and disease. Cell Death Differ *13*, 712-729.

Parrondo, R., de las Pozas, A., Reiner, T., Rai, P., and Perez-Stable, C. (2010). NF-kappaB activation enhances cell death by antimitotic drugs in human prostate cancer cells. Mol Cancer 9, 182.

Perkins, N.D., and Gilmore, T.D. (2006). Good cop, bad cop: the different faces of NF-kappaB. Cell Death Differ *13*, 759-772.

Petropoulos, L., and Hiscott, J. (1998). Association between HTLV-1 Tax and I kappa B alpha is dependent on the I kappa B alpha phosphorylation state. Virology *252*, 189-199.

Poole, L.B., Karplus, P.A., and Claiborne, A. (2004). Protein sulfenic acids in redox signaling. Annu Rev Pharmacol Toxicol *44*, 325-347.

Rabilloud, T., Heller, M., Gasnier, F., Luche, S., Rey, C., Aebersold, R., Benahmed, M., Louisot, P., and Lunardi, J. (2002). Proteomics analysis of cellular response to oxidative stress. Evidence for in vivo overoxidation of peroxiredoxins at their active site. J Biol Chem *277*, 19396-19401.

Rajendrasozhan, S., Yang, S.R., Edirisinghe, I., Yao, H., Adenuga, D., and Rahman, I. (2008). Deacetylases and NF-kappaB in redox regulation of cigarette smoke-induced lung inflammation: epigenetics in pathogenesis of COPD. Antioxid Redox Signal *10*, 799-811.

Realini, C., Jensen, C.C., Zhang, Z., Johnston, S.C., Knowlton, J.R., Hill, C.P., and Rechsteiner, M. (1997). Characterization of recombinant REGalpha, REGbeta, and REGgamma proteasome activators. J Biol Chem *272*, 25483-25492.

Rechsteiner, M., and Hill, C.P. (2005). Mobilizing the proteolytic machine: cell biological roles of proteasome activators and inhibitors. Trends Cell Biol *15*, 27-33.

Rechsteiner, M., and Rogers, S.W. (1996). PEST sequences and regulation by proteolysis. Trends Biochem Sci *21*, 267-271.

Reinheckel, T., Sitte, N., Ullrich, O., Kuckelkorn, U., Davies, K.J., and Grune, T. (1998). Comparative resistance of the 20S and 26S proteasome to oxidative stress. Biochem J *335 (Pt 3)*, 637-642.

Rogers, S., Wells, R., and Rechsteiner, M. (1986). Amino acid sequences common to rapidly degraded proteins: the PEST hypothesis. Science *234*, 364-368.

Salvat, C., Aquaviva, C., Jariel-Encontre, I., Ferrara, P., Pariat, M., Steff, A.M., Carillo, S., and Piechaczyk, M. (1999). Are there multiple proteolytic pathways contributing to c-Fos, c-Jun and p53 protein degradation in vivo? Mol Biol Rep *26*, 45-51.

Savinova, O.V., Hoffmann, A., and Ghosh, G. (2009). The Nfkb1 and Nfkb2 proteins p105 and p100 function as the core of high-molecular-weight heterogeneous complexes. Mol Cell *34*, 591-602.

Schmidt, F., Dahlmann, B., Hustoft, H.K., Koehler, C.J., Strozynski, M., Kloss, A., Zimny-Arndt, U., Jungblut, P.R., and Thiede, B. (2010). Quantitative proteome analysis of the 20S proteasome of apoptotic Jurkat T cells. Amino Acids.

Schmidt, F., Dahlmann, B., Janek, K., Kloss, A., Wacker, M., Ackermann, R., Thiede, B., and Jungblut, P.R. (2006). Comprehensive quantitative proteome analysis of 20S proteasome subtypes from rat liver by isotope coded affinity tag and 2-D gel-based approaches. Proteomics *6*, 4622-4632.

Schmittgen, T.D., and Livak, K.J. (2008). Analyzing real-time PCR data by the comparative C(T) method. Nat Protoc *3*, 1101-1108.

Schoonbroodt, S., Ferreira, V., Best-Belpomme, M., Boelaert, J.R., Legrand-Poels, S., Korner, M., and Piette, J. (2000). Crucial role of the amino-terminal tyrosine residue 42 and the carboxyl-terminal PEST

domain of I kappa B alpha in NF-kappa B activation by an oxidative stress. J Immunol *164*, 4292-4300.

Schreck, R., Rieber, P., and Baeuerle, P.A. (1991). Reactive oxygen intermediates as apparently widely used messengers in the activation of the NF-kappa B transcription factor and HIV-1. EMBO J *10*, 2247-2258.

Schwarz, K., Eggers, M., Soza, A., Koszinowski, U.H., Kloetzel, P.M., and Groettrup, M. (2000). The proteasome regulator PA28alpha/beta can enhance antigen presentation without affecting 20S proteasome subunit composition. Eur J Immunol *30*, 3672-3679.

Scott, M.L., Fujita, T., Liou, H.C., Nolan, G.P., and Baltimore, D. (1993). The p65 subunit of NF-kappa B regulates I kappa B by two distinct mechanisms. Genes Dev *7*, 1266-1276.

Sen, R., and Baltimore, D. (1986). Inducibility of kappa immunoglobulin enhancer-binding protein Nf-kappa B by a posttranslational mechanism. Cell *47*, 921-928.

Shringarpure, R., Grune, T., Mehlhase, J., and Davies, K.J. (2003). Ubiquitin conjugation is not required for the degradation of oxidized proteins by proteasome. J Biol Chem *278*, 311-318.

Singh, H., Sen, R., Baltimore, D., and Sharp, P.A. (1986). A nuclear factor that binds to a conserved sequence motif in transcriptional control elements of immunoglobulin genes. Nature *319*, 154-158.

Smith, D.M., Kafri, G., Cheng, Y., Ng, D., Walz, T., and Goldberg, A.L. (2005). ATP binding to PAN or the 26S ATPases causes association with the 20S proteasome, gate opening, and translocation of unfolded proteins. Mol Cell *20*, 687-698.

Song, X., von Kampen, J., Slaughter, C.A., and DeMartino, G.N. (1997). Relative functions of the alpha and beta subunits of the proteasome activator, PA28. J Biol Chem *272*, 27994-28000.

Spandidos, A., Wang, X., Wang, H., Dragnev, S., Thurber, T., and Seed, B. (2008). A comprehensive collection of experimentally validated primers for Polymerase Chain Reaction quantitation of murine transcript abundance. BMC Genomics *9*, 633.

Spandidos, A., Wang, X., Wang, H., and Seed, B. (2010). PrimerBank: a resource of human and mouse PCR primer pairs for gene expression detection and quantification. Nucleic Acids Res *38*, D792-799.

Stilmann, M., Hinz, M., Arslan, S.C., Zimmer, A., Schreiber, V., and Scheidereit, C. (2009). A nuclear poly(ADP-ribose)-dependent signalosome confers DNA damage-induced IkappaB kinase activation. Mol Cell *36*, 365-378.

Storz, P., Doppler, H., and Toker, A. (2004). Protein kinase Cdelta selectively regulates protein kinase D-dependent activation of NF-kappaB in oxidative stress signaling. Mol Cell Biol *24*, 2614-2626.

Storz, P., and Toker, A. (2003). Protein kinase D mediates a stress-induced NF-kappaB activation and survival pathway. EMBO J *22*, 109-120.

Strack, P.R., Waxman, L., and Fagan, J.M. (1996). Activation of the multicatalytic endopeptidase by oxidants. Effects on enzyme structure. Biochemistry *35*, 7142-7149.

Sullivan, J.C., Kalaitzidis, D., Gilmore, T.D., and Finnerty, J.R. (2007). Rel homology domain-containing transcription factors in the cnidarian Nematostella vectensis. Dev Genes Evol *217*, 63-72.

Sun, S.C., and Ley, S.C. (2008). New insights into NF-kappaB regulation and function. Trends Immunol *29*, 469-478.

Takada, Y., Mukhopadhyay, A., Kundu, G.C., Mahabeleshwar, G.H., Singh, S., and Aggarwal, B.B. (2003). Hydrogen peroxide activates NF-kappa B through tyrosine phosphorylation of I kappa B alpha and serine phosphorylation of p65: evidence for the involvement of I kappa B

alpha kinase and Syk protein-tyrosine kinase. J Biol Chem *278*, 24233-24241.

Takahashi, A., Aoshiba, K., and Nagai, A. (2002). Apoptosis of wound fibroblasts induced by oxidative stress. Exp Lung Res *28*, 275-284.

Tanahashi, N., Murakami, Y., Minami, Y., Shimbara, N., Hendil, K.B., and Tanaka, K. (2000). Hybrid proteasomes. Induction by interferon-gamma and contribution to ATP-dependent proteolysis. J Biol Chem *275*, 14336-14345.

Trachootham, D., Lu, W., Ogasawara, M.A., Nilsa, R.D., and Huang, P. (2008). Redox regulation of cell survival. Antioxid Redox Signal *10*, 1343-1374.

Valko, M., Leibfritz, D., Moncol, J., Cronin, M.T., Mazur, M., and Telser, J. (2007). Free radicals and antioxidants in normal physiological functions and human disease. Int J Biochem Cell Biol *39*, 44-84.

Valko, M., Rhodes, C.J., Moncol, J., Izakovic, M., and Mazur, M. (2006). Free radicals, metals and antioxidants in oxidative stress-induced cancer. Chem Biol Interact *160*, 1-40.

Veal, E.A., Day, A.M., and Morgan, B.A. (2007). Hydrogen peroxide sensing and signaling. Mol Cell *26*, 1-14.

Veal, E.A., Findlay, V.J., Day, A.M., Bozonet, S.M., Evans, J.M., Quinn, J., and Morgan, B.A. (2004). A 2-Cys peroxiredoxin regulates peroxide-induced oxidation and activation of a stress-activated MAP kinase. Mol Cell *15*, 129-139.

Veuger, S.J., Hunter, J.E., and Durkacz, B.W. (2009). Ionizing radiation-induced NF-kappaB activation requires PARP-1 function to confer radioresistance. Oncogene *28*, 832-842.

Voss, P., and Grune, T. (2007). The nuclear proteasome and the degradation of oxidatively damaged proteins. Amino Acids *32*, 527-534.

Wagner, E., Luche, S., Penna, L., Chevallet, M., Van Dorsselaer, A., Leize-Wagner, E., and Rabilloud, T. (2002). A method for detection of overoxidation of cysteines: peroxiredoxins are oxidized in vivo at the active-site cysteine during oxidative stress. Biochem J *366*, 777-785.

Wang, X., and Seed, B. (2003). A PCR primer bank for quantitative gene expression analysis. Nucleic Acids Res *31*, e154.

Wang, Y., Cui, H., Schroering, A., Ding, J.L., Lane, W.S., McGill, G., Fisher, D.E., and Ding, H.F. (2002). NF-kappa B2 p100 is a pro-apoptotic protein with anti-oncogenic function. Nat Cell Biol *4*, 888-893.

Wang, Y., Keogh, R.J., Hunter, M.G., Mitchell, C.A., Frey, R.S., Javaid, K., Malik, A.B., Schurmans, S., Tridandapani, S., and Marsh, C.B. (2004). SHIP2 is recruited to the cell membrane upon macrophage colony-stimulating factor (M-CSF) stimulation and regulates M-CSF-induced signaling. J Immunol *173*, 6820-6830.

Wardman, P., and Candeias, L.P. (1996). Fenton chemistry: an introduction. Radiat Res *145*, 523-531.

Werner, S.L., Barken, D., and Hoffmann, A. (2005). Stimulus specificity of gene expression programs determined by temporal control of IKK activity. Science *309*, 1857-1861.

Whitby, F.G., Masters, E.I., Kramer, L., Knowlton, J.R., Yao, Y., Wang, C.C., and Hill, C.P. (2000). Structural basis for the activation of 20S proteasomes by 11S regulators. Nature *408*, 115-120.

Woo, H.A., Chae, H.Z., Hwang, S.C., Yang, K.S., Kang, S.W., Kim, K., and Rhee, S.G. (2003a). Reversing the inactivation of peroxiredoxins caused by cysteine sulfinic acid formation. Science *300*, 653-656.

Woo, H.A., Jeong, W., Chang, T.S., Park, K.J., Park, S.J., Yang, J.S., and Rhee, S.G. (2005). Reduction of cysteine sulfinic acid by sulfiredoxin is specific to 2-cys peroxiredoxins. J Biol Chem *280*, 3125-3128.

Woo, H.A., Kang, S.W., Kim, H.K., Yang, K.S., Chae, H.Z., and Rhee, S.G. (2003b). Reversible oxidation of the active site cysteine of peroxiredoxins to cysteine sulfinic acid. Immunoblot detection with antibodies specific for the hyperoxidized cysteine-containing sequence. J Biol Chem *278*, 47361-47364.

Wood, Z.A., Schroder, E., Robin Harris, J., and Poole, L.B. (2003). Structure, mechanism and regulation of peroxiredoxins. Trends Biochem Sci *28*, 32-40.

Wu, Z.H., and Miyamoto, S. (2008). Induction of a pro-apoptotic ATM-NF-kappaB pathway and its repression by ATR in response to replication stress. EMBO J *27*, 1963-1973.

Xiao, J., Lv, Y., Lin, S., Jin, L., Zhang, Y., Wang, X., Ma, J., Hu, K., Feng, W., Cai, L.*, et al.* (2010). Cardiac protection by basic fibroblast growth factor from ischemia/reperfusion-induced injury in diabetic rats. Biol Pharm Bull *33*, 444-449.

Yang, K.S., Kang, S.W., Woo, H.A., Hwang, S.C., Chae, H.Z., Kim, K., and Rhee, S.G. (2002). Inactivation of human peroxiredoxin I during catalysis as the result of the oxidation of the catalytic site cysteine to cysteine-sulfinic acid. J Biol Chem *277*, 38029-38036.

Yu, S.W., Wang, H., Poitras, M.F., Coombs, C., Bowers, W.J., Federoff, H.J., Poirier, G.G., Dawson, T.M., and Dawson, V.L. (2002). Mediation of poly(ADP-ribose) polymerase-1-dependent cell death by apoptosis-inducing factor. Science *297*, 259-263.

Zhang, Z., Clawson, A., Realini, C., Jensen, C.C., Knowlton, J.R., Hill, C.P., and Rechsteiner, M. (1998). Identification of an activation region in the proteasome activator REGalpha. Proc Natl Acad Sci U S A *95*, 2807-2811.

Zmijewski, J.W., Zhao, X., Xu, Z., and Abraham, E. (2007). Exposure to hydrogen peroxide diminishes NF-kappaB activation, IkappaB-alpha degradation, and proteasome activity in neutrophils. Am J Physiol Cell Physiol *293*, C255-266.

Zong, C., Gomes, A.V., Drews, O., Li, X., Young, G.W., Berhane, B., Qiao, X., French, S.W., Bardag-Gorce, F., and Ping, P. (2006). Regulation of murine cardiac 20S proteasomes: role of associating partners. Circ Res 99, 372-380.

Zong, C., Young, G.W., Wang, Y., Lu, H., Deng, N., Drews, O., and Ping, P. (2008). Two-dimensional electrophoresis-based characterization of post-translational modifications of mammalian 20S proteasome complexes. Proteomics *8*, 5025-5037.